[American Journal of Science, Vol. 309, September, 2009, P. 549–602, DOI 10.2475/07.2009.02]

SYNOROGENIC EVOLUTION OF LARGE-SCALE DRAINAGE PATTERNS: ISOTOPE PALEOHYDROLOGY OF SEQUENTIAL LARAMIDE BASINS

STEVEN J. DAVIS*†, HARI T. MIX**, BETTINA A. WIEGAND***, ALAN R. CARROLL§, and C. PAGE CHAMBERLAIN**

ABSTRACT. In the past decade, we and others have compiled an extensive dataset of O, C and Sr isotope stratigraphies from sedimentary basins throughout the Paleogene North American Cordillera. In this study, we present new results from the Piceance Creek Basin of northwest Colorado, which record the evolving hydrology of the Eocene Green River Lake system. We then place the new data in the context of the broader Cordilleran dataset and summarize implications for understanding the synorogenic evolution of large-scale drainage patterns. The combined data reflect (1) a period of throughgoing foreland rivers heading in the Sevier fold-and-thrust belt and flowing east, (2) ponding of freshwater lakes in the foredeep as Laramide uplifts blocked drainage, (3) hydrologic closure that led to both intensive evaporation in the terminal sink of the Piceance Creek Basin and integration of catchments over length-scales >1000 km, (4) infilling of basin accommodation by southward migrating magmatism in distal catchments, leading to the freshening and demise of intraforeland lakes that also stepped south over time.

Key words: Isotope ratios, North American Cordillera, Green River Lakes, Sevier fold-and-thrust belt, paleoaltimetry, limnogeology

INTRODUCTION

Synorogenic sediments preserved in intermontane and foreland basins have long been appreciated as valuable archives of orogen and basin development, recording the complex linkage among tectonics, climate and landscape evolution. As such, clastic basin fill has been exploited by many studies using tools of sedimentary petrology and provenance, paleocurrent analysis, and kinematic histories (for example, Dickinson and others, 1986, 1988; Lawton, 1986; DeCelles, 1988; DeCelles and others, 1995; Smith and others, 2008a). In the past decade, numerous isotopic studies have also demonstrated the potential of authigenic sediments in reconstructing surface elevation and climate (for example, Koch and others, 1995; Chamberlain and Poage, 2000; Garzione and others, 2000; Fricke, 2003; Graham and others, 2005; Kent-Corson and others, 2006).

Unfortunately, very few isotopic studies have assembled large, regional datasets capable of distinguishing local and regional signals in the geologic past, and even fewer have considered the effect of large-scale drainage reorganization on their results (Davis and others, 2008). Here we add data to the most spatially and temporally dense dataset in existence, totaling more than 3000 isotopic analyses in multiple isotope systems on samples collected from 12 basins spanning ~1400 km along strike of the Tertiary North American Cordillera (table 1). Using this dataset, we summarize mounting isotopic evidence for the regional evolution of drainage patterns in both the hinterland and foreland of the orogen. Despite important changes in global climate during the Paleogene, we further conclude these regional changes in basin hydrology were driven by tectonic processes.

* Department of Global Ecology, Carnegie Institution of Washington, Stanford, California 94305, USA
** Environmental Earth System Science, Stanford University, Stanford, California 94305, USA; hmix@stanford.edu; chamb@stanford.edu
*** Geological and Environmental Sciences, Stanford University, Stanford, California 94305, USA; bwiegand@stanford.edu
§ Department of Geology and Geophysics, University of Wisconsin, Madison, Wisconsin 53706, USA; acarroll@geology.wisc.edu
† Corresponding author: sjdavis@stanford.edu

TABLE 1

Summary of isotopic and elemental data from the late Cretaceous and Paleogene Cental North American

Basin (State) Sampled Units ***Abbr. on fig. 2***	**Proxy Carbonate**	**Mean $\delta^{18}O_{calcite}$ (V-SMOW)**	**$\delta^{18}O_{calcite}$-$\delta^{13}C_{calcite}$ Covariance**	**Mean Sr/Ca (mmol/mol)**	**Mean $^{87}Sr/^{86}Sr$**	**Reference(s) and Locations on fig. 1**
Late Cretaceous - earliest Eocene (~70-52 Ma)						
Sage Creek Basin (MT/ID) Red Butte Conglomerate	Calcite Cement	20.5±1.1‰* (1σ, *n* = 5)	-	-	-	(Kent-Corson and others, 2006) ***a*** on fig. 1
Crazy Mountain Basin (MT) Unit not reported	Fossil Aragonite (Unionacea)	16.6±1.2‰* (1σ, *n* = 45)	W (r^2 = 0.11*)	-	-	(Dettman and Lohmann, 2000) ***b*** on fig. 1
Bighorn Basin (WY) Fort Union and lower Willwood Formations	Paleosol	22.1±0.5‰* (1σ, *n* = 90)	N (r^2 = 0.04*)	-	-	(Koch and others, 1995) ***c*** on fig. 1
Unit not reported	Fossil Aragonite (Unionacea)	19.6±0.8‰* (1σ, *n* = 272)	N (r^2 < 0.001*)	-	-	(Dettman and Lohmann, 2000) ***c*** on fig. 1
Fort Union and Willwood Formations	Fossil Biogenic Hydroxyapatite	20.2±1.3‰* (1σ, *n* = 49)	N (negative correlation, r^2 = 0.02*)	-	-	(Fricke and others, 1998) ***c*** on fig. 1
Powder River Basin (WY) Unit not reported	Fossil Aragonite (Unionacea)	16.6±4.4‰ (1σ, *n* = 110)	N (r^2 < 0.001*)	-	-	(Dettman and Lohmann, 2000) ***d*** on fig. 1
Greater Green River Basin (WY) Luman Tongue (Green River Formation), ***Tglu***	Fossil Aragonite (Unionacea)	23.1±1.8‰* (1σ, *n* = 59)	M (r^2 = 0.45*)	-	-	(Dettman and Lohmann, 2000) ***e*** on fig. 1
Luman Tongue (Green River Formation), ***Tglu***	Fossil Aragonite (Unionacea)	22.6±0.7‰* (1σ, *n* = 13)	-	-	-	(Morrill and Koch, 2002) ***e, f*** on fig. 1
Uinta Basin (UT) North Horn Formation, Flagstaff Member (Green River Formation), ***Tgf***, Colton Formation, ***Tc***	Lacustrine Precipitate, Calcite Cement	18.9±1.9‰ (1σ, *n* = 93)	N (r^2 = 0.05)	0.75±0.5 (1σ, *n* = 79)	0.7099±0.0002 (2σ, *n* = 3)	(Davis and others, 2008) ***g*** on fig. 1
Piceance Creek Basin (CO) Cow Ridge, ***Tgc*** and Anvil Points, ***Tga*** Members (Green River Formation)	Lacustrine Precipitate	20.3±3.9‰ (1σ, *n* = 42)	N (r^2 = 0.02)	1.3±0.8 (1σ, *n* = 33)	0.7105±0.0008 (2σ, *n* = 11)	(this study) **1** on fig. 1

TABLE 1
(continued)

Basin (State) Sampled Units ***Abbr. on fig. 2***	Proxy Carbonate	Mean $\delta^{18}O_{calcite}$ (V-SMOW)	$\delta^{18}O_{calcite}$-$\delta^{13}C_{calcite}$ Covariance	Mean Sr/Ca (mmol/mol)	Mean $^{87}Sr/^{86}Sr$	Reference(s) and Locations on fig. 1
Late Cretaceous - earliest Eocene (~70-52 Ma)						
Axhandle Basin (UT)	Lacustrine Precipitate, Paleosol	20.7±2.3‰ (1σ, *n* = 68)	N ($r^2 < 0.001$)	-	-	(Chamberlain, unpublished) ***h*** on fig. 1
North Horn and Flagstaff Formations						
North Horn Formation	Paleosol	22.0±1.2‰ (1σ, *n* = 262)	N ($r^2 = 0.03$)	-	-	(Bowen and Bowen, 2008) ***h*** on fig. 1
Flagstaff Basin (UT)	Lacustrine Precipitate (micrite)	21.7±0.9‰ (1σ, *n* = 48)	W ($r^2 = 0.11$)	-	-	(Bowen and others, 2008) ***i*** on fig. 1
Flagstaff Formation, ***Tf***	Lacustrine Precipitate	-	-	<0.1* (1σ, *n* = 38)	0.7100±0.0003 (2σ, *n* = 38)	(Gierlowski-Kordesch and others, 2008) ***i*** on fig. 1
Flagstaff Formation, ***Tf***	Lacustrine Precipitate	22.6±2.8‰ (1σ, *n* = 115)	M ($r^2 = 0.36$*)	-	-	(Weber, 1964) ***i*** on fig. 1
Early Eocene (~52-48.6 Ma)						
Sage Creek Basin (MT/ID)	Paleosol	23.2±1.8‰* (1σ, *n* = 9)	W ($r^2 = 0.26$*)	-	-	(Kent-Corson and others, 2006) ***a*** on fig. 1
Lower Sage Creek Formation						
Greater Green River Basin (WY)	Fossil Aragonite (Unionacea)	25.0‰ (1σ, *n* = 3)	-	-	-	(Morrill and Koch, 2002) ***j*** on fig. 1
Tipton Member (Green River Formation), ***Tgt***						
Wilkins Peak, ***Tgw*** and lower Laney, ***Tgl*** Members (Green River Formation)	Lacustrine Precipitate	28.3±0.7‰ (1σ and *n* not reported)	-	-	-	(Norris and others, 1996) ***k*** on fig. 1
†Laney Member (Green River Formation), ***Tgl***	Fossil Aragonite (Unionacea)	23.3±1.9‰ (1σ, *n* = 14)	-	-	-	(Morrill and Koch, 2002) ***l*** on fig. 1
†Laney Member (Green River Formation), ***Tgl***	Lacustrine Precipitate	-	-	-	0.7125±0.0006 (2σ, *n* = 22)	(Rhodes and others, 2002) ***m*** on fig. 1
Lower LaClede Bed, ***-l-***, Wilkins Peak Member (Green River Formation), ***Tgw***	Lacustrine Precipitate	27.0±1.9‰ (1σ, *n* = 122)	-	-	0.7123±0.0004 (2σ, *n* not reported)	(Carroll and others, 2008) ***m*** on fig. 1

TABLE 1
(continued)

Basin (State) Sampled Units *Abbr. on fig. 2*	Proxy Carbonate	Mean $\delta^{18}O_{calcite}$ (V-SMOW)	$\delta^{18}O_{calcite}$-$\delta^{13}C_{calcite}$ Covariance	Mean Sr/Ca (mmol/mol)	Mean $^{87}Sr/^{86}Sr$	Reference(s) and Locations on fig. 1
Early Eocene (~52-48.6 Ma						
Uinta Basin (UT) Lower Main Body (Green River Formation), ***Tgmb***	Lacustrine Precipitate	24.9±3.5‰ (1σ, *n* = 47)	S (r^2 = 0.61)	1.4±0.5 (1σ, *n* = 22)	0.7116±0.0010 (2σ, *n* = 7)	(Davis and others, 2008; Davis and others, 2009) ***n*** on fig. 1
Piceance Creek Basin (CO) Garden Gulch, ***Tgg***, Douglas Creek, ***Tgd,*** and Lower Parachute Creek, ***Tgp,*** Members (Green River Formation)	Lacustrine Precipitate	27.9±3.9‰ (1σ, *n* = 54)	S (r^2 = 0.61)	2.7±0.8 (1σ, *n* = 50)	0.7113±0.0005 (2σ, *n* = 9)	(this study) **2, 3** on fig. 1
Flagstaff Basin (UT) Lower Green River Formation, ***Tg***	Lacustrine Precipitate	26.7±2.0‰ (1σ, *n* =9)	S (r^2 = 0.65)	2.8±0.1 (1σ, *n* = 3)	-	(Davis and others, 2009) ***o*** on fig. 1
Early Middle Eocene (48.6-46 Ma)						
Sage Creek Basin (MT/ID) Upper Sage Creek Formation	Paleosol	12.7±0.5‰* (1σ, *n* = 10)	N (r^2 = 0.02*)	-	-	(Kent-Corson and others, 2006) ***a*** on fig. 1
Greater Green River Basin (WY) Upper LaClede Bed, (Green River Formation), ***-l-***	Lacustrine Precipitate	22.0±2.5‰ (1σ, *n* = 72)	-	-	0.7116±0.0003 (2σ, *n* = not reported)	(Carroll and others, 2008) ***m*** on fig. 1
Uinta Basin (UT) Upper Main Body (Green River Formation), ***Tgmb***	Lacustrine Precipitate	26.7±1.1‰ (1σ, *n* = 14)	M (r^2 = 0.33)	2.4±0.3 (1σ, *n* = 8)	0.7114±0.0024 (2σ, *n* = 2)	(Davis and others, 2008; Davis and others, 2009) ***n*** on fig. 1
Piceance Creek Basin (CO) Upper Parachute Creek Member (Green River Formation), ***Tgp***, Uinta Formation, ***Tu***, Tongues of Green River Formation	Lacustrine Precipitate	22.3±4.4‰ (1σ, *n* = 103)	S (r^2 = 0.61)	2.7±0.5 (1σ, *n* = 20)	0.7098±0.0024 (2σ, *n* = 10)	(this study) **3** on fig. 1
Flagstaff Basin (UT) Upper Green River Formation, ***Tg***	Lacustrine Precipitate	27.4±2.5‰ (1σ, *n* =19)	N (r^2 = 0.09)	1.8±0.7 (1σ, *n* = 6)	-	(Davis and others, 2009) ***o*** on fig. 1

TABLE 1
(continued)

Basin (State) Sampled Units *Abbr. on fig. 2*	Proxy Carbonate	Mean $\delta^{18}O_{calcite}$ (V-SMOW)	$\delta^{18}O_{calcite}$-$\delta^{13}C_{calcite}$ Covariance	Mean Sr/Ca (mmol/mol)	Mean $^{87}Sr/^{86}Sr$	Reference(s) and Locations on fig. 1
Late Middle Eocene (~46-37.2 Ma)						
Sage Creek Basin (MT/ID) Dell, Spring Hollow, and Antelope Lakes Formations	Calcite Cement, Paleosol, Lacustrine Precipitate	13.6±1.6‰* (1σ, *n* = 57)	N (negative correlation, $r^2 = 0.12$*)	-	-	(Kent-Corson and others, 2006) ***a*** on fig. 1
Elko Basin (NV) Upper Elko Formation	Lacustrine Precipitate	22.4±2.5‰ (1σ, *n* = 19)	M ($r^2 = 0.47$)	2.9±3.6 (1σ, *n* = 12)	-	(Horton and others, 2004) ***p*** on fig. 1
Ibapah Basin (NV/UT) White Sage Formation	Lacustrine Precipitate	19.8±2.2‰ (1σ, *n* = 21)	W ($r^2 = 0.20$)	-	-	(Davis, unpublished) ***q*** on fig. 1
Uinta Basin (UT) Saline Facies, ***Tgs***, Sandstone and Limestone Facies, ***Tgsl*** (Green River Formation)	Lacustrine Precipitate	27.0±3.1‰ (1σ, *n* = 61)	M ($r^2 = 0.45$)	2.9±0.9 (1σ, *n* = 28)	0.7100±0.0006 (2σ, *n* = 13)	(Davis and others, 2008; Davis and others, 2009) ***r*** on fig. 1
Flagstaff Basin (UT) Crazy Hollow, ***Tcr***, and Bald Knoll Formations	Calcite Cement	17.0±2.6‰ (1σ, *n* =29)	N ($r^2 = 0.06$)	0.5±0.1 (1σ, *n* = 4)	-	(Davis and others, 2009) ***s*** on fig. 1
Claron Basin (UT) Claron Formation	Lacustrine Precipitate	20.3±2.2‰ (1σ, *n* =32)	N ($r^2 = 0.07$)	-	-	(Davis and others, 2009) ***t*** on fig. 1
Galisteo Basin (NM) Galisteo Formation	Lacustrine Precipitate, Calcite Cement	21.9±1.2‰ (1σ, *n* =36)	N ($r^2 < 0.001$)	-	-	(Davis, unpublished) ***u*** on fig. 1
Late Eocene – Early Oligocene (37.2-28.4 Ma)						
Sage Creek Basin (MT/ID) Upper Antelope Lakes and Cook Ranch Formations	Calcite Cement, Paleosol	14.3±0.9‰* (1σ, *n* = 27)	N (negative correlation, $r^2 = 0.26$*)	-	-	(Kent-Corson and others, 2006) ***a*** on fig. 1
Elko Basin (NV) Indian Wells Formation	Lacustrine Precipitate	13.9±1.5‰ (1σ, *n* = 3)	-	0.5±0.5 (1σ, *n* = 2)	-	(Horton and others, 2004) ***p*** on fig. 1
Uinta Basin (UT) Duchesne River Formation, ***Tdr***	Calcite Cement	17.7±3.5‰ (1σ, *n* = 40)	N ($r^2 = 0.09$)	0.4±0.2 (1σ, *n* = 7)	-	(Davis and others, 2009) ***v*** on fig. 1

TABLE 1
(continued)

Basin (State) Sampled Units *Abbr. on fig. 2*	Proxy Carbonate	Mean $\delta^{18}O_{calcite}$ (V-SMOW)	$\delta^{18}O_{calcite}$-$\delta^{13}C_{calcite}$ Covariance	Mean Sr/Ca (mmol/mol)	Mean $^{87}Sr/^{86}Sr$	Reference(s) and Locations on fig. 1
Late Eocene – Early Oligocene (37.2-28.4 Ma)						
Flagstaff Basin (UT) Dipping Vat Formation	Calcite Cement	15.4±0.4‰ (1σ, *n* =11)	N (r^2 = 0.01)	0.4±0.02 (1σ, *n* = 3)	-	(Davis and others, 2009) ***s*** on fig. 1
Claron Basin (UT) Brian Head Formation	Lacustrine Precipitate, Calcite Cement	14.8±1.4‰ (1σ, *n* =34)	N (negative correlation, r^2 = 0.10)	0.3±0.1 (1σ, *n* = 9)	-	(Davis and others, 2009) ***w*** on fig. 1
Galisteo Basin (NM) Espinaso Formation	Calcite Cement	21.8±0.9‰ (1σ, *n* =16)	W (r^2 = 0.27)	-	-	(Davis, unpublished) ***u*** on fig. 1

*Calculated based on published data.

†Note that the Luman Tongue of the Green River Formation in the Greater Green River Basin spans a major hydrologic shift (see, Carroll and others, 2008), and the precise stratigraphic location of these samples is not reported. Covariance reported as N (none), W (weak), M (moderate), or S (strong), evaluated by Pearson product-moment coefficient. Dashes indicate analyses not performed or data not reported.

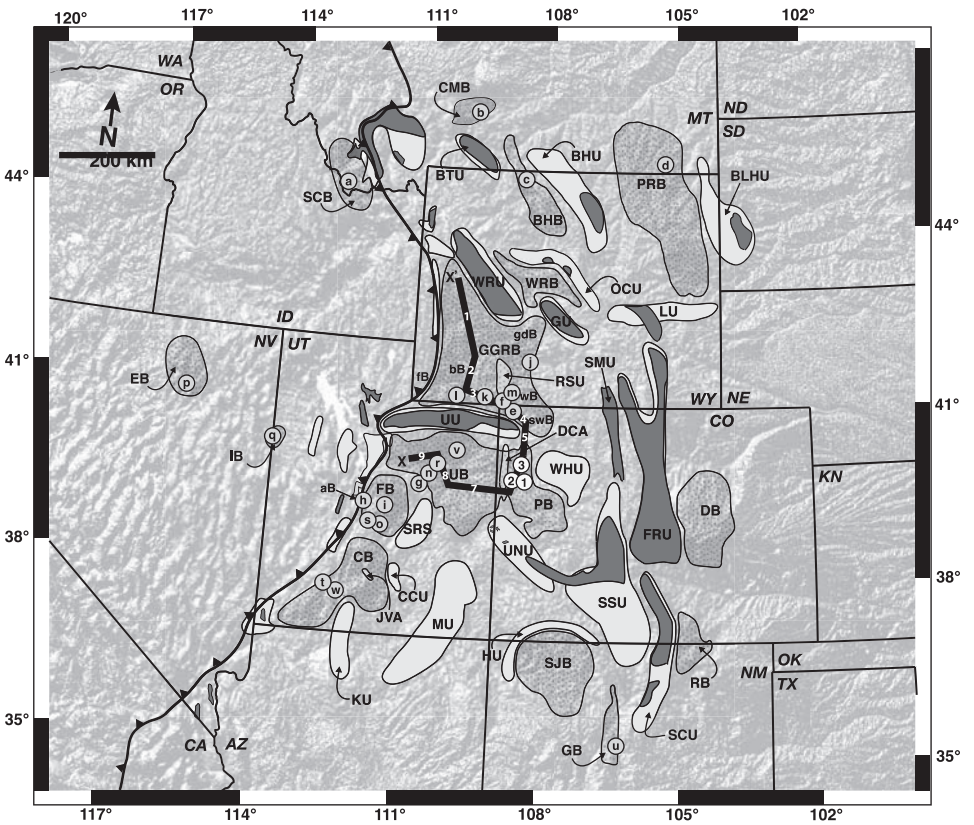

Fig. 1. Digital elevation map of modern topography of the central North American Cordillera (UTM Zone 13N) with Paleogene structures superimposed (location and extent of structures after Dickinson and others, 1986, 1988). Basins are lightly stippled and uplifts are shaded gray. Darker shading indicates exposed Precambrian rock where $^{87}Sr/^{86}Sr$ ratios can be in excess of 1.0, while lighter shading indicates exposures of Paleozoic and Mesozoic rocks with $^{87}Sr/^{86}Sr$ ratios <0.710 [extent of basins and uplifts after Dickinson and others (1988), Precambrian exposures from Foster and others (2006), and isotopic composition from sources cited in text and listed in table A6 of Appendix A]. Bold line shows the Sevier fold-and-thrust belt, teeth on the upper plate. Cross-section chronostratigraphy along X-X′ shown in figure 2. Major structures are labeled as follows: BHB, Bighorn Basin; BHU, Bighorn Uplift; BLHU, Black Hills Uplift; BTU, Beartooth Uplift; CB, Claron Basin; CCU, Circle Cliffs Uplift; CMB, Crazy Mountain Basin; CMU, Crazy Mountain Uplift; DB, Denver Basin; DCA, Douglas Creek Arch; EB, Elko Basin; FB, Flagstaff Basin (sub-basin: aB, Axhandle Basin); FRU, Front Range Uplift; GB, Galisteo Basin; GGRB, Greater Green River Basin (sub-basins: bB, Bridger Basin; gdB, Great Divide Basin; wB, Washakie Basin; swB, Sand Wash Basin); GU, Granite Mountain Uplift; HM, Hogback Monocline; IB, Ibapah Basin; JVA, Johns Valley and Upper Valley Anticlines; KU, Kaibab Uplift; LU, Laramie Uplift; MU, Monument Upwarp; OCU, Owl Creek Uplift; PB, Piceance Creek Basin; PRB, Powder River Basin; RB, Raton Basin; RSU, Rock Springs Uplift; SCB, Sage Creek Basin; SCU, Sangre de Cristo Uplift; SJB, San Juan Basin; SMU, Sierra Madre Uplift; SSU, Sawatch-San Luis Uplift; SRS, San Rafael Swell; UB, Uinta Basin; UNU, Uncompahgre Uplift; UU, Uinta Uplift; WHU, White River Uplift; WRB, Wind River Basin; WRU, Wind River Uplift. Numbered and lettered circles correspond to sampling localities of this study and previous studies, respectively, as listed in table 1.

Samples of lacustrine carbonate are particularly useful isotopic proxies of paleoenvironment because of the continuity of lake deposits and their sensitivity to climatic and tectonic processes (Carroll and Bohacs, 1999; Bohacs and others, 2000). We analyzed lacustrine carbonate samples from the Piceance Creek Basin of northwest Colorado (fig. 1) for oxygen, carbon, and strontium isotope composition, as well as calcium and strontium concentrations.

GEOLOGIC SETTING AND STRATIGRAPHY

Evidence of each phase in the development of Cordilleran drainage patterns is preserved by lacustrine units in the intraforeland Piceance Creek Basin of northwest Colorado (fig. 1). Four Laramide uplifts bound the Piceance Creek Basin: the White River Uplift to the northeast, the Uinta Uplift to the northwest, the Uncompahgre Uplift to the southwest, and the Sawatch Uplift to the southeast (fig. 1). Units sampled for isotopic analyses belong to two formations:

Green River Formation

Lacustrine deposits in the Piceance Creek Basin are part of the carbonate-rich Green River Formation (Hayden, 1869; Bradley, 1931). Though the lake in the Piceance Creek Basin has often been referred to as Lake Uinta by earlier workers acknowledging its merger with the lake in the Uinta Basin during a lake highstand at 48.6 Ma (Smith and others, 2008a), it is herein distinguished as the Piceance lake. Lacustrine deposition first expanded across the Piceance Creek Basin in the Early Eocene as recorded by the shallow lacustrine, paludal, and fluvial beds of the Cow Ridge Member (***Tgc***, fig. 2) which occur in the basin center isolated between fluvial redbeds of the main body and an overlying tongue of the DeBeque (Wasatch) Formation (***Td***, fig. 2, Donnell, 1969; Johnson, 1984; Kihm, ms, 1984). At ~52 Ma, the freshwater Piceance lake returned and expanded widely, evidenced by the fossiliferous Long Point bed (***lp***, fig. 2, denoted by cross symbols at ~100m in fig. 3) (Johnson, 1984). This Long Point transgression marks the base of three roughly time-equivalent facies: The Anvil Points and Douglas Creek Members (***Tga*** and ***Tgd***, respectively, fig. 2) are arenaceous, nearshore lake facies deposited along the eastern and western basin margins, respectively. The Garden Gulch Member (***Tgg***, fig. 2) is made up of argillaceous, profundal deposits in the basin center (Hail, 1992). Overlying these older members in the Piceance Creek Basin are marl, oil shale (kerogen-rich marl), and evaporite deposits belonging to the Parachute Creek Member (***Tgp***, fig. 2), which includes the well-known Mahogany Zone (***m***, fig. 2) of rich oil shale deposited during the lake highstand at 48.6 Ma (Brobst and Tucker, 1973; Smith and others, 2008a).

Uinta Formation

In the Middle Eocene, at ~48 Ma, sandy, volcaniclastic sediments assigned to the Uinta Formation (***Tu***, fig. 2) prograded south into the Piceance Creek Basin (Surdam and Stanley, 1980; Smith and others, 2008a). Strata of the Uinta Formation intertongue with the Parachute Creek Member of the Green River Formation over several hundred meters (Hail, 1987). Although the tongues of the Uinta Formation have not been named, a number of the regressing lacustrine marls are useful stratigraphic markers that have been formally named tongues of the Green River Formation, giving them status as formation members (Duncan and others, 1974; O'Sullivan, 1975; Hail, 1977). Named tongues sampled in this study include (from oldest to youngest) the Yellow Creek, Dry Fork, Black Sulphur, Coughs Creek, and Stewart Gulch Tongues. By ~47 Ma, the encroaching Uinta Formation overwhelmed the lake, and fluvial deposits of the Uinta Formation completely filled the basin shortly thereafter.

ISOTOPIC APPROACHES TO BASIN EVOLUTION

In order to characterize the paleohydrology of the Piceance Creek Basin, we assembled O isotopic profiles of exposed lacustrine sediments of Paleogene age. C isotopes and Sr/Ca ratios of carbonate were then used to evaluate the role of evaporation on the O isotope record. Evaporative effects can be assessed by the degree of covariance of $\delta^{13}C$-$\delta^{18}O$ values and Sr/Ca ratios in carbonate samples. If evaporation is relatively high $\delta^{13}C$ and $\delta^{18}O$ values will covary because hydrologically closed lakes have long residence times allowing preferential outgassing of ^{12}C-rich CO_2

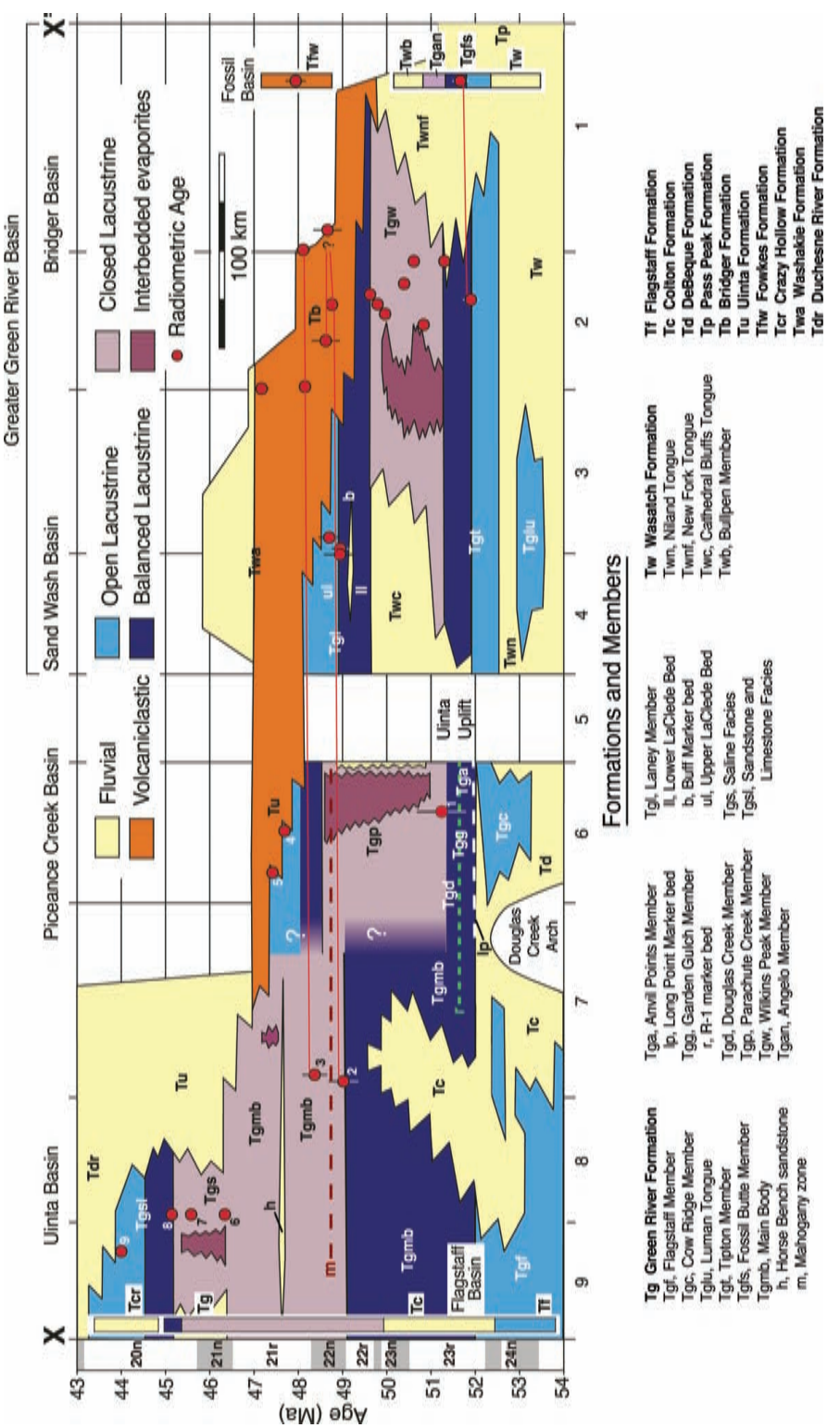

Fig. 2. Chronostratigraphy of the Green River Lake basins, after Smith and others, 2008a. Numbered radiometric ages are those used to constrain samples presented in figure 3 and are detailed in table A3 and figure A1. All other ages are detailed in Smith and others, 2008a. Location of cross-section shown on figure 1.

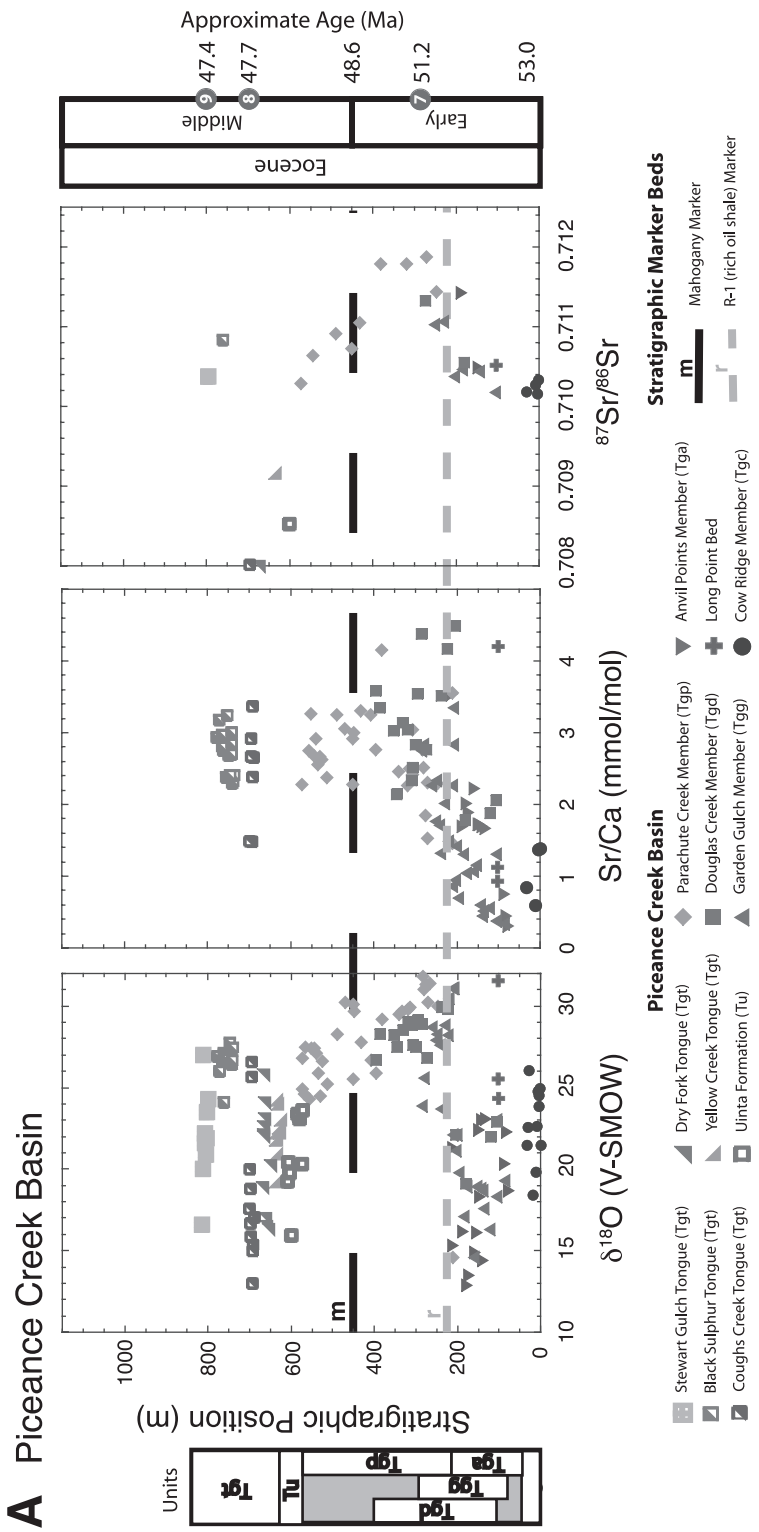

Fig. 3. (A) Panel A shows isotopic and elemental data from the Piceance Creek Basin presented in this study.

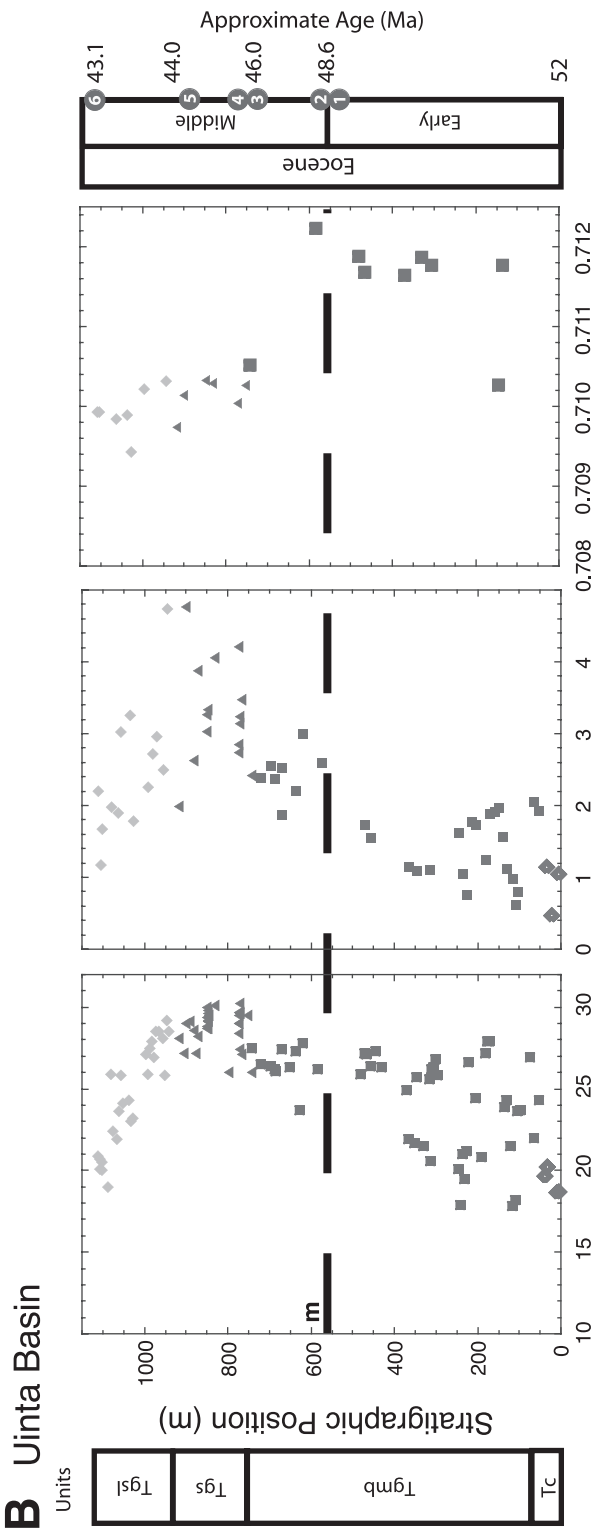

Fig. 3. (B) Panel B shows similar data from the Uinta Basin presented in Davis and others (2008) and Davis and others (2009).

accompanied by evaporative enrichment of ^{18}O (Talbot and Kelts, 1990). Sr/Ca ratios will also be high in evaporative lakes as the partitioning of Sr between host water and authigenic carbonate is proportional to the ratio of Sr^{2+} to Ca^{2+} in the water (Müller and others, 1972). In hydrologically closed lakes, Sr^{2+} is not flushed from the lake, and as Ca^{2+} is taken up by precipitating $CaCO_3$, Sr^{2+} is progressively concentrated and incorporated into authigenic carbonates (Eugster and Kelts, 1983). Carbon isotopes can also be used to assess the role of diagenesis on the O isotope composition of carbonates. Late stage diagenesis often results in relatively low O isotope values (Morrill and Koch, 2002) as a result of equilibration of carbonate with meteoric waters at high temperatures. Conversely, $\delta^{13}C$ values of early diagenetic carbonates may be affected by bacterially mediated redox reactions, while $\delta^{18}O$ values of such diagenetic phases continue to record the isotopic composition of sediment pore waters (Talbot and Kelts, 1990), resulting in non-covariance of C and O isotopes in lacustrine sediments (Talbot, 1990; Talbot and Kelts, 1990).

We used Sr isotopes of authigenic carbonate to determine whether the source of the water supplied to these lakes has changed over time. The ratio of $^{87}Sr/^{86}Sr$ in lacustrine carbonates has been recognized as a valuable method for reconstructing lake paleohydrology (Rhodes and others, 2002; Hart and others, 2004; Davis and others, 2008; Gierlowski-Kordesch and others, 2008). Mass-dependent fractionation of $^{87}Sr/^{86}Sr$ ratios is insignificant and corrected for during analysis, meaning that authigenic minerals record the Sr isotope composition of lake water at the time of their precipitation. The $^{87}Sr/^{86}Sr$ ratio of waters is controlled by contact with rocks in the drainage area, and especially more soluble carbonate rocks (Palmer and Edmond, 1992; Jacobsen and Blum, 2000). In the Paleogene Cordillera, basement uplifts in many cases exposed Precambrian crystalline rocks with high $^{87}Sr/^{86}Sr$ ratios (commonly >1.0) which were in turn flanked by Paleozoic and Mesozoic carbonates and siliclastics with much lower $^{87}Sr/^{86}Sr$ ratios (≤ 0.710, see fig. 1). Such heterogeneities in the Sr isotope ratios of lithologies present in the drainage basin are homogenized in lake water so that when carbonate precipitates, its Sr isotope composition reflects the weighted average of isotopically distinct inflows to the lake.

Although differential weathering of minerals can cause the concentration of radiogenic strontium in solid weathering products (for example, clays), research indicates that this effect is generally quite small, and that the isotopic composition and abundance of source rocks effectively control the $^{87}Sr/^{86}Sr$ ratio of strontium in solution (Brass, 1975). Furthermore, it has been demonstrated that the $^{87}Sr/^{86}Sr$ ratios of soil carbonate (also a product of weathering reactions) are similar to stratigraphically equivalent fish and mollusk fossils (which reflect surface water) (Quade and others, 1997).

Finally, in order to better characterize the maximum depositional age of lacustrine deposits and also examine the potential of detrital zircon data as an indicator of provenance, we also sampled tuffaceous lake beds where they occurred.

MATERIALS AND METHODS

Sample Collection

We collected authigenic carbonate samples from 11 stratigraphic sections of Paleogene lacustrine facies in 3 localities of the Piceance Creek Basin (fig. 1 and tables A1 and A2) and analyzed their O and C isotope composition ($n=186$), Sr isotope composition ($n=30$) and Sr/Ca ratios ($n=114$). Samples were predominantly limestone, although carbonate was variably argillaceous (that is, marls or "oil-shales") and, less commonly, arenaceous. Isotopic analyses were performed only on micritic samples with no evidence of recrystallization. Where present, we

also collected tuffaceous arenites for U-Pb geochronologic analyses of zircon. Detailed information and key references of each sampled section are included in Appendix A (fig. A1 and tables A1, A3 and A4).

U-Pb Geochronologic Analyses of Zircon

U-Pb geochronological analyses of 7 tuffaceous samples from the Piceance Creek Basin as well as 2 samples from the Uinta Basin (details in Appendix A) were carried out using both the Stanford/U.S. Geological Survey (USGS) Sensitive High-Resolution Ion Microprobe (SHRIMP-RG) and a laser ablation multicollector inductively coupled plasma mass spectrometer (LA-MC-ICPMS) at the University of Arizona.

For ion microprobe analyses, zircon separates were mounted in epoxy, polished, imaged by cathodoluminescence on a JEOL 5600LLV scanning electron microscope, and gold coated. Analytical spots 25 to 30 μm in diameter on the zircon grains were sputtered using an ~10 nA primary beam of $^{16}O_2^-$ ions. After rastering the spot for 90 s to remove surficial contaminants, the secondary ion beam was repeatedly scanned for $^{90}Zr_2{}^{16}O$, ^{204}Pb, ^{206}Pb, ^{207}Pb, ^{238}U, $^{232}Th^{16}O$ and $^{238}U^{16}O$. Zircon standard R33 (419 Ma from monzodiorite, Braintree Complex, Vermont) was used as a concentration standard. Concentration measurements were corrected and reduced using SQUID software (Version 1.02; Ludwig, 2001).

Samples failing to yield a coherent age group were assumed detrital, and were further analyzed by LA-MC-ICPMS using methods described by Gehrels and others (2008). Gold coat was quantitatively removed from microprobe zircon mounts by immersion in a saturated solution of potassium iodide (KI) for an hour at 80 to 90 °C. Mounts were then placed in an LA-MC-ICMP and ablated with a New Wave DUV193 Excimer laser (operating at a wavelength of 193 nm) using a spot diameter of 25 or 35 μm, depending on zircon grain size. Entrained in helium gas, ablated material was carried into the plasma source of a Micromass Isoprobe where U, Th, and Pb isotopes were measured simultaneously. All measurements were made in static mode, using Faraday detectors for ^{238}U, ^{232}Th, $^{208-206}Pb$, and an ion-counting channel for ^{204}Pb. Each analysis consisted of one 12 s integration on peaks with the laser off (for backgrounds), twelve 1 s integrations with the laser firing, and a 30 s delay to purge the previous sample and prepare for the next analysis. A Sri Lanka zircon standard (563.5 ± 3.2 Ma, 2σ) was used as a concentration standard (Gehrels, unpublished data).

Isotopic and Elemental Analyses of Carbonate

Sr, C and O isotope values of the carbonate samples were measured in the mass spectrometry laboratories at Stanford University. For Sr isotope analysis, Sr was extracted from bulk carbonate samples using 1M acetic acid (CH_3COOH) to ensure that potentially existing silicate minerals were not dissolved. The solution was centrifuged, transferred into clean Teflon vials, and evaporated. The evaporate was then treated with concentrated HNO_3 to oxidize traces of organic material and facilitate re-dissolution of the sample with 2.5N HCl. Aliquots of each sample were loaded onto cation exchange columns using Biorad AG50x8 (200-400 mesh) resin, and eluted with 2.5N HCl. All reagents were distilled. Purified Sr fractions were measured on a Finnigan MAT262 Thermal Ionization Mass Spectrometer using Ta single filaments and 0.25N H_3PO_4. Ratios of ^{88}Sr, ^{87}Sr, ^{86}Sr, and ^{84}Sr were scanned at least 80 times per sample. $^{87}Sr/^{86}Sr$ ratios were corrected for instrumental fractionation using the natural $^{88}Sr/^{86}Sr$ ratio of 8.375209. Routine standard measurements yield a $^{87}Sr/^{86}Sr$ ratio of 0.71033 ± 0.00001 (2σ: n = 64) for the NBS-987 Sr standard. The analytical precision is 0.003 percent or less. Blanks were less than 0.5 ng Sr.

O and C isotope analyses of carbonate were determined using the phosphoric acid digestion method of McCrea (1950) coupled on-line with a gas ratio mass spectrometer. Using this method, between 300 to 500 μg of sample material was drilled from each sample, sealed in reaction vials, flushed with helium and reacted with pure H_3PO_4 at 72°C. Evolved CO_2 in the vial headspace was then sampled using a Finnigan GasBench II, connected to a Finnigan MAT Delta^{Plus} XL mass spectrometer. Replicate analyses of NBS-19 (limestone) and laboratory standards yielded a precision ± 0.2 permil or better for both $\delta^{18}O$ and $\delta^{13}C$.

Sr/Ca ratios of carbonate were measured using an inductively coupled plasma-atomic emission spectrometer (ICP-AES) at Stanford University. Samples were first digested in concentrated HNO_3, diluted with Mega-Pure water and filtered. Total dissolved Ca^{2+} and Sr^{2+} were measured at wavelengths 317.9 and 407 nm, respectively (for example, de Villiers and others, 2002). Replicate analyses of prepared blanks and standard solutions of varying known concentrations indicated detection limits for Ca^{2+} and Sr^{2+} of 6 and 0.1 μg L^{-1}, respectively, and precision better than 15 μg L^{-1} for Ca^{2+} and 1 μg L^{-1} for Sr^{2+} (that is, better than 0.1 mmol/mol for Sr/Ca ratios).

RESULTS

Analyses of carbonate from the Piceance Creek Basin show first order trends that are here presented as three stratigraphic/temporal intervals (table 1).

U-Pb Geochronological Analyses

Of the 7 Piceance samples analyzed, 2 from Tongues of the Green River Formation yielded coherent age groups that we interpret as maximum depositional ages (numbered 8 and 9 in figs. 2 and 3A; data and diagrams in Appendix A). The other 5 Piceance samples and 2 additional samples from the Uinta Basin contained zircons of variable ages that do not help to constrain depositional age, but which are useful as indicators of provenance (fig. 4). Such detrital samples from older units (DeBeque Formation and Anvil Points in the Piceance Basin and Flagstaff Member and Colton Formation in the Uinta Basin) contain few zircons older than 800 Ma. Samples from younger units (Garden Gulch Member, Kimball Mountain Tuff Bed, and Coughs Creek Tongue in the Piceance Basin) increasingly contain Grenville- (1315−1000 Ma) and Paleoproterozoic-age (1615−1800 Ma) grains.

Prior to ~52 Ma

Samples deposited between the formation of the Piceance lake (fig. 2, ***Tgc***) and ~52 Ma (fig. 2, including parts or all of ***Tga***, ***Tgd***, and ***Tgg***) give a mean $\delta^{18}O_{calcite}$ value of 20.3 permil (fig. 3A), a mean Sr/Ca ratio of 1.3 mmol/mol (figs. 3A and 5), and a mean $^{87}Sr/^{86}Sr$ ratio of 0.7105 (fig. 3A, $2\sigma = 0.0008$, n = 11). $\delta^{18}O_{calcite}$ and $\delta^{13}C_{calcite}$ do not covary in samples from this period ($r^2 = 0.02$, fig. 6, panels ***Tgc*** and ***Tga***). Here as well as in all other units, samples from similar stratigraphic intervals yield similar Sr isotope ratios irrespective of mineralogy, texture, O isotope composition and Sr/Ca ratio.

Between ~52 and 48.6 Ma

Beginning at ~52 Ma (as constrained by radiometric age of the overlying Yellow Tuff, #1 in figs. 2 and 3), the mean $\delta^{18}O_{calcite}$ value of samples increased by ~7.6 permil from 20.3 permil to 27.9 permil (fig. 3A). During the same interval, the mean Sr/Ca ratio increases to 2.7 mmol/mol (figs. 3A and 5), and $\delta^{18}O_{calcite}$-$\delta^{13}C_{calcite}$ values in deposited units display strong covariance ($r^2 = 0.61$, fig. 6, panels ***Tgd***, ***Tgg***, ***Tgp***). Coincident with these shifts, $^{87}Sr/^{86}Sr$ ratios increase steadily to a maximum of 0.7119 (fig. 3A, mean = 0.7113, $1\sigma = 0.0005$, n = 9).

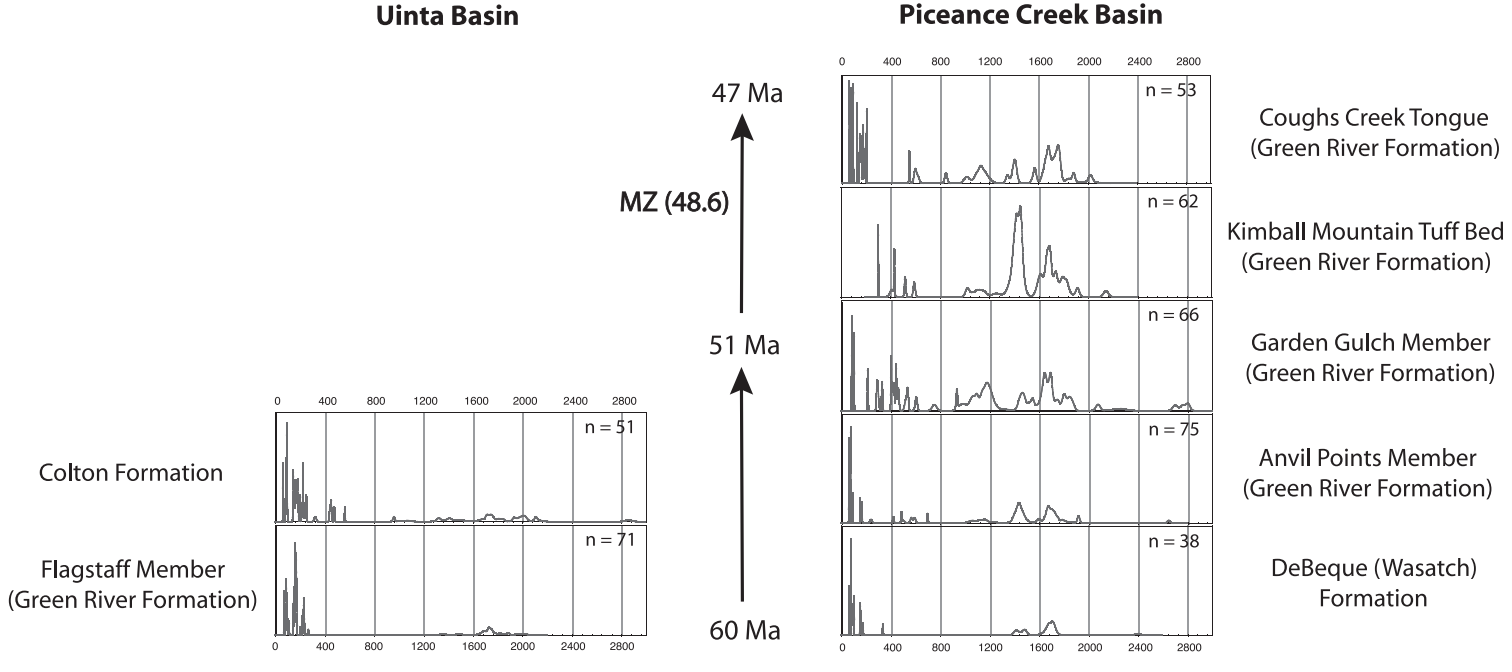

Fig. 4. Probability distributions of zircon U-Pb ages in detrital samples from the Uinta and Piceance Creek and Basins.

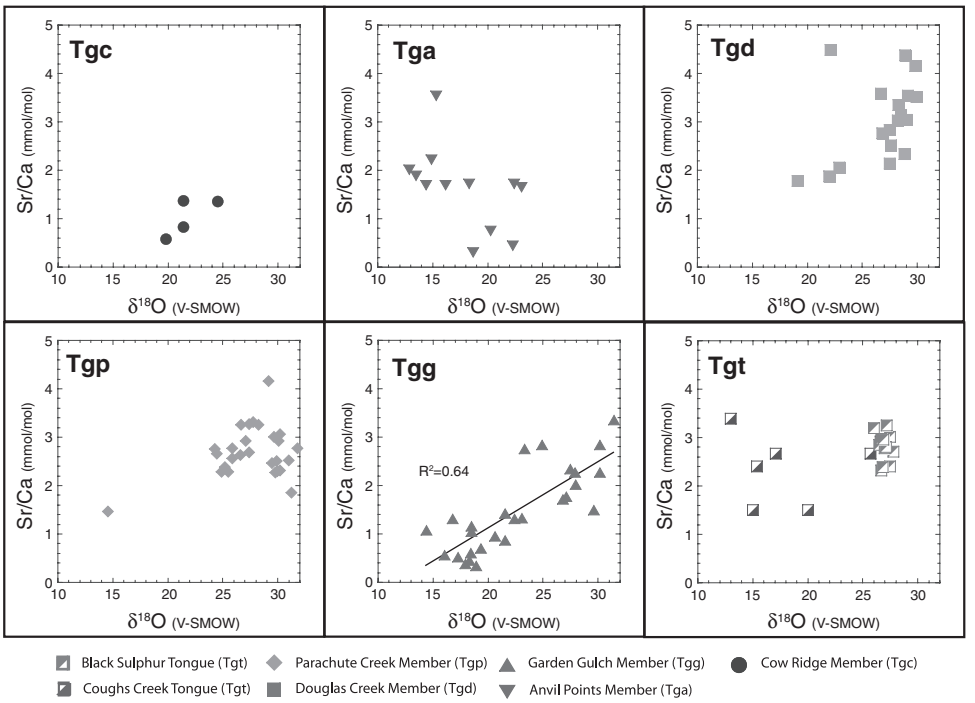

Fig. 5. Relationship of $\delta^{18}O_{calcite}$ and Sr/Ca ratios in sampled units of the Piceance Creek Basin.

Between 48.6 and ~47 Ma

Beginning at 48.6 Ma, $\delta^{18}O_{calcite}$ values decrease in two recognizable stages, first by ~1.2 permil from 27.9 permil to 26.7 permil in the upper Parachute Creek Member (fig. 3A, ***Tgp***) and then continuing more sharply at ~48 Ma to a mean value of 21.5 permil in the Uinta Formation and tongues of the Green River Formation (fig. 3A, ***Tu*** and ***Tgt***). The two stages are also delineated by $^{87}Sr/^{86}Sr$ ratios, which first decrease to a mean of 0.7106 in the upper Parachute Creek Member (fig. 3A, $2\sigma = 0.0005$, $n = 4$) and then drop as low as 0.7080 in the Uinta Formation and Tongues of the Green River Formation (fig. 3A, mean = 0.7092, $2\sigma = 0.0024$, $n = 6$). Sr/Ca ratios in samples of the upper Parachute Creek Member (the first stage) maintain the same mean value, 2.7 mmol/mol, as samples from the interval between ~52 and 48.6 Ma with little variability (figs. 3A and 5, $1\sigma = 0.3$, $n = 13$). Sr/Ca ratios remain high in samples of the Tongues of the Green River Formation deposited during this second stage (mean = 2.7 mmol/mol, figs. 3A and 5, $1\sigma = 0.5$, $n = 20$) and $\delta^{18}O_{calcite}$-$\delta^{13}C_{calcite}$ values from the combined Uinta Formation and Tongues continue to display strong covariance ($r^2 = 0.61$, fig. 6, panel ***Tu-Tgt***).

Discussion

The isotopic and elemental results from the Piceance Creek Basin are here interpreted in the context of results from previous studies of the central North American Cordillera (table 1)—especially recent work in the neighboring Greater Green River (Rhodes and others, 2002; Carroll and others, 2008) and Uinta (Davis and others, 2008, 2009) Basins which contained other large lakes of the Green

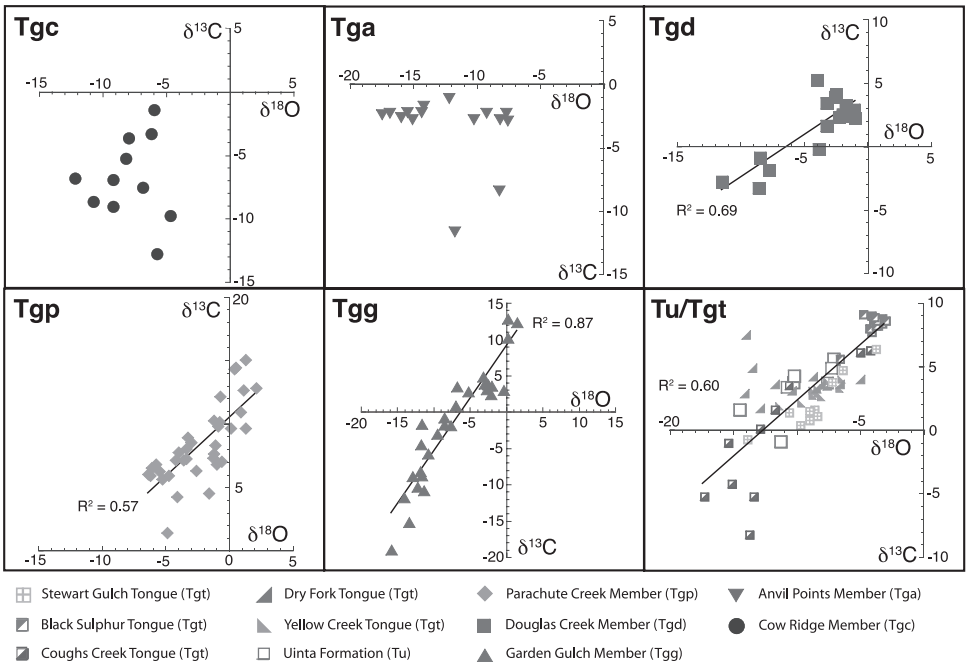

Fig. 6. Isotopic covariance of $\delta^{18}O_{calcite}$-$\delta^{13}C_{calcite}$ in sampled units of the Piceance Creek Basin. $\delta^{18}O_{calcite}$ is plotted relative to the PeeDee Belemnite standard (V-PDB).

River lake system during the Paleogene (figs. 1 and 2). Where relevant, interpretations also reference Pleistocene Lake Bonneville and the modern Great Salt Lake of Utah, whose location, hydrology and catchment geology closely resemble the Green River lakes, which preceded them. The new results thereby add to a growing consensus that topographic growth during the Laramide Orogeny caused large-scale integration of Cordilleran drainage patterns that in turn dictated the hydrologic regime of intraforeland lake basins. Following is a summary of the new and published isotopic and elemental results in support of this interpretation, presented chronologically.

Sevier-Laramide Transition (Late Cretaceous-earliest Eocene)

Between the Campanian and earliest Eocene, coeval with the onset of Laramide-style deformation in the foreland, the highstanding Sevier fold-and-thrust belt drained east into a broad, low-relief foreland (fig. 7, panel 53 Ma; for example, Lawton, 1986; Goldstrand, 1994; Janecke and others, 2000; DeCelles, 2004; Gierlowski-Kordesch and others, 2008). Within the foreland, shallow lakes and rivers drained northeast from Utah and Colorado and southeast from Montana and Idaho to an outlet in the northeast Greater Green River Basin (Wyoming) that debouched eastward into the ancestral Great Plains (see for example, Hansen, 1965, 1985; Steidtmann, 1969; Dorr Jr. and others, 1977; Stanley and Collinson, 1979; Moncure and Surdam, 1980; Cole, 1985; Sklenar and Anderson, 1985; Roehler, 1993).

Isotopic and elemental data support a hydrologically open foreland receiving water from catchments in the fold-and-thrust belt. First, mean $\delta^{18}O_{calcite}$ values of basinal proxies formed during this period are ~20 permil (table 1, for example

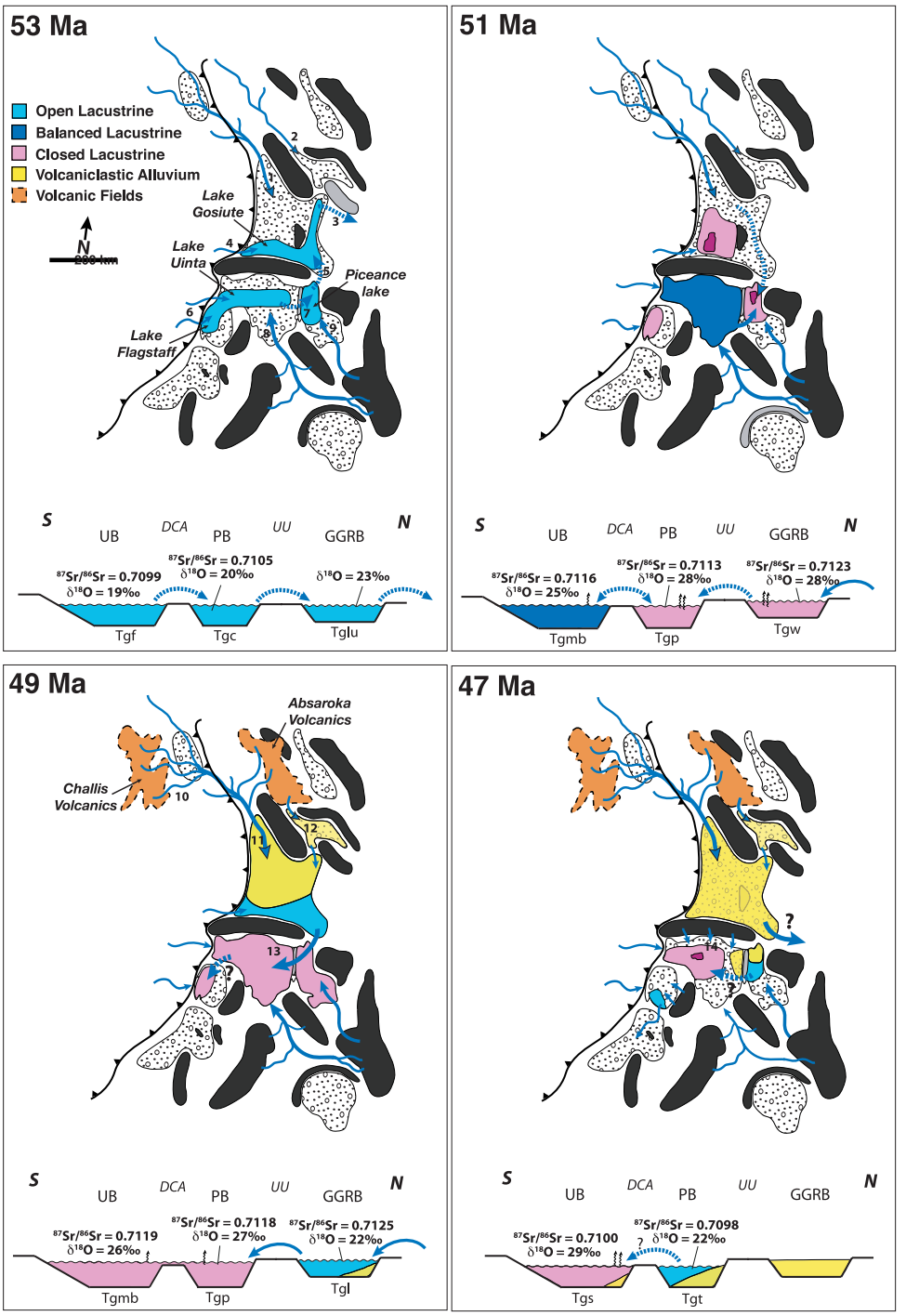

Fig. 7. Inferred development of foreland lakes and Cordilleran drainage patterns at four key times during the Paleogene (refer to fig. 1 for names of major structures and basins). Schematized cross-sections at bottom of each panel show the hydrology and isotopic compositions of the Greater Green River Basin (GGRB), Piceance Creek Basin (PCB) and Uinta Basin (UB), as separated by sills of the Uinta Uplift (UU) and the Douglas Creek Arch (DCA). Abbreviations of units deposited in each basin are shown in figure 2. Paleoflows are dashed where flow of surface waters was periodic, and are numbered according to the supporting references listed in Appendix A, table A5.

"non-evaporitic" lakes of Drummond and others, 1993), with a minimum of 16.6 permil in the Crazy Mountain and Powder River Basins in the northern Cordillera (Dettman and Lohmann, 2000) and maxima of 22.1 permil in the Bighorn Basin (Koch and others, 1995), 22.6 permil in the Flagstaff Formation of central Utah (Weber, 1964), and 23.1 permil in the Luman Tongue in the Greater Green River Basin (Bridger subbasin) (Dettman and Lohmann, 2000). Such values are consistent with $\delta^{18}O$ values of freshwater marls from Pleistocene Lake Bonneville (Provo- and Bonneville-age samples reported in Oviatt and others, 1994; Nelson and others, 2005) and imply Eocene surface waters between −4 permil and −8 permil (compare, Fricke, 2003). Second, $\delta^{18}O_{calcite}$ and $\delta^{13}C_{calcite}$ values from these samples generally do not covary (table 1 and fig. 6). Moderate covariance in samples of the Flagstaff Formation and Luman Tongue (Weber, 1964; Dettman and Lohmann, 2000; see table 1) suggests the early Lakes Gosiute and Flagstaff, respectively, may have been hydrologically closed at intervals, helping to explain slightly higher $\delta^{18}O_{calcite}$ values of those samples. Third, where Sr/Ca ratios of these samples have been measured, they are relatively low (table 1): mean values range from 1.3 ± 0.8 mmol/mol in the Piceance Creek Basin (this study, fig. 3), 0.75 ± 0.47 mmol/mol in the Uinta Basin (Davis and others, 2008) and <0.1 mmol/mol in the Flagstaff Basin (Gierlowski-Kordesch and others, 2008). Lastly, the $^{87}Sr/^{86}Sr$ ratios observed during this time in the Flagstaff, Uinta and Piceance Creek Basins (figs. 2 and 7, ***Tf***, ***Tgf*** and ***Tgc***, respectively) are consistently ~0.710 (table 1), suggesting catchments draining Paleozoic and Mesozoic carbonates then exposed in the fold-and-thrust belt to the west (Davis and others, 2008; Gierlowski-Kordesch and others, 2008). Modern rivers draining these rocks also have $^{87}Sr/^{86}Sr$ ratios ≤0.710 and tend to have a disproportionately strong influence on the isotopic composition of the lakes they flow into due to their high [Sr] (Hart and others, 2004; Bright, 2009).

Hydrologic Closure of the Green River Lake System (Early Eocene)

At ~52 Ma, the central Laramide foredeep became hydrologically closed, as recorded by the system of lakes which occupied the Greater Green River, Piceance Creek, and Uinta Basins (the Green River lake system). At lowstands, the Piceance Creek Basin was the final evaporating (that is, terminal) basin in the system, receiving periodic inflows from both the Greater Green River and Uinta Basins (fig. 7, panel 51 Ma). When prompted by climatic changes or increased inflows from upstream basins, the expanded Piceance lake coalesced with Lake Uinta overtop the Douglas Creek Arch (stratigraphy indicates lakes interconnected as early as the R-1 marker bed, Bartov and others, 2007; Smith and others, 2008a). Thus, the final evaporating basin of the closed lake system incorporated both the Uinta and Piceance Creek Basins when the lakes merged at highstands (for example, Kelts, 1988).

Isotopic and elemental results suggest changing foreland hydrology at this time. Mean $\delta^{18}O_{calcite}$ values of samples from the Green River lakes increase in each basin by 5 to 8 permil, shifting to values ≥ 25 permil (table 1), with maxima of 28.3 permil in the Wilkins Peak (***Tgw***) and lower Laney (***Tgl***) Members of the Greater Green River Basin (Norris and others, 1996; Carroll and others, 2008) and 27.9 permil in the Garden Gulch (***Tgg***), Douglas Creek (***Tgd***) and lower Parachute Creek (***Tgp***) Members of the Piceance Creek Basin (this study). Explanation of these high values by hydrologic closure and evaporative enrichment is supported by strong covariance of $\delta^{18}O_{calcite}$-$\delta^{13}C_{calcite}$ values (table 1 and fig. 6) and elevated Sr/Ca ratios (table 1, figs. 3 and 6). Modern carbonates from the analogous, closed Great Salt Lake display very similar $\delta^{18}O_{calcite}$ values (~26−28‰) which also covary with $\delta^{13}C_{calcite}$ (Spencer and others, 1984). The mean $\delta^{18}O_{calcite}$ value and

Sr/Ca ratio of Uinta Basin samples are somewhat lower than the other lake basins, 24.9 permil and 1.4 mmol/mol, respectively, reflecting only episodic connections with the intensely evaporative Piceance lake.

Despite high values from Greater Green River Basin samples, Sr isotope ratios indicate periodic outflows from that basin south to the terminal Piceance Creek and Uinta Basins. The mean $^{87}Sr/^{86}Sr$ ratio of Greater Green River Basin (Washakie subbasin) samples at this time is >0.7120 (Rhodes and others, 2002; Carroll and others, 2008), evidence of catchments draining radiogenic rocks in adjacent, craton-cored uplifts (for example, the Wind River Uplift). Because groundwater fluxes have in some cases been observed to have a very strong effect on the $^{87}Sr/^{86}Sr$ ratio of modern river and lake waters in Utah (Jones and Faure, 1972; Hart and others, 2004; Bright, 2009), it is likely that springs flowing into the Greater Green River Basin were also a significant flux of radiogenic Sr given the greater duration water-rock contact and elevated temperatures at depth. Importantly, though, rocks in the subsurface rocks of foreland basin systems are generally no different than those exposed in surface.

Beginning ~52 Ma, samples from the Uinta (Davis and others, 2008) and Piceance Creek (this study) Basins increase from ~0.7100 to 0.7116 and 0.7113, respectively. Lack of radiogenic rocks in the uplifts adjacent to and south of these basins indicates the integration of catchments in the northern Cordillera (Davis and others, 2008), and suggests hydrologic closure throughout at least 500 km of the north central foreland.

Integration of Axial Drainage and the Mahogany Highstand (early Middle Eocene)

At ~49 Ma, the Greater Green River Basin captured drainages flowing through the Challis volcanic field and Sage Creek Basin from headwaters in high-altitude north central Idaho (Kent-Corson and others, 2006; Carroll and others, 2008). Captured waters and their volcaniclastic sediment load quickly freshened and overfilled Lake Gosiute so that outflow to the Piceance Creek Basin became continuous (fig. 7, panel 49 Ma, Surdam and Stanley, 1980; Carroll and others, 2008). In turn, the continuous overspilling of Lake Gosiute led to a persistent merging of the Piceance lake with Lake Uinta by 48.6 Ma, when rich oil shales of the Mahogany Zone were deposited throughout the expanded yet evaporative lake (m, figs. 2 and 3). Connection of these sequential basins integrated axial drainage in the foreland over at least 1000 km from north central Idaho to northeast Utah (Davis and others, 2008).

Isotopic and elemental data record the expansion of the drainage basin and attendant changes in basin hydrology. At ~49 Ma, mean $\delta^{18}O_{calcite}$ values in the Sage Creek Basin of southwest Montana decrease by ~10 permil (table 1, Kent-Corson and others, 2006) as high-altitude catchments began draining through the basin. At about the same time, the mean $\delta^{18}O_{calcite}$ values downstream in Lake Gosiute decrease by ~6 permil in the span of 100 kyr (Carroll and others, 2008). Water spilling south from the newly freshened Lake Gosiute into the Piceance Creek Basin caused mean $\delta^{18}O_{calcite}$ values in the latter to decrease by ~1.2 permil as the combined (and terminal) Lake Uinta equilibrated with the increased volume of low-$\delta^{18}O$ water flowing in from the north (fig. 3, Tgp above ***m***). Owing to the persistent connection with the Piceance Creek Basin, mean $\delta^{18}O_{calcite}$ values in the Uinta Basin increase by ~2 permil (matching time-equivalent samples from the Piceance Creek Basin) and display less variability (table 1, fig. 3, Davis and others, 2008). As expected of a terminal lake, $\delta^{13}C_{calcite}$-$\delta^{18}O_{calcite}$ values covary in samples from both the Uinta and Piceance Creek Basins (table 1 and fig. 6, panels ***Tgp*** and ***Tu/Tgt***), and Sr/Ca ratios are similarly high (table 1 and fig. 3).

With the capture of catchments draining the Challis and Absaroka volcanic fields in the northern Cordillera, $^{87}Sr/^{86}Sr$ ratios of samples from Greater Green River Basin decrease to a mean of ~0.7116 after ~49 Ma (Carroll and others, 2008) likely due to the less radiogenic composition of the volcanic rocks (from 0.704−0.709, see table A6). As this water spilled south, a corresponding shift is seen in $^{87}Sr/^{86}Sr$ ratios of Piceance Creek Basin samples, from ~0.7119 at ~51 Ma to ~0.7109 at 48.6 Ma (fig. 3A). Upsection, $^{87}Sr/^{86}Sr$ ratios continue to decrease over ~150 m to ~0.7102 (fig. 3A). In the Uinta Basin, the sparsity of analyzed samples reveal only end members of what we infer to be a similarly decreasing trend in $^{87}Sr/^{86}Sr$ ratios, from a maximum of 0.7122 near the Mahogany marker to mean values of 0.7100 at ~46 Ma (fig. 3B). Although the initial decrease in $^{87}Sr/^{86}Sr$ ratios likely reflects the influence of new, less radiogenic catchments, there are several reasons to think that the continuing decline of $^{87}Sr/^{86}Sr$ ratios after ~46 Ma may mark decreasing inflows from the Greater Green River Basin. First, unlike $^{87}Sr/^{86}Sr$ ratios measured in lacustrine carbonates of both the Piceance Creek and Uinta Basins, those from the Greater Green River Basin never fall below 0.711. Second, mean $^{87}Sr/^{86}Sr$ ratios in both the Piceance Creek and Uinta Basins after 48.6 Ma are ~0.710, statistically indistinguishable from the ratios of older lacustrine rocks deposited when the same basins contained open lakes that drained west and north (table 1 and fig. 3A, ***Tgf*** and ***Tgc***). Third, marginal lacustrine sediments of the upper Washakie Formation deposited in the Greater Green River Basin after 47 Ma regress northward (Roehler, 1973, fig. 2), suggesting that a lingering deposystem in the Sand Wash sub-basin either drained internally or from a different outlet away from the Piceance Creek Basin. Fourth, the progradation of volcaniclastic sediments into the easternmost Uinta Basin (the Uinta Formation) tapers off between ~47 to 46 Ma (Prothero, 1990, 1996; Smith and others, 2008a). Finally, growth structures observed in synorogenic deposits of the Duchesne River Formation in the northern Uinta Basin reveal active tectonism of the Uinta Uplift as late as ~40 Ma (Anderson and Picard, 1974; see also Stucky and others, 1996), which may have interfered with the connection between the Greater Green River and Piceance Creek Basins (Davis and others, 2008).

Detrital zircon data (fig. 4) suggest a growing contribution of Grenville- (1315−1000 Ma) and Paleoproterozoic-age (1615−1800 Ma) grains to the Piceance Creek Basin over Eocene time. This trend is consistent with both large-scale axial drainage integration of the foreland and recycling of easily-eroded Mesozoic sediments that were progressively exposed along the flanks of rising Laramide uplifts (for example, Dickinson and Gehrels, 2003; Carroll and others, 2006; Smith and others, 2008b).

Piceance Creek Basin samples abruptly shift to $^{87}Sr/^{86}Sr$ ratios as low as 0.7080 in the Uinta Formation and lower tongues of the Green River Formation before returning to 0.7106 in two samples from the upper tongues (fig. 3A). We are not certain how to interpret the lowest observed values, but offer two possible explanations: As the lake in the Piceance Creek Basin contracted and shallowed, the depocenter may have become segmented, with some areas dominated by localized catchments draining easily weathered rocks with low $^{87}Sr/^{86}Sr$ (that is, Paleozoic carbonates). As an analog, when Pleistocene Lake Gunnison became discrete from Lake Bonneville, the $^{87}Sr/^{86}Sr$ ratio of its waters was identically low—0.708 (Oviatt, 1988; Hart and others, 2004). Another possibility regards the presence of substantial volcaniclastic grains contained in the carbonates with the lowest $^{87}Sr/^{86}Sr$ ratios. Though our method should prevent contamination by Sr^{2+} derived from the siliclastic component, it is possible that dissolution of these sediments in the depositional environment affected the Sr isotope composition of precipitating carbonate.

Demise of the Green River Lakes (early and late Middle Eocene)

Lacustrine deposition in the Greater Green River Basin ended ~48 Ma, overwhelmed by volcaniclastic alluvium that thereafter prograded southward into the Piceance Creek Basin (fig. 2, Surdam and Stanley, 1980; Smith and others, 2008a). The Piceance lake responded just as Lake Gosiute had before, freshening and increasingly passing water west into the Uinta Basin, which may have in turn periodically overspilled south into the Flagstaff Basin (fig. 2, Surdam and Stanley, 1980; Smith and others, 2008a; Davis and others, 2009). By ~47 Ma, accommodation in both the Greater Green River and Piceance Creek Basins was depleted (Franczyk and others, 1992; Hail, 1992).

Although large-scale integration of axial drainage was probably disrupted by Late Laramide topographic growth of the Uinta Uplift, evaporative lakes in the Uinta and Flagstaff Basins persisted as terminal sinks within the foreland until ~45 and ~43 Ma, respectively (Smith and others, 2008a; Davis and others, 2009). It has been suggested that the later demise of these lakes nonetheless conforms to the pattern of evolving Cordilleran drainage, driven by the expansion of distal catchments in tectonically and magmatically active areas of the hinterland (Davis and others, 2009). Although lacustrine deposition ended in the smaller Flagstaff Basin at ~45 Ma, presumably for lack of accommodation, Lake Uinta freshened and infilled between ~45 and 43.1 Ma, coeval with the southward migration of hinterland magmatism into northeastern Nevada, where paleorivers flowed east to the Uinta Basin (that is, Copper Basin and Tuscarora volcanics, Christensen and Yeats, 1992; Henry, 2008).

Isotopic and elemental data record the changes in basin hydrology as the Green River lakes disappeared. Between ~49 and ~48 Ma, samples from the vanishing Lake Gosiute (table 1, ***ul***) give a mean $\delta^{18}O_{calcite}$ value of 22.0 permil (fig. 7, panel 49 Ma). Between ~48 and ~47 Ma, as volcaniclastic sediment filled accommodation in the Piceance Creek Basin and its lake freshened, mean $\delta^{18}O_{calcite}$ values decrease again by ~5.1 permil to a similar mean of 22.2 permil (table 1, figs. 3A and 7, panel 47 Ma, ***Tu*** and ***Tgt***). The cessation of distal inflows from the northern Cordilleran catchments to Lake Uinta between ~47 and 46 Ma caused an increase in mean $\delta^{18}O_{calcite}$ values and Sr/Ca ratios to 28.8 permil ($1\sigma = 1.1$, n = 35) and 3.3 mmol/mol ($1\sigma = 0.7$, n = 15), respectively (figs. 2, 3B, and 7, ***Tgmb/Tgs***). To the south, mean $\delta^{18}O_{calcite}$ values in Flagstaff Basin sediments also increase slightly, perhaps reflecting the influence of Lake Uinta (table 1, Upper ***Tg***).

The end of lacustrine deposition in the Flagstaff Basin at ~45 Ma is obscured by a brief period of erosion that seems to have removed isotopic evidence of the lake's final freshening (Davis and others, 2009). Uinta Basin samples do record the final stage of Lake Uinta between ~44 and 43.1 Ma (fig. 3B, ***Tgsl***), showing a ~6 permil decrease in $\delta^{18}O_{calcite}$ values to ~20 permil and a 3 mmol/mol decrease in Sr/Ca ratios to 1.1 mmol/mol (Davis and others, 2009). $^{87}Sr/^{86}Sr$ ratios from Uinta Basin samples hold steady at ~0.710 during this time, a ratio consistent with inflows from hinterland catchments to the west (Davis and others, 2008; Gierlowski-Kordesch and others, 2008).

Magmatism Sweeps South (late Middle Eocene-Late Eocene)

Restoring Neogene extension of the Basin and Range, the hinterland of northeastern Nevada and northwestern Utah was situated roughly 100 to 200 km west of the Uinta Basin. Though exact basin geometries are difficult to reconstruct in light of subsequent extension and erosion, sizeable lakes were also present in that area during Eocene time, preserved as deposits of the Elko, White Sage and Sheep Pass Formations (Winfrey, 1960; Fouch, 1979; Wingate, 1983; Good,

1987; Dubiel and others, 1996). Some studies have used these lacustrine rocks to document a phase of Eocene and Oligocene extension that immediately precedes the migration of magmatism through the region (Axen and others, 1993; Potter and others, 1995).

Isotopic data from these lakes is also important to the interpretation of Cordilleran drainage patterns. Mean $\delta^{18}O_{calcite}$ values in the late Middle Eocene upper Elko and White Sage Formations are 22.4 permil and 19.8 permil, respectively (table 1). A ~8.5 permil decrease in mean $\delta^{18}O_{calcite}$ values between ~45 and 37 Ma in the Elko Basin (table 1) has been interpreted as surface uplift related to the coeval magmatism in the region (Horton and others, 2004). As noted above, ash-filled paleovalleys in the Elko area indicate eastward paleoflow (Henry, 2008), such that the expansion and uplift of local catchments in the late Middle Eocene would likely have influenced the hydrology and isotopic composition of Lake Uinta in the subjacent foreland (Davis and others, 2009).

The lake in the Claron Basin of southwest Utah, shallower and fresher than Lake Uinta in the late Middle Eocene, also records a decrease in mean $\delta^{18}O_{calcite}$ values by 5.5 permil between ~40 and 35 Ma (table 1), again interpreted as the effect of coeval uplift and drainage reorganization in northern Arizona (Elston and Young, 1991; Flowers and others, 2008; Davis and others, 2009). Interestingly, fluvial-lacustrine deposits to the east in the Galisteo Basin of central New Mexico remain more or less constant over the same period (table 1), suggesting differential uplift of the southeastern Colorado Plateau.

Localized Depocenters (Late Eocene-Early Oligocene)

By the post-Laramide Late Eocene, few large lakes remained anywhere in the Cordillera. Accommodation was primarily created through slow subsidence (compare, McMillan and others, 2006) while volcanism in the central and southern Cordillera (compare, Tintic, Marysvale, San Juan, Datil and Espinaso centers; see Lipman and others, 1972; Ingersoll and others, 1990) generated prodigious volcaniclastic sediments. As a result, depocenters were localized and fluvial (for example, the Brian Head Formation of the Claron Basin, the Bald Knoll and Dipping Vat Formations of the Flagstaff Basin, the Espinaso Formation of the Galisteo Basin). Outside of these depocenters, erosion dominated large regions of the Cordillera (for example, Epis and Chapin, 1975; Dickinson, 2004).

Isotopic and elemental data from this period are consistent with throughgoing rivers draining highstanding adjacent topography as well as the cooler and more arid climate prevailing in the Oligocene (for example, Wolfe, 1994; Zachos and others, 2001; Sheldon and Retallack, 2004). Mean $\delta^{18}O_{calcite}$ values in sampled basins of Utah, Nevada and Montana are generally low (14−15‰, table 1), resembling unevaporated, meteoric water possibly incorporating snowmelt (for example, Norris and others, 1996; Dettman and Lohmann, 2000). Mean values of samples from the Galisteo and Uinta Basins are 21.8 and 17.7 permil, respectively (table 1). Lack of evaporation is further indicated by $\delta^{18}O_{calcite}$-$\delta^{13}C_{calcite}$ values that do not covary in any of the basins (except weakly in the Galisteo Basin) and mean Sr/Ca ratios that are everywhere <0.5 (table 1).

CONCLUSIONS

Isotopic and elemental composition of lacustrine carbonate samples from the Piceance Creek Basin of northwest Colorado record dramatic changes in basin hydrology during the Early and Middle Eocene. Interpreted alongside a large dataset of isotopic stratigraphies from sedimentary basins throughout the Paleogene Cordillera, the new data reflect the evolution of orogen-scale drainage

patterns. Although changes in global and regional climate during the Paleogene undoubtedly influenced the Cordilleran paleoenvironment, the hydrology of neighboring basins in some cases trended in opposite directions, defying explanation by changes in climate alone. Instead, the data suggest changes in Cordilleran hydrology were tectonically forced, as accommodation was first created and then dissected and filled by processes of downwarping, uplift, and magmatism.

1. During the transition from thin-skinned Sevier-style thrusting to thick-skinned Laramide-style deformation during the Late Cretaceous and Paleocene, large river systems flowed east from the highstanding hinterland through the foreland and out to the ancestral Great Plains. Isotopic and elemental data substantiate this hydrologic regime with relatively low values (~20‰), minimal evidence of evaporation, and $^{87}Sr/^{86}Sr$ ratios in the central foreland (Utah) consistent with inflows of hinterland provenance.
2. By the earliest Eocene, downwarping of the foredeep and block uplifts further east impounded a system of large (>10,000 km^2) freshwater lakes in the central foreland (the Green River Lakes of Wyoming, Utah and Colorado). $\delta^{18}O_{calcite}$ values in these early lakes remain low, and lack of an evaporative signal supports their open hydrology. $^{87}Sr/^{86}Sr$ ratios continue to reflect hinterland catchments to the west.
3. At ~52 Ma, the hydrology of foreland lakes became closed and waters that had formerly exited the Cordillera to the east were diverted axially to the terminal Piceance Creek Basin. $\delta^{18}O_{calcite}$ values in the Green River Lakes rise to 25 permil or higher at this time and covary with $\delta^{13}C_{calcite}$, and Sr/Ca ratios also increase, all indicating internal drainage and attendant evaporation. A marked increase in the $^{87}Sr/^{86}Sr$ ratio of Piceance Creek and Uinta Basin lacustrine carbonate reflects the integration of foreland drainage.
4. Beginning ~49 Ma, magmatism in the northern Cordillera (that is, the Challis and Absaroka volcanic fields) led to the capture of drainages heading in north-central Idaho by Lake Gosiute. The influx of water and sediment freshened and infilled the lake basin, and affected the downstream Piceance Creek and Uinta Basins in sequence. Late Laramide rise of the Uinta Uplift interrupted axial drainage in the foreland between 47 to 46 Ma. $\delta^{18}O_{calcite}$ values in the Sage Creek and Greater Green River Basins record the drainage capture event as a 10 and 6 permil decrease, respectively, at ~49 Ma. $\delta^{18}O_{calcite}$ values in the Piceance Creek and Uinta Basins, joined by a Lake Uinta highstand, also record the event. $^{87}Sr/^{86}Sr$ ratios in each of the Green River Lakes decrease with the integration of catchments draining Tertiary volcanics. $^{87}Sr/^{86}Sr$ ratios in the Piceance Creek and Uinta Basins decline further as inflows from the Greater Green River Basin cease.
5. Filled in by volcaniclastics, sedimentation in the Piceance Creek Basin ended at ~47 Ma. Yet the southward sweep of magmatism through the Cordillera had a similar effect on adjacent intraforeland basins: lakes in the Flagstaff and Uinta Basins freshened and infilled at ~45 and 43 Ma, respectively, coeval with magmatism in their catchments to the west in northern Nevada (that is, the Copper Basin and Tuscarora volcanics). $\delta^{18}O_{calcite}$ values decrease in each of the Elko, Flagstaff and Uinta Basins during this time by 7 to 10 permil. Between ~40 and 37 Ma, drainage patterns in northern Arizona reverse, perhaps related to episodes of uplift and/or magmatism to the south in central Arizona and south-central New Mexico, and $\delta^{18}O_{calcite}$ values in the downstream Claron Basin of southern Utah also decrease by 5.5 permil.

6. The Late Eocene and Oligocene Cordillera was characterized by further magmatism and localized depocenters of throughgoing fluvial systems. $\delta^{18}O_{calcite}$ values from throughout the Cordillera are low (~14–18‰) and lack signs of evaporative enrichment, evidencing a cooler, more arid climate than previously in the Paleogene.

ACKNOWLEDGMENTS

We acknowledge the support of National Science Foundation grant EAR-0609649 to C. P. Chamberlain and a Stanford University Earth Sciences McGee grant to S. J. Davis. We thank Trevor Dumitru, Joe Wooden, Frank Mazdab, and George Gehrels for assistance in the processing and analysis of geochronological samples, and Jim Sweeney for help in the laboratory. U-Pb analyses of detrital zircon samples at the Arizona LaserChron Center were supported in part by funding from National Science Foundation grant EAR-732436. The manuscript was much improved by discussions with Stephan Graham, Pete DeCelles and Jim Ingle, as well as thorough reviews by Greg Retallack, Jay Quade and Majie Fan.

APPENDIX A

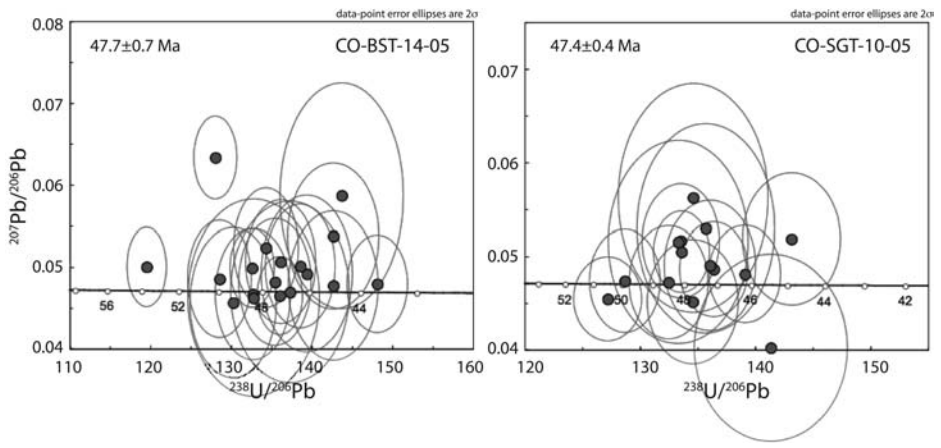

Fig. A1. Tera-Waserburg plots of U-Pb analyses of zircon separates from the Black Sulphur and Stewart Gulch Tongues (BST, SGT, respectively) of the Green River Formation in the Piceance Creek Basin. Samples represent coherent age groups that constrain maximum depositional age, and appear as #4 and #5, respectively, in figures 2 and 3.

Table A1

Details and key references of sampled exposures in the Piceance Creek

Unit	Location Name	GPS Coordinates	Reference(s)
Uinta Formation	Piceance Creek	39°41.935' N 108°0.128' W	Brobst and Tucker, 1973
Green River Formation	Jackrabbit Ridge	Type section (between U.S. 13 and Stewart Gulch): 39°41.935' N 108°0.128' W	O'Sullivan, 1987
Jackrabbit Marl			
Stewart Gulch Tongue	Middle Fork of Stewart Gulch	Type section: 39°43.884' N 108°10.065' W	Hail, 1977
Coughs Creek Tongue	West side of Cow Creek	Type section: 39°42.634' N 107°59.887' W	O'Sullivan, 1975
Black Sulphur Tongue	Black Sulphur Creek	Type section: 39°51.279 N 108°22.375' W	Duncan and others, 1974
Dry Fork Tongue	Near confluence of the main stem and the Dry Fork of Piceance Creek	Type section: 40°00.481 N 108°14.385' W	Duncan and others, 1974
Yellow Creek Tongue	East side of Yellow Creek	Type section: 40°5.119 N 108°20.082' W	Duncan and others, 1974
Parachute Creek Member	Piceance Creek	Complete section: 39°41.935' N 108°0.128' W	Brobst and Tucker, 1973
Garden Gulch Member	West side of Yellow Creek	Type section: 40°9.652 N 108°23.706' W	Hail, 1990
Douglas Creek Member	Douglas Pass	Principal reference section: 39°36.209' N 108°46.847' W	Johnson, 1984
Long Point Bed / Kimball Mountain Tuff Bed		Type section of Long Point Bed: 39°26.338 N 108°0.294' W	Johnson, 1984
Anvil Points Member		Type section of Long Point Bed: 39°26.338 N 108°0.294' W	Johnson, 1984
Cow Ridge Member	Cow Ridge	Type section: 39°23.641 N 108°22.388 W	Johnson, 1984

TABLE A2

Isotopic and elemental compositions of samples

Unit / Sample Number	$\delta^{18}O_{calcite}$ (V-SMOW)	$\delta^{13}C_{calcite}$ (V-PDB)	Sr/Ca (mmol/mol)	$^{87}Sr/^{86}Sr_i$	Stratigraphic Position (m)
Uinta Formation / Tongues of the ***Green River Formation***					
CO-YCT-06-13	18.09	1.14			621.0
CO-YCT-06-14	18.76	2.31			623.0
CO-YCT-06-15	22.88	3.95			625.0
CO-YCT-06-02	22.14	3.19			627.5
CO-YCT-06-03	22.44	2.62			631.6
CO-YCT-06-04	23.88	3.26			632.5
CO-YCT-06-05	24.09	3.98			635.0
CO-YCT-06-06	21.72	3.15			635.4
CO-YCT-06-07	20.83	2.07			635.8
CO-YCT-06-08	21.73	2.67			637.5
CO-YCT-06-09	19.06	1.90		0.70918	637.9
CO-YCT-06-10	22.10	2.92			638.7
CO-YCT-06-11	18.74	1.37			641.7
CO-YCT-06-12	16.33	-1.44			643.7
CO-DFT-06-02	20.50	2.95			645.0
CO-DFT-06-03	18.51	1.69			647.0
CO-DFT-06-04	20.29	3.07			650.0
CO-DFT-06-05	16.44	2.88			654.4
CO-DFT-06-07	16.60	7.51			658.0
CO-DFT-06-11	17.09	4.85			661.5
CO-DFT-06-12	24.24	3.63			664.0
CO-DFT-06-13	23.16	3.45			665.1
CO-DFT-06-14	22.20	3.26			665.8
CO-DFT-06-15	22.71	3.63			666.2
CO-DFT-06-16	22.08	4.16			666.6
CO-DFT-06-17	25.90	4.01			667.3
CO-DFT-06-18	18.96	3.57			668.0
CO-DFT-06-21	17.74	1.72		0.70803	671.3
CO-BST-06-05	17.14	-5.21	2.65		690.0
CO-BST-06-06	15.03	-1.00	1.49		692.9
CO-BST-06-07	13.05	-5.21	3.37		692.9
CO-BST-06-08	15.36	-4.24	2.39		693.7
CO-BST-06-10	25.74	6.15	2.66		695.1
CO-BST-06-11	26.62	6.29	2.91		695.5
CO-BST-06-12	15.92	-13.26			696.5
CO-BST-06-13	18.85	1.56		0.70802	696.9
CO-BST-06-15	16.73	-8.23			698.0
CO-BST-06-16	20.01	3.46	1.49		698.8
CO-BST-06-17	17.64	0.10			699.1
CO-BST-06-18	13.74	-2.15			703.1
CO-CCT-06-02	18.80	5.76	3.52		736.8
CO-CCT-06-04	27.47	8.39	2.39		740.0
CO-CCT-06-05	27.48	8.79	3.00		741.2
CO-CCT-06-06	26.68	7.66	2.30		743.7
CO-CCT-06-07	26.52	8.04	2.83		745.7
CO-CCT-06-08	27.76	8.58	2.70		748.7
CO-CCT-06-09	27.19	8.23	3.23		752.7
CO-CCT-06-10	26.82	8.54	2.37		754.7
CO-CCT-06-12	27.01	8.19	2.77		759.7
CO-CCT-06-13	24.06	5.60			761.2
CO-CCT-06-14	27.08	8.58	2.79		763.2
CO-CCT-06-16	26.68	9.04	2.96	0.71083	766.8

TABLE A2
(continued)

Unit / Sample Number	$\delta^{18}O_{calcite}$ (V-SMOW)	$\delta^{13}C_{calcite}$ (V-PDB)	Sr/Ca (mmol/mol)	$^{87}Sr/^{86}Sr_i$	Stratigraphic Position (m)
Uinta Formation / Tongues of the ***Green River Formation***					
CO-CCT-06-17	25.96	9.07	3.18		772.2
CO-CCT-06-18	26.91	8.87	2.95		776.2
CO-SGT-06-01	21.47	0.68			798.0
CO-SGT-06-03	24.28	4.71		0.71039	800.0
CO-SGT-06-04	23.47	3.76			803.0
CO-SGT-06-05	22.03	1.59			804.1
CO-SGT-06-06	20.86	0.38			805.1
CO-SGT-06-07	21.68	0.78			806.6
CO-SGT-06-08	21.62	1.48			807.6
CO-SGT-06-09	22.23	1.10			808.6
CO-SGT-06-11	19.99	1.41			812.2
CO-SGT-06-14	26.98	6.45			813.2
CO-SGT-06-15	16.58	-0.73			815.2
CO-SGT-06-16	22.18	0.96			817.2
CO-SGT-06-17	16.75	0.25			818.2
CO-SGT-06-20	26.34	7.75			800.0
CO-UF-06-01	27.53	8.88			566.4
CO-UF-06-02	24.61	6.53			568.4
CO-UF-06-04	26.82	7.67		0.71030	571.9
CO-UF-06-05	23.59	5.57			572.4
CO-UF-06-06	20.31	3.79			575.4
CO-UF-06-07	23.12	3.69			580.4
CO-UF-06-08	23.42	4.86			585.4
CO-UF-06-11	15.91	1.61		0.70854	599.4
CO-UF-06-12	19.82	3.40			603.4
CO-UF-06-13	20.36	4.27			605.4
CO-UF-06-14	19.23	-0.92			609.4
Green River Formation Garden Gulch Member					
CO-GRGG-06-105	31.12	12.92	2.26		51.7
CO-GRGG-06-104	32.40	12.44	3.35		51.7
CO-GRGG-06-103	31.14	10.20	2.83		51.7
CO-GRGG-06-01	19.31	-10.81	0.33		87.4
CO-GRGG-06-02	18.33	-10.32	0.38		106.5
CO-GRGG-06-03	23.03	-1.84	1.30	0.71018	106.6
CO-GRGG-06-04	16.35	-11.69	0.56		122.5
CO-GRGG-06-05	17.62	-8.81	0.52		136.9
CO-GRGG-06-06	18.74	-8.08	0.44		138.5
CO-GRGG-06-07	18.84	-4.36	0.60	0.71044	144.9
CO-GRGG-06-09	18.93	-1.55	1.15		153.6
CO-GRGG-06-10	14.65	-18.91	1.07		161.6
CO-GRGG-06-12	18.94	-8.73	1.04		177.6
CO-GRGG-06-13	17.08	-15.07	1.31	0.71046	184.0
CO-GRGG-06-15	19.82	-5.66	0.70		196.0
CO-GRGG-06-16	22.10	-1.70	1.42		201.5
CO-GRGG-06-17	21.10	-2.99	0.95	0.71038	203.1
CO-GRGG-06-20	22.12	-0.66	0.86		211.9
CO-GRGG-06-21	30.50	3.04	1.49		219.9
CO-GRGG-06-22	28.16	3.05			223.1
CO-GRGG-06-23	28.80	3.63	2.02	0.71106	231.1
CO-GRGG-06-24	23.70	0.91	1.32		239.1
CO-GRGG-06-25	27.56	4.92	1.71		243.1
CO-GRGG-06-26	28.31	3.80	2.34		249.4
CO-GRGG-06-27	27.86	3.89	1.76	0.71103	252.6

TABLE A2
(continued)

Unit / Sample Number	$\delta^{18}O_{calcite}$ (V-SMOW)	$\delta^{13}C_{calcite}$ (V-PDB)	Sr/Ca (mmol/mol)	$^{87}Sr/^{86}Sr_i$	Stratigraphic Position (m)
Green River Formation					
Garden Gulch Member					
CO-GRGG-06-28	28.71	2.49	2.27		262.2
CO-GRGG-06-31	25.58	2.93	2.83		281.4
Green River Formation					
Parachute Creek Member					
CO-GRPC-06-01	32.06	12.59	3.56		211.9
CO-GRPC-06-101	14.58	-1.86	1.46		212.17
CO-GRPC-06-02	30.00	9.80	2.29	0.71144	245.7
CO-GRPC-06-03	31.41	14.37			265.9
CO-GRPC-06-05	32.29	15.00	1.53		271.3
CO-GRPC-06-04	30.15	12.07	2.30	0.71188	271.3
CO-GRPC-06-06	31.32	14.34	1.85		274.7
CO-GRPC-06-07	31.03	9.61	2.52		280.1
CO-GRPC-06-08	31.82	10.93	2.76		282.8
CO-GRPC-06-10	32.23	9.62	3.04		307.1
CO-GRPC-06-11	33.02	12.82	2.42		307.2
CO-GRPC-06-12	29.87	6.81	2.50		315.3
CO-GRPC-06-13	29.78	8.26	2.26	0.71179	318.1
CO-GRPC-06-14	29.67	7.57			333.4
CO-GRPC-06-15	29.54	7.33	2.46		340.2
CO-GRPC-06-17	29.22	4.53	4.15	0.71179	380.7
CO-GRPC-06-204	25.89	1.44	2.76		396.8
CO-GRPC-06-201	26.70	4.20	3.25		406.8
CO-GRPC-06-18	27.77	8.52	3.30	0.71105	432.2
CO-GRPC-06-19	29.71	10.24	3.00		448.7
CO-GRPC-06-21	30.05	10.09	2.92		449.5
CO-GRPC-06-20	25.49	5.63	2.28	0.71072	451.4
CO-GRPC-06-24	30.24	6.99	3.06		471.1
CO-GRPC-06-25	28.27	6.32	3.25	0.71091	489.2
CO-GRPC-06-27	25.19	6.21	2.38		513.0
CO-GRPC-06-29	26.57	7.09	2.62		523.8
CO-GRPC-06-30	24.54	5.88	2.66		529.2
CO-GRPC-06-31	25.95	5.94	2.56		534.6
CO-GRPC-06-32	27.15	7.10	2.92		540.0
CO-GRPC-06-33	27.43	7.17	2.68	0.71064	545.4
CO-GRPC-06-34	27.39	8.05	3.27		550.8
CO-GRPC-06-35	24.32	6.01	2.75		556.2
Green River Formation					
Douglas Creek Member					
CO-GRDC-06-29	31.47	4.28	4.20		102.8
CO-GRDC-06-28	22.89	-1.85	2.06		106.8
CO-GRDC-06-27	22.04	-3.34	1.88		119.7
CO-GRDC-06-25	19.10	-2.82	1.78	0.71055	180.4
CO-GRDC-06-22	22.13	-0.94	4.49		203.6
CO-GRDC-06-21B	29.79	2.93	4.16		224.3
CO-GRDC-06-21A	29.88	2.19	3.51		237.2
CO-GRDC-06-19					257.9
CO-GRDC-06-18	26.84	-0.17	2.77	0.71133	273.4
CO-GRDC-06-15	28.86	2.43	4.38		286.3
CO-GRDC-06-14	29.09	3.21	3.54		294.0
CO-GRDC-06-13	27.52	1.65	2.84		299.2
CO-GRDC-06-12	27.58	1.63	2.52		306.9
CO-GRDC-06-11	28.81	2.54	2.34		309.5
CO-GRDC-06-08	28.99	2.48	3.04		319.8
CO-GRDC-06-09	28.54	2.30	3.14		330.2
CO-GRDC-06-07	27.51	3.40	2.14		345.7
CO-GRDC-06-06	28.25	3.94	3.03		353.4

TABLE A2
(continued)

Unit / Sample Number	$\delta^{18}O_{calcite}$ (V-SMOW)	$\delta^{13}C_{calcite}$ (V-PDB)	Sr/Ca (mmol/mol)	$^{87}Sr/^{86}Sr_i$	Stratigraphic Position (m)
Green River Formation					
Garden Gulch Member					
CO-GRDC-06-02	28.30	4.11	3.35		387.0
CO-GRDC-06-01	26.74	5.18	3.58		394.8
Green River Formation					
Anvil Points Member					
CO-GRAP-06-102	18.70	-11.63	0.30		76.4
CO-GRAP-06-103	22.35	-8.36	0.44		81.4
CO-GRAP-06-101	20.32	-2.79	0.75		86.4
CO-LPB-06-01	25.46	-13.11	1.13		102.7
CO-LPB-06-02	24.27	-8.02	0.92	0.71051	102.8
CO-GRAP-06-01	23.10	-2.90	1.66		133.0
CO-GRAP-06-02	14.39	-2.65	1.69		138.1
CO-GRAP-06-03	22.95	-2.26			141.9
CO-GRAP-06-04	18.34	-1.05	1.72	0.71049	145.7
CO-GRAP-06-05	22.41	-2.79	1.72		149.5
CO-GRAP-06-07	16.11	-2.21			154.8
CO-GRAP-06-08	14.93	-2.21	2.22		157.3
CO-GRAP-06-10	13.52	-2.29	1.89		172.5
CO-GRAP-06-11	12.88	-2.38	2.02		177.5
CO-GRAP-06-12	16.23	-1.75	1.69	0.71142	186.4
CO-GRAP-06-13	21.33	-2.27			211.7
Green River Formation					
Cow Ridge Member					
CO-GRCR-06-01	21.42	-6.93	1.37		0
CO-GRCR-06-02	24.91	-12.74		0.71033	2
CO-GRCR-06-03	23.81	-7.47			5
CO-GRCR-06-04	24.52	-3.34	1.36	0.71015	6
CO-GRCR-06-05	24.71	-1.44			8.5
CO-GRCR-06-06	22.64	-3.60		0.71026	9.7
CO-GRCR-06-07	19.80	-8.60	0.59		12.7
CO-GRCR-06-09	18.35	-6.78			20.2
CO-GRCR-06-11	26.02	-9.72			28.2
CO-GRCR-06-12	22.50	-5.23		0.71017	32.2

TABLE A3

Age constraints of sampled units in the Piceance Creek Basin

Unit	Reported Age	Method	Details	Reference(s)
Green River Formation				
Tongues				
Stewart Gulch Tongue	47.4±0.3 Ma	U-Pb Zircon (SHRIMP-RG)	**(#5 in figs. 2 and 3)**	this study
Black Sulphur Tongue	47.7±0.7 Ma	U-Pb Zircon (SHRIMP-RG)	**(#4 in figs. 2 and 3)**	this study
Parachute Creek Member				
Wavy Tuff	48.37 ± 0.23 Ma	^{40}Ar-^{39}Ar	(~50 m above Mahogany Marker in Uinta Basin) N 39°50′59.3″ W 110°15′17.5″ **(#3 in figs. 2 and 3)**	Smith and others, 2008
Curly Tuff	49.02 ± 0.30 Ma	^{40}Ar-^{39}Ar	(~25 m below Mahogany Marker in Uinta Basin) N 39°50′33.8″ W 110°15′3.1″ **(#2 in figs. 2 and 3)**	Smith and others, 2008
Yellow Tuff	51.24 ± 0.52 Ma	^{40}Ar-^{39}Ar	(1.5 - 6 m above base of Parachute Creek Member) N 40°1′1.9″ W 108°6′53.2″ **(#1 in fig. 2 and 3)**	Pipiringos and Johnson, 1975; Smith and others, 2008

Table A4

Geochronological analyses of U-Pb in zircons using LA-ICPMS

Analysis	U (ppm)	$^{206}Pb/^{204}Pb$	U/Th	$^{206}Pb^*/^{207}Pb^*$	± (%)	Isotope Ratios					Apparent Ages (Ma)						Best age (Ma)	± (Ma)
						$^{207}Pb^*/^{235}U^*$	± (%)	$^{206}Pb^*/^{238}U$	± (%)	Err. corr	$^{206}Pb^*/^{238}U^*$	± (Ma)	$^{207}Pb^*/^{235}U$	± (Ma)	$^{206}Pb^*/^{207}Pb^*$	± (Ma)		
CCT-14	126	363	1.9	24.6108	15.4	0.0551	15.6	0.0098	2.7	0.17	63.1	1.7	54.5	8.3	-310.6	396.6	63.1	1.7
CCT-61	139	828	1.0	26.4517	22.0	0.0611	22.3	0.0117	4.0	0.18	75.2	3.0	60.2	13.1	-498.9	591.1	75.2	3.0
CCT-48	144	1029	0.8	28.3254	30.0	0.0607	30.0	0.0125	1.0	0.03	79.8	0.8	59.8	17.4	-684.7	845.4	79.8	0.8
CCT-63	526	3297	1.7	21.9414	6.4	0.0891	8.1	0.0142	5.0	0.61	90.8	4.5	86.7	6.7	-24.7	154.7	90.8	4.5
CCT-12	384	3576	0.9	22.0187	6.3	0.0949	6.6	0.0151	2.1	0.32	96.9	2.0	92.0	5.8	-33.3	152.3	96.9	2.0
CCT-9	166	573	0.9	17.9376	22.7	0.1524	22.8	0.0198	1.8	0.08	126.5	2.3	144.0	30.6	442.4	511.4	126.5	2.3
CCT-23	647	5217	1.9	20.6635	4.5	0.1562	5.4	0.0234	2.9	0.54	149.2	4.3	147.4	7.4	118.6	106.6	149.2	4.3
CCT-67	1014	5082	0.7	19.9757	3.1	0.1726	7.4	0.0250	6.7	0.91	159.2	10.6	161.7	11.0	197.8	71.6	159.2	10.6
CCT-43	143	2814	1.4	21.7403	7.1	0.1597	8.5	0.0252	4.5	0.54	160.3	7.2	150.4	11.8	-2.5	172.4	160.3	7.2
CCT-60	753	6951	1.7	20.5173	2.4	0.1872	3.3	0.0279	2.3	0.68	177.1	3.9	174.2	5.3	135.3	56.7	177.1	3.9
CCT-65	676	6363	3.9	17.5413	4.1	0.2293	9.0	0.0292	8.0	0.89	185.4	14.6	209.7	17.0	491.8	90.3	185.4	14.6
CCT-64	2098	5382	2.0	17.7074	3.3	0.2528	3.6	0.0325	1.3	0.37	206.0	2.6	228.9	7.3	471.0	73.2	206.0	2.6
CCT-13	188	6879	0.9	17.1949	2.3	0.7187	2.6	0.0896	1.2	0.45	553.3	6.3	549.9	11.1	535.6	51.2	553.3	6.3
CCT-40	215	10827	2.0	16.9219	3.0	0.7930	4.3	0.0973	3.0	0.71	598.7	17.4	592.8	19.1	570.6	64.9	598.7	17.4
CCT-56	45	2010	2.2	15.5953	3.0	0.8899	5.5	0.1007	4.6	0.83	618.3	26.9	646.3	26.2	745.6	64.1	618.3	26.9
CCT-10	1319	46515	4.1	13.6686	1.4	1.4211	2.8	0.1409	2.5	0.88	849.6	19.7	897.8	16.9	1018.4	27.5	849.6	19.7
CCT-57	131	19857	1.8	13.6759	2.0	1.7830	4.1	0.1768	3.6	0.88	1049.7	35.1	1039.3	26.8	1017.3	40.0	1017.3	40.0
CCT-44	26	1947	1.2	13.3505	4.2	1.8799	6.3	0.1820	4.7	0.75	1078.0	46.8	1074.0	41.8	1065.9	84.1	1065.9	84.1
CCT-21	679	31521	3.5	13.1248	1.8	1.9577	2.1	0.1863	1.0	0.48	1101.6	10.1	1101.1	13.9	1100.1	36.2	1100.1	36.2
CCT-34	109	10032	1.8	12.9686	2.2	2.0523	6.5	0.1930	6.1	0.94	1137.8	63.9	1133.1	44.5	1124.0	44.2	1124.0	44.2
CCT-30	318	32058	3.1	12.9148	1.4	1.8450	2.2	0.1728	1.6	0.75	1027.6	15.4	1061.7	14.2	1132.3	28.3	1132.3	28.3
CCT-58	143	9435	1.7	12.7591	1.9	2.1337	2.6	0.1974	1.8	0.68	1161.6	18.8	1159.8	18.1	1156.4	38.3	1156.4	38.3
CCT-52	49	3345	1.8	12.6721	2.7	2.2714	4.4	0.2088	3.5	0.79	1222.2	38.9	1203.4	31.2	1169.9	54.0	1169.9	54.0
CCT-46	368	57204	3.2	12.5170	3.0	2.1261	4.6	0.1930	3.5	0.76	1137.7	36.3	1157.3	31.6	1194.3	58.4	1194.3	58.4
CCT-22	149	14835	2.6	11.5600	1.4	2.3874	2.9	0.2002	2.5	0.88	1176.2	27.0	1238.8	20.4	1349.5	26.1	1349.5	26.1
CCT-8	140	12915	1.1	11.2747	2.0	2.8725	6.4	0.2349	6.1	0.95	1360.1	74.2	1374.7	48.0	1397.6	38.0	1397.6	38.0
CCT-17	92	7410	2.5	11.2213	1.5	2.9592	3.3	0.2408	2.9	0.89	1391.0	36.8	1397.2	25.0	1406.6	28.2	1406.6	28.2
CCT-35	604	27210	0.9	11.2101	1.7	2.9833	3.0	0.2426	2.5	0.82	1400.0	31.1	1403.4	23.0	1408.6	33.3	1408.6	33.3
CCT-28	630	42981	4.9	11.1597	1.5	2.7857	1.9	0.2255	1.2	0.62	1310.7	14.2	1351.7	14.4	1417.2	28.7	1417.2	28.7
CCT-32	213	46989	1.6	10.3334	1.6	3.6514	2.8	0.2737	2.4	0.83	1559.3	32.5	1560.8	22.7	1562.8	30.0	1562.8	30.0
CCT-19	145	14139	1.1	10.2660	1.1	3.6852	1.5	0.2744	1.0	0.67	1563.0	13.9	1568.2	11.9	1575.1	20.7	1575.1	20.7
CCT-20	2316	150312	8.9	9.8561	1.8	3.3920	4.2	0.2425	3.8	0.90	1399.5	47.6	1502.5	32.8	1651.0	33.4	1651.0	33.4
CCT-53	215	23760	3.6	9.8356	2.9	3.0476	5.5	0.2174	4.7	0.85	1268.1	53.6	1419.6	41.9	1654.8	53.2	1654.8	53.2

TABLE A4

(continued)

Analysis	U (ppm)	$^{206}Pb/^{204}Pb$	U/Th	$^{206}Pb^*/^{207}Pb^*$	± (%)	Isotope Ratios					Apparent Ages (Ma)						Best age (Ma)	± (Ma)
						$^{207}Pb^*/^{235}U^*$	± (%)	$^{206}Pb^*/^{238}U$	± (%)	Err. corr	$^{206}Pb^*/^{238}U^*$	± (Ma)	$^{207}Pb^*/^{235}U$	± (Ma)	$^{206}Pb^*/^{207}Pb^*$	± (Ma)		
CCT-38	223	15435	1.1	9.7912	4.8	4.2637	6.5	0.3028	4.4	0.68	1705.1	66.5	1686.4	53.8	1663.2	88.7	1663.2	88.7
CCT-68	83	11496	1.5	9.7649	1.7	4.1330	3.9	0.2927	3.5	0.90	1655.1	51.7	1660.9	32.2	1668.2	32.0	1668.2	32.0
CCT-36	1564	15105	1.5	9.7171	2.1	3.1084	3.8	0.2191	3.2	0.83	1276.9	36.7	1434.8	29.4	1677.3	39.6	1677.3	39.6
CCT-42	4003	25680	4.3	9.6797	1.9	1.3579	8.3	0.0953	8.1	0.97	587.0	45.2	871.0	48.5	1684.4	35.3	1684.4	35.3
CCT-1	635	22155	12.1	9.6717	1.0	3.6551	1.5	0.2564	1.2	0.75	1471.3	15.1	1561.6	12.3	1685.9	18.8	1685.9	18.8
CCT-31	1057	184245	4.0	9.6094	3.2	4.4316	3.4	0.3089	1.1	0.33	1735.1	16.9	1718.3	28.1	1697.8	59.2	1697.8	59.2
CCT-7	1857	78630	21.0	9.5167	2.2	4.2641	2.9	0.2943	1.9	0.66	1663.1	28.3	1686.5	24.0	1715.7	40.1	1715.7	40.1
CCT-37	108	9441	0.9	9.5065	2.3	4.4870	6.5	0.3094	6.1	0.94	1737.6	93.5	1728.6	54.4	1717.6	41.4	1717.6	41.4
CCT-41	94	30900	1.6	9.4103	3.2	4.6979	4.0	0.3206	2.4	0.60	1792.8	37.6	1766.9	33.7	1736.3	59.3	1736.3	59.3
CCT-24	966	112869	6.1	9.3759	1.8	4.5530	4.1	0.3096	3.7	0.90	1738.8	55.9	1740.7	34.0	1743.0	32.8	1743.0	32.8
CCT-54	862	85479	1.3	9.3563	2.3	3.4228	10.1	0.2323	9.9	0.97	1346.4	119.9	1509.6	79.7	1746.9	41.2	1746.9	41.2
CCT-62	252	14094	2.1	9.3117	3.6	4.1931	3.9	0.2832	1.5	0.39	1607.4	21.2	1672.7	31.7	1755.6	65.4	1755.6	65.4
CCT-50	121	9963	1.2	9.2871	1.9	4.4278	2.3	0.2982	1.3	0.57	1682.6	19.5	1717.5	19.2	1760.4	34.9	1760.4	34.9
CCT-49	336	42135	2.8	9.2812	1.4	4.6186	2.2	0.3109	1.7	0.78	1745.1	26.3	1752.6	18.4	1761.6	25.1	1761.6	25.1
CCT-45	578	64338	2.2	9.2308	1.5	4.7271	3.3	0.3165	2.9	0.89	1772.5	44.9	1772.1	27.4	1771.6	27.4	1771.6	27.4
CCT-6	588	51873	2.5	9.2151	1.5	4.1122	2.2	0.2748	1.6	0.73	1565.3	22.4	1656.7	18.0	1774.7	27.4	1774.7	27.4
CCT-59	1659	145578	3.1	8.8443	2.5	5.2050	5.0	0.3339	4.3	0.87	1857.1	69.9	1853.4	42.6	1849.3	45.2	1849.3	45.2
CCT-66	523	47595	0.7	8.6494	1.2	5.4225	1.6	0.3402	1.0	0.63	1887.4	16.4	1888.4	13.7	1889.5	22.3	1889.5	22.3
CCT-3	685	40407	4.8	8.1200	7.6	5.2941	8.4	0.3118	3.5	0.41	1749.5	52.9	1867.9	71.5	2002.4	135.4	2002.4	135.4
CCT-5	135	42813	3.5	8.0114	1.7	6.3786	2.4	0.3706	1.7	0.69	2032.3	28.8	2029.3	20.9	2026.3	30.5	2026.3	30.5
CO22-35	949	4557	2.1	19.6780	4.7	0.0690	5.2	0.0099	2.1	0.40	63.2	1.3	67.8	3.4	232.6	109.1	63.2	1.3
CO22-20	194	1287	1.4	19.3923	12.8	0.0942	13.5	0.0132	4.2	0.31	84.8	3.5	91.4	11.8	266.2	295.1	84.8	3.5
CO22-46	105	1329	1.3	21.7646	15.6	0.0880	15.9	0.0139	3.5	0.22	88.9	3.0	85.6	13.1	-5.2	377.4	88.9	3.0
CO22-13	473	4143	2.3	18.8477	7.1	0.1032	7.4	0.0141	2.0	0.27	90.3	1.8	99.7	7.0	331.2	161.1	90.3	1.8
CO22-16	213	2196	2.0	18.2755	5.1	0.1099	5.5	0.0146	2.0	0.36	93.2	1.8	105.8	5.5	400.7	114.3	93.2	1.8
CO22-48	1239	4740	3.7	20.5607	3.6	0.0989	4.1	0.0147	2.0	0.48	94.4	1.8	95.7	3.8	130.3	85.0	94.4	1.8
CCT-19	145	14139	1.1	10.2660	1.1	3.6852	1.5	0.2744	1.0	0.67	1563.0	13.9	1568.2	11.9	1575.1	20.7	1575.1	20.7
CO22-61	533	3852	1.4	20.9751	5.5	0.0975	5.9	0.0148	2.0	0.34	95.0	1.9	94.5	5.3	83.2	131.2	95.0	1.9
CO22-68	933	4611	2.0	19.9378	2.3	0.1077	3.2	0.0156	2.3	0.71	99.6	2.3	103.9	3.2	202.2	52.3	99.6	2.3
CO22-69	810	2832	1.4	19.8979	3.3	0.1588	5.1	0.0229	3.9	0.76	146.1	5.6	149.6	7.1	206.9	76.5	146.1	5.6
CO22-64	960	2853	1.7	19.8539	3.9	0.1595	4.3	0.0230	1.7	0.41	146.4	2.5	150.2	6.0	212.0	90.6	146.4	2.5
CO22-2	668	4845	1.6	20.7826	3.5	0.1568	4.6	0.0236	2.9	0.64	150.6	4.3	147.9	6.3	105.0	83.1	150.6	4.3
CO22-70	475	2625	1.7	17.7266	6.4	0.1838	7.0	0.0236	3.0	0.42	150.6	4.4	171.3	11.1	468.6	141.0	150.6	4.4
CO22-5	297	4737	1.1	21.2089	4.5	0.1573	4.8	0.0242	1.7	0.35	154.1	2.5	148.4	6.7	56.8	107.9	154.1	2.5

Table A4
(continued)

Analysis	U (ppm)	$^{206}Pb/^{204}Pb$	U/Th	$^{206}Pb^*/^{207}Pb^*$	± (%)	Isotope Ratios $^{207}Pb^*/^{235}U^*$	± (%)	$^{206}Pb^*/^{238}U$	± (%)	Err. corr	Apparent Ages (Ma) $^{206}Pb^*/^{238}U^*$	± (Ma)	$^{207}Pb^*/^{235}U$	± (Ma)	$^{206}Pb^*/^{207}Pb^*$	± (Ma)	Best age (Ma)	± (Ma)
CO22-45	315	5463	1.0	20.1081	4.2	0.1718	5.1	0.0251	2.9	0.57	159.5	4.6	161.0	7.6	182.4	98.0	159.5	4.6
CO22-56	480	11514	1.8	20.0011	1.9	0.1782	3.1	0.0258	2.5	0.81	164.5	4.1	166.5	4.8	194.8	43.1	164.5	4.1
CO22-8	345	4653	1.7	20.9696	4.2	0.1716	4.7	0.0261	2.1	0.44	166.1	3.4	160.8	7.0	83.8	100.6	166.1	3.4
CO22-19	98	1533	2.1	18.1033	9.3	0.2041	9.5	0.0268	1.8	0.19	170.4	3.1	188.6	16.3	421.9	207.8	170.4	3.1
CO22-57	216	5010	2.3	20.4910	5.8	0.1803	6.7	0.0268	3.3	0.50	170.5	5.6	168.3	10.3	138.3	135.7	170.5	5.6
CO22-36	113	2424	1.4	20.1489	10.7	0.1898	11.1	0.0277	2.9	0.26	176.4	5.0	176.5	18.0	177.7	251.2	176.4	5.0
CO22-31	173	6405	1.9	18.1518	6.2	0.2154	6.4	0.0284	1.9	0.29	180.2	3.4	198.1	11.6	415.9	137.9	180.2	3.4
CO22-44	140	2076	1.7	20.9378	9.0	0.1906	9.1	0.0289	1.2	0.14	184.0	2.2	177.2	14.8	87.4	214.3	184.0	2.2
CO22-40	383	4152	1.0	19.4622	2.6	0.2087	4.1	0.0295	3.2	0.78	187.2	5.9	192.5	7.2	258.0	59.0	187.2	5.9
CO22-33	97	4008	4.3	19.5704	12.3	0.2227	12.3	0.0316	1.5	0.12	200.6	2.9	204.2	22.8	245.2	283.2	200.6	2.9
CO22-4	396	14925	3.4	19.5639	3.1	0.2459	5.8	0.0349	5.0	0.85	221.1	10.8	223.3	11.7	246.0	71.6	221.1	10.8
CO22-23	657	30585	3.1	17.2365	3.9	0.2798	5.1	0.0350	3.3	0.65	221.6	7.1	250.5	11.2	530.4	84.6	221.6	7.1
CO22-29	1148	4740	3.8	17.3399	3.3	0.2828	3.5	0.0356	1.0	0.29	225.3	2.2	252.9	7.8	517.2	73.2	225.3	2.2
CO22-52	685	15777	2.7	19.5774	3.8	0.2530	4.4	0.0359	2.2	0.50	227.5	4.9	229.0	9.0	244.4	87.1	227.5	4.9
CO22-25	191	2916	1.7	16.5692	4.3	0.3191	7.7	0.0383	6.4	0.83	242.6	15.2	281.2	18.9	616.2	93.1	242.6	15.2
CO22-49	353	6591	2.3	19.9581	6.0	0.2775	6.1	0.0402	1.3	0.21	253.9	3.2	248.7	13.5	199.8	139.2	253.9	3.2
CO22-53	208	11121	2.0	16.0282	26.9	0.4452	27.5	0.0518	5.3	0.19	325.3	16.7	373.9	86.1	687.5	584.9	325.3	16.7
CO22-38	289	9648	3.4	17.1026	4.1	0.5784	4.4	0.0718	1.8	0.40	446.7	7.6	463.5	16.6	547.4	89.2	446.7	7.6
CO22-59	278	13239	1.4	18.0750	3.3	0.5474	4.4	0.0718	3.0	0.68	446.8	12.9	443.3	15.8	425.4	72.6	446.8	12.9
CO22-12	135	4041	0.7	15.1922	2.8	0.6639	3.0	0.0732	1.0	0.34	455.1	4.4	517.0	12.0	800.7	58.4	455.1	4.4
CO22-42	118	5769	2.2	16.9179	3.8	0.6301	4.0	0.0773	1.2	0.30	480.1	5.6	496.2	15.7	571.1	83.0	480.1	5.6
CO22-17	320	17769	3.8	14.4849	2.5	0.8716	2.7	0.0916	1.0	0.37	564.8	5.4	636.4	12.7	899.8	51.2	564.8	5.4
CO22-7	57	10851	4.4	14.1562	2.7	1.5681	3.3	0.1610	1.9	0.58	962.3	17.0	957.7	20.4	947.0	55.1	962.3	17.0
CO22-51	30	4548	1.8	13.3990	3.5	1.8124	3.7	0.1761	1.0	0.28	1045.8	9.8	1050.0	24.2	1058.6	71.5	1058.6	71.5
CO22-41	265	32895	7.3	11.7112	1.5	2.4133	1.8	0.2050	1.0	0.55	1202.0	11.0	1246.6	13.1	1324.3	29.7	1324.3	29.7
CO22-28	71	8055	3.4	11.5435	4.3	2.2889	4.5	0.1916	1.0	0.23	1130.2	10.6	1208.9	31.5	1352.2	83.6	1352.2	83.6
CO22-26	221	19461	6.3	11.2011	1.9	2.3196	3.3	0.1884	2.7	0.82	1112.9	27.8	1218.3	23.6	1410.1	36.8	1410.1	36.8
CO22-58	94	26445	3.7	11.0259	4.3	3.0745	4.9	0.2459	2.4	0.49	1417.1	30.8	1426.3	37.8	1440.2	81.8	1440.2	81.8
CO22-32	52	12192	5.0	10.6540	3.2	2.7442	3.7	0.2120	1.9	0.52	1239.7	21.8	1340.5	27.5	1505.3	59.6	1505.3	59.6
CO22-39	286	12675	5.8	10.0458	3.8	1.1442	7.3	0.0834	6.2	0.85	516.2	30.6	774.5	39.4	1615.6	71.4	1615.6	71.4
CO22-54	50	16305	1.4	9.7076	2.0	4.1631	5.9	0.2931	5.5	0.94	1657.1	80.7	1666.8	48.2	1679.1	37.4	1679.1	37.4
CO22-3	178	13869	1.2	9.5304	1.2	4.1269	4.7	0.2853	4.5	0.97	1617.8	64.7	1659.6	38.1	1713.0	21.2	1713.0	21.2
CO22-63	719	19137	1.8	9.4114	2.0	3.5249	2.3	0.2406	1.1	0.46	1389.8	13.4	1532.8	18.2	1736.1	37.4	1736.1	37.4
CO22-65	168	14832	1.0	9.3981	2.5	4.0300	4.5	0.2747	3.7	0.82	1564.6	51.1	1640.3	36.4	1738.7	46.4	1738.7	46.4

TABLE A4

(continued)

Analysis	U (ppm)	$^{206}Pb/^{204}Pb$	U/Th	$^{206}Pb^*/^{207}Pb^*$	± (%)	Isotope Ratios					Apparent Ages (Ma)						Best age (Ma)	± (Ma)
						$^{207}Pb^*/^{235}U^*$	± (%)	$^{206}Pb^*/^{238}U$	± (%)	Err. corr	$^{206}Pb^*/^{238}U^*$	± (Ma)	$^{207}Pb^*/^{235}U$	± (Ma)	$^{206}Pb^*/^{207}Pb^*$	± (Ma)		
CO22-67	192	26874	1.7	9.3686	2.2	4.0615	2.7	0.2760	1.6	0.58	1571.0	22.3	1646.6	22.4	1744.5	40.9	1744.5	40.9
CO22-50	91	36681	1.0	9.2829	1.9	4.5039	2.6	0.3032	1.8	0.69	1707.3	26.4	1731.7	21.3	1761.3	34.2	1761.3	34.2
CO22-66	444	36174	1.9	9.0473	1.7	4.3628	2.0	0.2863	1.1	0.54	1622.9	15.5	1705.3	16.6	1808.1	30.9	1808.1	30.9
CO22-18	361	47022	1.5	8.8709	1.8	4.0560	2.5	0.2610	1.7	0.70	1494.7	23.1	1645.5	20.2	1843.8	32.0	1843.8	32.0
CO22-34	49	5229	3.7	8.4372	1.5	5.0465	2.4	0.3088	1.8	0.77	1734.8	27.5	1827.2	19.9	1934.1	26.9	1934.1	26.9
CO22-15	362	21129	2.7	8.3036	3.3	4.9940	4.1	0.3008	2.4	0.58	1695.1	35.6	1818.3	34.8	1962.6	59.6	1962.6	59.6
CO22-43	116	16230	3.3	8.2346	2.2	5.7588	3.2	0.3439	2.3	0.72	1905.6	37.9	1940.2	27.7	1977.5	39.7	1977.5	39.7
CO22-24	164	29157	2.5	8.0877	2.7	5.2933	4.0	0.3105	3.0	0.74	1743.1	45.8	1867.8	34.5	2009.5	47.9	2009.5	47.9
CO22-22	97	28377	2.1	8.0651	2.0	5.1094	2.6	0.2989	1.6	0.61	1685.7	23.3	1837.7	21.7	2014.4	35.8	2014.4	35.8
CO22-27	134	38760	2.2	8.0027	2.5	5.3199	2.9	0.3088	1.5	0.51	1734.7	22.2	1872.1	24.6	2028.2	43.9	2028.2	43.9
CO22-14	298	24030	7.0	7.6392	1.2	5.7296	5.9	0.3174	5.7	0.98	1777.3	88.9	1935.9	50.6	2110.1	21.6	2110.1	21.6
CO22-11	85	11067	4.9	7.5518	3.5	6.0244	5.9	0.3300	4.7	0.80	1838.2	75.8	1979.4	51.4	2130.3	61.3	2130.3	61.3
CO22-37	43	13257	2.7	4.8909	3.3	14.7897	5.3	0.5246	4.2	0.79	2718.8	93.2	2801.8	50.7	2862.1	53.4	2862.1	53.4
GRAP-89	150	756	1.0	25.7538	20.3	0.0508	20.5	0.0095	3.3	0.16	60.8	2.0	50.3	10.1	-428.2	536.0	60.8	2.0
GRAP-7	139	575	1.1	24.4766	14.5	0.0562	14.5	0.0100	1.0	0.07	64.0	0.6	55.5	7.9	-296.6	371.9	64.0	0.6
GRAP-79	286	1989	1.9	24.2404	14.8	0.0796	15.2	0.0140	3.1	0.21	89.6	2.8	77.8	11.3	-271.9	378.7	89.6	2.8
GRAP-85	334	2334	1.3	23.9805	13.8	0.0675	13.8	0.0117	1.4	0.10	75.3	1.0	66.4	8.9	-244.6	349.2	75.3	1.0
GRAP-73	272	2136	1.3	22.7968	14.0	0.0589	14.2	0.0097	2.5	0.17	62.5	1.5	58.1	8.0	-118.2	346.0	62.5	1.5
GRAP-15	286	2274	1.7	22.7807	8.8	0.0728	8.9	0.0120	1.0	0.11	77.1	0.8	71.4	6.1	-116.5	217.6	77.1	0.8
GRAP-11	145	1215	1.5	22.0246	8.3	0.1495	8.5	0.0239	1.9	0.22	152.2	2.8	141.5	11.3	-33.9	202.3	152.2	2.8
GRAP-32	131	2610	2.3	21.8073	8.3	0.1568	9.6	0.0248	4.8	0.50	157.9	7.5	147.9	13.2	-9.9	201.4	157.9	7.5
GRAP-75	82	1221	0.7	21.5670	6.6	0.1668	7.5	0.0261	3.7	0.49	166.0	6.0	156.6	10.9	16.7	157.9	166.0	6.0
GRAP-6	575	2165	1.8	21.5040	4.5	0.0932	4.9	0.0145	2.0	0.40	93.1	1.8	90.5	4.3	23.7	108.1	93.1	1.8
GRAP-23	1473	5760	0.7	21.2702	2.6	0.0633	3.2	0.0098	1.8	0.58	62.7	1.1	62.4	1.9	49.9	61.6	62.7	1.1
GRAP-35	869	5145	2.0	20.8862	9.2	0.0778	10.1	0.0118	4.1	0.40	75.5	3.0	76.1	7.4	93.2	218.3	75.5	3.0
GRAP-50	565	9771	1.8	20.5427	4.1	0.1719	5.6	0.0256	3.8	0.68	163.0	6.1	161.0	8.3	132.4	95.7	163.0	6.1
GRAP-34	246	6273	2.3	18.2019	2.2	0.5111	3.4	0.0675	2.6	0.76	420.9	10.5	419.2	11.6	409.7	48.8	420.9	10.5
GRAP-69	289	12726	6.4	17.9784	4.5	0.6022	4.7	0.0785	1.4	0.29	487.3	6.5	478.7	18.1	437.3	100.9	487.3	6.5
GRAP-78	242	8874	1.6	17.2540	3.3	0.6445	6.2	0.0807	5.3	0.85	500.0	25.4	505.1	24.7	528.1	72.3	500.0	25.4
GRAP-58	98	5607	1.4	16.9589	3.2	0.7674	7.5	0.0944	6.8	0.90	581.4	37.8	578.3	33.2	565.8	70.5	581.4	37.8
GRAP-64	241	6732	2.5	16.7418	2.1	0.7960	3.5	0.0966	2.9	0.80	594.7	16.2	594.6	16.0	593.8	45.9	594.7	16.2
GRAP-87	75	1563	2.5	16.2527	10.6	0.3228	12.9	0.0381	7.4	0.57	240.8	17.5	284.1	32.0	657.7	227.1	240.8	17.5
GRAP-61	266	5622	1.7	16.2338	3.5	0.7795	4.4	0.0918	2.7	0.62	566.0	14.8	585.2	19.6	660.2	74.4	566.0	14.8
GRAP-8	172	2655	0.9	15.7428	2.4	1.0022	2.6	0.1144	1.0	0.39	698.4	6.6	705.0	13.1	725.7	50.3	698.4	6.6

Table A4
(continued)

Analysis	U (ppm)	$^{206}Pb/^{204}Pb$	U/Th	$^{206}Pb^*/^{207}Pb^*$	± (%)	Isotope Ratios $^{207}Pb^*/^{235}U^*$	± (%)	$^{206}Pb^*/^{238}U$	± (%)	Err. corr	Apparent Ages (Ma) $^{206}Pb^*/^{238}U^*$	± (Ma)	$^{207}Pb^*/^{235}U$	± (Ma)	$^{206}Pb^*/^{207}Pb^*$	± (Ma)	Best age (Ma)	± (Ma)
CO22-67	192	26874	1.7	9.3686	2.2	4.0615	2.7	0.2760	1.6	0.58	1571.0	22.3	1646.6	22.4	1744.5	40.9	1744.5	40.9
GRAP-67	82	7281	2.8	13.5186	2.8	1.8733	7.5	0.1837	6.9	0.93	1087.0	69.2	1071.7	49.4	1040.7	55.8	1040.7	55.8
GRAP-71	139	23685	3.5	13.3709	2.0	1.7502	6.5	0.1697	6.2	0.95	1010.6	58.0	1027.2	42.1	1062.8	39.7	1062.8	39.7
GRAP-51	435	33648	30.4	13.0271	1.9	1.9632	6.0	0.1855	5.7	0.95	1096.9	57.9	1103.0	40.7	1115.0	38.1	1115.0	38.1
GRAP-59	99	7110	2.3	12.9108	3.5	2.0672	3.9	0.1936	1.6	0.42	1140.7	16.8	1138.0	26.4	1132.9	69.9	1132.9	69.9
GRAP-47	90	6789	2.1	12.7645	2.4	2.1575	8.0	0.1997	7.6	0.95	1173.9	81.7	1167.5	55.4	1155.5	47.9	1155.5	47.9
GRAP-56	213	18468	1.3	12.6968	1.9	2.1152	3.6	0.1948	3.1	0.85	1147.2	32.3	1153.8	25.0	1166.1	38.1	1166.1	38.1
GRAP-45	167	9564	2.6	12.2899	2.5	2.1907	3.8	0.1953	2.8	0.75	1149.9	29.8	1178.1	26.3	1230.3	49.1	1230.3	49.1
GRAP-38	49	7875	1.9	11.3392	2.7	2.8828	5.1	0.2371	4.3	0.84	1371.5	53.2	1377.4	38.5	1386.6	52.7	1386.6	52.7
GRAP-5	135	5915	1.7	11.2547	1.4	2.9852	3.3	0.2437	3.0	0.90	1405.8	37.9	1403.9	25.2	1400.9	27.1	1400.9	27.1
GRAP-13	188	15095	0.8	11.2268	1.6	3.0151	2.5	0.2455	1.9	0.76	1415.2	24.1	1411.4	19.0	1405.7	31.0	1405.7	31.0
GRAP-17	134	13782	1.1	11.1736	2.6	2.9272	2.8	0.2372	1.1	0.38	1372.2	13.3	1389.0	21.4	1414.8	50.0	1414.8	50.0
GRAP-80	95	22758	1.9	11.1382	2.0	2.9488	4.2	0.2382	3.7	0.88	1377.4	45.3	1394.5	31.6	1420.9	38.3	1420.9	38.3
GRAP-41	118	14757	2.6	11.0760	2.6	3.0451	4.5	0.2446	3.7	0.82	1410.6	47.0	1419.0	34.7	1431.6	50.0	1431.6	50.0
GRAP-13b	195	14292	2.5	11.0723	1.4	3.0315	2.5	0.2434	2.1	0.82	1404.6	25.9	1415.6	19.1	1432.2	27.5	1432.2	27.5
GRAP-76	64	11028	2.4	11.0531	1.8	3.1050	4.0	0.2489	3.6	0.90	1432.9	46.3	1433.9	30.8	1435.5	33.4	1435.5	33.4
GRAP-90	156	18267	2.2	11.0518	2.6	2.8837	4.3	0.2311	3.4	0.79	1340.5	41.3	1377.6	32.4	1435.7	49.8	1435.7	49.8
GRAP-81	106	16014	2.5	11.0454	1.6	3.0599	4.0	0.2451	3.7	0.92	1413.3	47.2	1422.7	30.9	1436.8	29.8	1436.8	29.8
GRAP-39	169	33567	2.4	11.0435	1.9	3.0216	4.3	0.2420	3.9	0.90	1397.1	48.7	1413.1	32.9	1437.2	35.9	1437.2	35.9
GRAP-25	116	21612	2.5	11.0393	1.4	3.1551	2.2	0.2526	1.7	0.77	1451.9	22.0	1446.2	16.9	1437.9	26.7	1437.9	26.7
GRAP-26	169	32976	2.3	10.9624	2.0	3.1498	2.6	0.2504	1.6	0.62	1440.7	20.8	1445.0	20.0	1451.2	38.8	1451.2	38.8
GRAP-72	126	20424	1.2	10.9303	2.3	3.0466	6.6	0.2415	6.2	0.94	1394.6	77.6	1419.4	50.4	1456.8	42.8	1456.8	42.8
GRAP-44	171	19821	1.2	10.8891	2.1	3.1075	8.2	0.2454	7.9	0.97	1414.8	100.6	1434.5	62.9	1464.0	39.0	1464.0	39.0
GRAP-66	141	28551	1.6	10.8798	2.4	3.2458	3.4	0.2561	2.4	0.70	1470.0	31.2	1468.2	26.2	1465.6	45.8	1465.6	45.8
GRAP-88	122	5055	2.9	10.8565	1.9	3.2198	2.5	0.2535	1.6	0.66	1456.6	21.4	1461.9	19.3	1469.7	35.5	1469.7	35.5
GRAP-55	388	25461	2.4	10.8035	3.4	3.2967	4.2	0.2583	2.4	0.58	1481.2	32.2	1480.3	32.6	1478.9	64.7	1478.9	64.7
GRAP-63	100	12615	1.6	10.7414	3.0	3.4206	4.4	0.2665	3.3	0.74	1522.9	44.5	1509.1	34.8	1489.9	56.3	1489.9	56.3
GRAP-27	1284	11640	13.5	10.6779	3.7	0.1727	5.7	0.0134	4.3	0.75	85.7	3.7	161.8	8.5	1501.1	70.7	85.7	3.7
GRAP-53	62	7431	1.7	10.6255	7.6	3.0343	9.9	0.2338	6.4	0.65	1354.6	78.3	1416.3	76.0	1510.4	143.6	1510.4	143.6
GRAP-70	136	29019	1.4	10.1456	1.4	3.7094	6.4	0.2729	6.3	0.98	1555.7	86.8	1573.4	51.5	1597.1	26.3	1597.1	26.3
GRAP-65	215	36258	4.9	10.1321	2.1	3.8310	3.1	0.2815	2.3	0.75	1599.0	33.1	1599.3	25.2	1599.6	38.6	1599.6	38.6
GRAP-2	656	39015	29.1	9.8468	1.8	3.8698	2.4	0.2764	1.6	0.66	1573.0	22.3	1607.4	19.5	1652.7	33.6	1652.7	33.6
GRAP-10	88	7495	1.0	9.8260	2.3	4.1947	2.7	0.2989	1.5	0.54	1686.0	22.0	1673.0	22.4	1656.7	42.6	1656.7	42.6
GRAP-4	152	10320	2.2	9.7584	2.6	4.2637	2.9	0.3018	1.1	0.39	1700.0	16.6	1686.4	23.6	1669.4	48.9	1669.4	48.9

TABLE A4
(continued)

Analysis	U (ppm)	$^{206}Pb/^{204}Pb$	U/Th	$^{206}Pb^*/^{207}Pb^*$	± (%)	Isotope Ratios: $^{207}Pb^*/^{235}U^*$	± (%)	$^{206}Pb^*/^{238}U$	± (%)	Err. corr	Apparent Ages (Ma): $^{206}Pb^*/^{238}U^*$	± (Ma)	$^{207}Pb^*/^{235}U$	± (Ma)	$^{206}Pb^*/^{207}Pb^*$	± (Ma)	Best age (Ma)	± (Ma)
GRAP-3	72	8675	1.3	9.7553	1.8	4.1632	2.0	0.2946	1.0	0.50	1664.3	14.7	1666.8	16.5	1670.0	32.4	1670.0	32.4
GRAP-18	1485	158898	23.4	9.7531	1.3	3.3985	1.7	0.2404	1.1	0.62	1388.8	13.4	1504.1	13.5	1670.4	24.8	1670.4	24.8
GRAP-12	709	89745	5.9	9.7333	1.0	4.2537	3.2	0.3003	3.1	0.95	1692.7	46.0	1684.4	26.7	1674.2	18.5	1674.2	18.5
GRAP-74	166	25680	2.8	9.7306	2.1	4.1627	3.1	0.2938	2.3	0.74	1660.4	33.8	1666.7	25.6	1674.7	39.0	1674.7	39.0
GRAP-68	746	21018	38.3	9.6944	2.8	3.7860	4.5	0.2662	3.6	0.79	1521.5	48.8	1589.8	36.6	1681.6	51.4	1681.6	51.4
GRAP-24	86	10509	1.2	9.6257	2.5	4.1872	2.9	0.2923	1.6	0.54	1653.1	23.0	1671.5	24.1	1694.7	45.8	1694.7	45.8
GRAP-12b	109	26931	1.7	9.6244	1.6	4.1538	4.0	0.2899	3.6	0.92	1641.3	52.7	1665.0	32.4	1695.0	28.8	1695.0	28.8
GRAP-29	337	13524	1.3	9.5994	2.1	3.7260	2.3	0.2594	1.0	0.43	1486.8	13.3	1577.0	18.6	1699.7	38.6	1699.7	38.6
GRAP-40	465	86466	6.2	9.5761	1.9	4.2053	5.1	0.2921	4.8	0.93	1651.8	69.5	1675.1	42.2	1704.2	35.2	1704.2	35.2
GRAP-84	707	17193	1.9	9.5421	1.3	3.4644	5.3	0.2398	5.2	0.97	1385.4	64.6	1519.2	42.0	1710.8	23.2	1710.8	23.2
GRAP-42	664	160860	6.3	9.5165	2.6	4.4293	3.3	0.3057	2.0	0.62	1719.6	30.3	1717.8	27.0	1715.7	47.1	1715.7	47.1
GRAP-48	230	37518	2.4	9.5119	2.2	4.2457	4.3	0.2929	3.8	0.87	1656.0	55.1	1682.9	35.7	1716.6	39.5	1716.6	39.5
GRAP-86	356	29190	2.1	9.4413	1.1	4.4404	2.5	0.3041	2.3	0.90	1711.4	34.0	1719.9	20.9	1730.3	20.6	1730.3	20.6
GRAP-22	479	43251	3.4	9.4063	1.4	3.9798	4.1	0.2715	3.9	0.94	1548.4	53.5	1630.1	33.5	1737.1	25.5	1737.1	25.5
GRAP-60	139	33225	1.8	9.3166	1.0	4.5681	3.4	0.3087	3.3	0.96	1734.1	50.0	1743.5	28.7	1754.7	18.7	1754.7	18.7
GRAP-83	395	37824	6.5	9.1589	1.5	4.5016	3.1	0.2990	2.7	0.87	1686.5	39.5	1731.3	25.4	1785.8	27.4	1785.8	27.4
GRAP-52	346	50385	2.3	9.0422	2.6	4.3564	9.5	0.2857	9.1	0.96	1620.0	130.7	1704.1	78.5	1809.2	47.6	1809.2	47.6
GRAP-82	2111	4455	3.5	8.7685	5.6	0.8318	7.8	0.0529	5.5	0.70	332.3	17.7	614.6	36.0	1864.8	100.9	1864.8	100.9
GRAP-46	116	7671	2.7	8.5068	1.0	5.5125	3.2	0.3401	3.0	0.95	1887.2	48.9	1902.6	27.1	1919.3	18.0	1919.3	18.0
GRAP-54	127	26547	2.1	8.5006	1.1	5.4714	5.0	0.3373	4.9	0.98	1873.8	79.5	1896.1	43.0	1920.6	19.4	1920.6	19.4
GRAP-14	137	23754	2.7	5.5660	1.5	12.0014	2.2	0.4845	1.6	0.75	2546.8	34.5	2604.5	20.5	2649.7	24.1	2649.7	24.1
GRF10-57	181	1160	0.9	20.3009	14.1	0.0760	14.3	0.0112	2.3	0.16	71.7	1.6	74.3	10.3	160.1	331.9	71.7	1.6
GRF10-6	230	1485	0.8	20.9367	15.2	0.0743	15.3	0.0113	1.8	0.12	72.3	1.3	72.7	10.7	87.5	361.8	72.3	1.3
GRF10-35	143	5180	2.9	20.8527	19.8	0.0769	20.0	0.0116	2.6	0.13	74.6	1.9	75.3	14.5	97.0	473.6	74.6	1.9
GRF10-58	198	1270	0.6	22.4981	25.1	0.0720	25.2	0.0117	1.9	0.07	75.3	1.4	70.6	17.2	-85.8	623.4	75.3	1.4
GRF10-50	284	1955	1.5	18.1401	40.5	0.0965	40.6	0.0127	2.1	0.05	81.3	1.7	93.5	36.3	417.3	941.5	81.3	1.7
GRF10-37	527	2255	1.4	16.3503	12.2	0.1132	12.6	0.0134	2.8	0.22	85.9	2.4	108.9	13.0	644.9	264.0	85.9	2.4
GRF10-10	1120	11530	1.4	20.8761	6.3	0.0926	6.5	0.0140	1.5	0.22	89.7	1.3	89.9	5.6	94.4	149.9	89.7	1.3
GRF10-59	710	7320	3.0	19.9751	8.1	0.0983	8.2	0.0142	1.6	0.19	91.1	1.4	95.2	7.5	197.9	187.6	91.1	1.4
GRF10-68	408	2435	2.1	20.5778	6.8	0.0961	7.1	0.0143	2.0	0.28	91.8	1.8	93.1	6.3	128.4	159.9	91.8	1.8
GRF10-62	206	1635	0.8	20.7650	14.3	0.0975	14.6	0.0147	2.7	0.18	94.0	2.5	94.5	13.2	107.0	340.4	94.0	2.5
GRF10-75	144	835	0.8	17.8369	8.7	0.1138	8.9	0.0147	2.1	0.24	94.2	2.0	109.4	9.3	454.9	193.1	94.2	2.0
GRF10-39	1153	6600	1.2	20.5699	4.2	0.0989	7.7	0.0147	6.5	0.84	94.4	6.1	95.7	7.0	129.3	98.4	94.4	6.1
GRF10-13	675	2220	1.4	12.6098	15.7	0.1658	15.9	0.0152	2.3	0.15	97.0	2.2	155.8	23.0	1179.7	312.8	97.0	2.2

Table A4
(continued)

Analysis	U (ppm)	$^{206}Pb/^{204}Pb$	U/Th	$^{206}Pb^*/^{207}Pb^*$	± (%)	Isotope Ratios					Apparent Ages (Ma)						Best age (Ma)	± (Ma)
						$^{207}Pb^*/^{235}U^*$	± (%)	$^{206}Pb^*/^{238}U$	± (%)	Err. corr	$^{206}Pb^*/^{238}U^*$	± (Ma)	$^{207}Pb^*/^{235}U$	± (Ma)	$^{206}Pb^*/^{207}Pb^*$	± (Ma)		
GRF10-56	111	1275	1.9	21.5758	22.4	0.1004	22.5	0.0157	2.5	0.11	100.5	2.5	97.1	20.9	15.7	544.1	100.5	2.5
GRF10-12	599	6815	1.6	20.5377	5.6	0.1132	6.2	0.0169	2.5	0.41	107.8	2.7	108.9	6.4	133.0	132.1	107.8	2.7
GRF10-5	1074	4240	2.1	18.4840	24.8	0.1323	25.0	0.0177	3.0	0.12	113.3	3.4	126.1	29.6	375.2	565.9	113.3	3.4
GRF10-8	216	3820	0.6	20.7570	11.6	0.1519	11.7	0.0229	1.8	0.15	145.7	2.6	143.6	15.7	107.9	275.0	145.7	2.6
GRF10-7	149	2140	2.0	19.4009	6.5	0.1643	6.6	0.0231	1.4	0.21	147.3	2.1	154.4	9.5	265.2	148.4	147.3	2.1
GRF10-18	44	10165	0.6	23.8305	29.8	0.1368	30.2	0.0236	4.7	0.15	150.7	7.0	130.2	36.9	-228.8	766.3	150.7	7.0
GRF10-42	75	1170	0.6	22.2674	28.0	0.1480	28.1	0.0239	1.0	0.04	152.3	1.5	140.1	36.8	-60.6	695.7	152.3	1.5
GRF10-23	58	10830	1.7	25.8109	46.4	0.1277	46.4	0.0239	1.4	0.03	152.3	2.0	122.0	53.4	-434.1	1277.2	152.3	2.0
GRF10-45	279	3440	0.8	20.4446	7.7	0.1664	8.7	0.0247	4.1	0.47	157.1	6.4	156.3	12.6	143.6	179.9	157.1	6.4
GRF10-53	560	7555	2.1	20.2046	3.9	0.1709	4.5	0.0250	2.2	0.49	159.5	3.4	160.2	6.6	171.3	90.5	159.5	3.4
GRF10-65	463	5180	1.4	20.1689	3.7	0.1719	4.0	0.0251	1.5	0.36	160.1	2.3	161.0	5.9	175.4	86.7	160.1	2.3
GRF10-26	369	4940	0.8	20.4112	8.4	0.1713	8.6	0.0254	1.9	0.22	161.5	3.0	160.6	12.8	147.5	197.1	161.5	3.0
GRF10-38	299	5890	1.7	20.7562	7.6	0.1694	8.3	0.0255	3.3	0.40	162.4	5.2	158.9	12.2	108.0	179.5	162.4	5.2
GRF10-28	1724	29560	0.6	19.8710	2.0	0.1778	2.4	0.0256	1.4	0.57	163.1	2.2	166.2	3.7	210.0	46.4	163.1	2.2
GRF10-74	713	5740	0.6	19.7858	3.1	0.1791	5.5	0.0257	4.5	0.83	163.6	7.3	167.3	8.4	219.9	70.7	163.6	7.3
GRF10-25	946	17285	1.2	20.1881	2.6	0.1758	3.3	0.0257	2.1	0.62	163.9	3.3	164.5	5.1	173.2	61.3	163.9	3.3
GRF10-73	771	8650	1.5	20.2298	2.5	0.1755	2.6	0.0258	1.0	0.38	163.9	1.6	164.2	4.0	168.4	57.3	163.9	1.6
GRF10-34	76	1220	1.1	23.6211	34.1	0.1508	34.1	0.0258	1.0	0.03	164.4	1.6	142.6	45.4	-206.6	877.9	164.4	1.6
GRF10-20	292	4355	0.5	19.6143	3.8	0.1835	3.9	0.0261	1.0	0.25	166.1	1.6	171.1	6.2	240.1	87.9	166.1	1.6
GRF10-51	1199	15370	1.3	18.1608	20.3	0.2013	20.4	0.0265	2.7	0.13	168.7	4.4	186.2	34.8	414.8	457.0	168.7	4.4
GRF10-32	505	7045	1.0	20.0714	4.7	0.1832	5.2	0.0267	2.0	0.39	169.7	3.4	170.9	8.1	186.7	110.6	169.7	3.4
GRF10-61	780	6860	0.8	20.3236	3.6	0.1816	3.7	0.0268	1.0	0.27	170.3	1.7	169.4	5.8	157.5	83.2	170.3	1.7
GRF10-71	539	7410	1.0	19.9011	4.7	0.1867	4.8	0.0269	1.0	0.21	171.4	1.7	173.8	7.6	206.5	108.1	171.4	1.7
GRF10-33	265	3605	1.9	20.1079	7.7	0.1848	8.2	0.0270	2.7	0.33	171.5	4.5	172.2	13.0	182.5	180.6	171.5	4.5
GRF10-49	382	6810	2.0	19.8900	2.1	0.1878	4.1	0.0271	3.6	0.86	172.3	6.1	174.8	6.6	207.8	48.6	172.3	6.1
GRF10-52	201	4190	1.9	20.2058	6.5	0.1861	6.9	0.0273	2.1	0.31	173.5	3.7	173.3	11.0	171.1	153.0	173.5	3.7
GRF10-66	259	3190	2.1	19.7169	4.8	0.1909	5.8	0.0273	3.3	0.57	173.6	5.7	177.4	9.5	228.0	110.5	173.6	5.7
GRF10-1	416	5895	1.5	20.2378	4.0	0.1862	4.1	0.0273	1.0	0.24	173.8	1.7	173.4	6.5	167.4	92.8	173.8	1.7
GRF10-27	283	5270	1.9	20.3134	6.1	0.1876	6.3	0.0276	1.7	0.27	175.8	2.9	174.6	10.2	158.7	142.9	175.8	2.9
GRF10-48	338	5045	2.2	20.0674	7.9	0.1912	8.1	0.0278	1.7	0.21	176.9	2.9	177.7	13.2	187.1	184.3	176.9	2.9
GRF10-43	229	2135	0.8	19.3696	5.2	0.1993	5.5	0.0280	1.5	0.28	178.0	2.7	184.5	9.2	268.9	120.2	178.0	2.7
GRF10-31	651	13525	2.8	19.9302	3.6	0.2232	4.5	0.0323	2.7	0.60	204.7	5.4	204.5	8.3	203.1	83.0	204.7	5.4
GRF10-3	624	12820	1.5	19.7771	3.7	0.2393	3.8	0.0343	1.0	0.26	217.6	2.1	217.8	7.5	221.0	85.7	217.6	2.1
GRF10-60	167	3190	1.4	19.2887	4.7	0.2545	5.0	0.0356	1.8	0.36	225.5	4.0	230.2	10.3	278.5	107.2	225.5	4.0

TABLE A4
(continued)

Analysis	U (ppm)	$^{206}Pb/^{204}Pb$	U/Th	$^{206}Pb^*/^{207}Pb^*$	± (%)	Isotope Ratios $^{207}Pb^*/^{235}U^*$	± (%)	$^{206}Pb^*/^{238}U$	± (%)	Err. corr	Apparent Ages (Ma) $^{206}Pb^*/^{238}U^*$	± (Ma)	$^{207}Pb^*/^{235}U$	± (Ma)	$^{206}Pb^*/^{207}Pb^*$	± (Ma)	Best age (Ma)	± (Ma)
GRF10-9	585	15715	2.6	19.7058	1.0	0.2540	1.4	0.0363	1.0	0.71	229.9	2.3	229.8	2.9	229.3	23.2	229.9	2.3
GRF10-14	1269	21860	2.8	19.3911	2.0	0.2591	2.7	0.0364	1.9	0.68	230.8	4.2	234.0	5.7	266.4	45.7	230.8	4.2
GRF10-30	649	14415	2.9	19.4508	3.3	0.2604	3.5	0.0367	1.0	0.29	232.6	2.3	235.0	7.3	259.3	76.4	232.6	2.3
GRF10-4	775	12270	2.1	19.3024	2.3	0.2634	2.6	0.0369	1.1	0.43	233.5	2.5	237.4	5.4	276.9	53.0	233.5	2.5
GRF10-64	216	3500	2.2	19.1773	4.6	0.2693	4.7	0.0375	1.0	0.21	237.0	2.3	242.1	10.2	291.8	105.4	237.0	2.3
GRF10-67	175	2970	1.7	19.0405	5.7	0.3087	6.3	0.0426	2.8	0.44	269.1	7.3	273.2	15.2	308.1	129.8	269.1	7.3
GRF10-41	135	16895	1.7	11.4947	3.1	2.7464	3.8	0.2290	2.2	0.57	1329.1	26.1	1341.1	28.2	1360.4	59.8	1360.4	59.8
GRF10-40	187	24190	1.1	10.7323	1.9	3.2043	3.9	0.2494	3.4	0.87	1435.5	44.0	1458.2	30.3	1491.5	36.0	1491.5	36.0
GRF10-55	28	5985	1.2	9.7136	3.6	4.3036	3.8	0.3032	1.0	0.26	1707.1	15.0	1694.0	31.1	1677.9	67.3	1677.9	67.3
GRF10-63	308	35715	2.3	9.6980	2.7	4.1798	4.0	0.2940	2.9	0.74	1661.4	42.8	1670.1	32.5	1680.9	49.5	1680.9	49.5
GRF10-70	157	25780	2.3	9.6436	1.4	4.2968	3.1	0.3005	2.8	0.89	1693.9	41.3	1692.8	25.6	1691.3	25.8	1691.3	25.8
GRF10-24	187	18955	1.6	9.6225	3.5	3.9939	3.9	0.2787	1.8	0.45	1584.9	24.6	1632.9	31.5	1695.3	63.8	1695.3	63.8
GRF10-54	487	28160	1.4	9.4712	2.3	3.7361	3.1	0.2566	2.1	0.67	1472.6	27.4	1579.1	25.0	1724.5	42.6	1724.5	42.6
GRF10-2	171	28105	1.8	9.4462	1.0	4.4512	1.4	0.3050	1.0	0.71	1715.8	15.1	1721.9	11.7	1729.3	18.4	1729.3	18.4
GRF10-21	624	87750	1.6	9.4390	1.3	4.1787	1.7	0.2861	1.0	0.60	1621.8	14.3	1669.9	13.6	1730.7	24.4	1730.7	24.4
GRF10-47	361	21185	1.3	9.3686	1.7	4.0304	2.4	0.2739	1.7	0.70	1560.4	23.4	1640.4	19.5	1744.5	31.2	1744.5	31.2
GRF10-72	293	27805	2.3	9.3475	1.4	4.6080	1.7	0.3124	1.0	0.60	1752.5	15.5	1750.7	14.1	1748.6	24.9	1748.6	24.9
GRF10-11	389	69705	5.2	9.3030	1.5	4.6113	3.4	0.3111	3.1	0.90	1746.3	46.7	1751.3	28.4	1757.3	27.4	1757.3	27.4
GRF10-69	275	18655	1.6	9.1656	6.4	4.4828	6.9	0.2980	2.5	0.36	1681.4	36.4	1727.8	57.0	1784.5	116.8	1784.5	116.8
GRF10-17	420	23365	1.8	9.1565	2.4	4.3906	2.8	0.2916	1.3	0.49	1649.4	19.5	1710.6	22.8	1786.3	43.9	1786.3	43.9
GRF10-15	555	20980	1.4	8.9347	2.1	3.4150	11.2	0.2213	11.0	0.98	1288.7	128.3	1507.9	88.0	1830.9	37.6	1830.9	37.6
GRF10-19	618	122660	2.0	8.6707	1.2	5.1684	1.7	0.3250	1.3	0.74	1814.2	20.2	1847.4	14.6	1885.1	20.7	1885.1	20.7
GRF10-36	1020	935	3.3	8.1931	5.2	0.2684	5.6	0.0159	2.2	0.39	102.0	2.2	241.4	12.1	1986.5	92.7	1986.5	92.7
GRF10-29	3733	7265	6.8	8.1251	6.1	1.5663	7.4	0.0923	4.3	0.58	569.1	23.2	957.0	45.9	2001.3	107.6	2001.3	107.6
GRGG-41	409	3981	1.9	21.2708	5.3	0.0863	7.1	0.0133	4.7	0.67	85.2	4.0	84.0	5.7	49.9	126.4	85.2	4.0
GRGG-68	252	1566	1.3	21.3826	8.5	0.0890	9.1	0.0138	3.2	0.35	88.4	2.8	86.6	7.5	37.3	204.0	88.4	2.8
GRGG-74	285	987	1.2	21.3384	8.6	0.1067	9.0	0.0165	2.5	0.27	105.6	2.6	102.9	8.8	42.3	206.6	105.6	2.6
GRGG-17	111	2211	1.1	20.3474	7.6	0.2290	8.0	0.0338	2.5	0.31	214.3	5.3	209.4	15.1	154.8	177.6	214.3	5.3
GRGG-63	788	951	2.6	10.5123	5.9	0.6044	6.9	0.0461	3.7	0.53	290.4	10.5	480.0	26.6	1530.6	110.6	290.4	10.5
GRGG-24	96	3153	0.8	19.6953	8.1	0.3318	9.4	0.0474	4.7	0.51	298.5	13.8	290.9	23.7	230.5	186.6	298.5	13.8
GRGG-55	306	13020	2.1	18.5776	2.4	0.3910	3.4	0.0527	2.3	0.69	331.0	7.5	335.1	9.6	363.9	55.0	331.0	7.5
GRGG-71	440	5589	6.5	17.5147	4.7	0.5086	4.9	0.0646	1.2	0.25	403.6	4.8	417.5	16.7	495.2	103.9	403.6	4.8
GRGG-60	508	8226	2.2	18.1055	2.4	0.5014	3.8	0.0658	2.9	0.76	411.1	11.5	412.7	12.8	421.6	54.5	411.1	11.5
GRGG-39	308	10311	2.0	18.0479	3.0	0.5201	3.8	0.0681	2.3	0.61	424.6	9.5	425.2	13.1	428.7	66.1	424.6	9.5

Table A4
(continued)

Analysis	U (ppm)	$^{206}Pb/^{204}Pb$	U/Th	$^{206}Pb^*/^{207}Pb^*$	± (%)	Isotope Ratios $^{207}Pb^*/^{235}U^*$	± (%)	$^{206}Pb^*/^{238}U$	± (%)	Err. corr	Apparent Ages (Ma) $^{206}Pb^*/^{238}U^*$	± (Ma)	$^{207}Pb^*/^{235}U$	± (Ma)	$^{206}Pb^*/^{207}Pb^*$	± (Ma)	Best age (Ma)	± (Ma)
GRGG-28	228	9330	1.5	18.0013	3.6	0.5462	7.5	0.0713	6.6	0.88	444.0	28.3	442.5	26.9	434.5	79.9	444.0	28.3
GRGG-45	260	14412	1.8	17.4335	4.6	0.5653	4.7	0.0715	1.3	0.28	445.0	5.7	455.0	17.4	505.4	100.3	445.0	5.7
GRGG-59	77	2634	1.3	18.3659	5.4	0.5586	6.0	0.0744	2.5	0.42	462.7	11.3	450.6	21.8	389.6	122.1	462.7	11.3
GRGG-12	578	5493	0.9	15.2200	3.1	0.7675	5.1	0.0847	4.0	0.79	524.3	20.3	578.4	22.5	796.9	66.0	524.3	20.3
GRGG-46	422	13467	1.4	17.2371	1.4	0.6968	2.7	0.0871	2.3	0.85	538.4	11.7	536.9	11.1	530.3	31.0	538.4	11.7
GRGG-50	146	11286	1.9	16.4485	2.3	0.8285	3.6	0.0988	2.8	0.78	607.6	16.1	612.8	16.4	632.0	48.5	607.6	16.1
GRGG-35	59	4227	1.7	15.1582	3.4	1.1291	6.3	0.1241	5.3	0.84	754.3	37.4	767.3	33.8	805.4	71.9	754.3	37.4
GRGG-62	231	19008	1.8	13.8944	1.4	1.5510	1.9	0.1563	1.3	0.68	936.1	11.5	950.9	12.0	985.1	29.1	936.1	11.5
GRGG-33	129	18426	2.3	13.9967	2.7	1.6189	4.6	0.1643	3.7	0.81	980.9	33.8	977.6	28.9	970.2	55.5	970.2	55.5
GRGG-44	187	7299	2.9	13.8072	3.2	1.7112	3.4	0.1714	1.3	0.38	1019.6	12.3	1012.7	22.1	997.9	64.9	997.9	64.9
GRGG-56	425	65265	3.1	13.4149	2.6	1.7801	3.8	0.1732	2.8	0.73	1029.7	26.3	1038.2	24.7	1056.2	52.4	1056.2	52.4
GRGG-4	121	10089	1.0	13.3623	1.7	1.6934	2.0	0.1641	1.0	0.50	979.6	9.1	1006.0	12.9	1064.1	35.2	1064.1	35.2
GRGG-51	64	4806	2.2	13.2395	4.2	1.6857	4.5	0.1619	1.6	0.36	967.1	14.7	1003.1	28.7	1082.7	84.1	1082.7	84.1
GRGG-22	78	6795	0.9	13.1342	1.3	1.7650	4.8	0.1681	4.6	0.96	1001.8	43.0	1032.7	31.1	1098.7	25.4	1098.7	25.4
GRGG-8	395	27315	1.7	13.0523	3.0	1.9164	4.0	0.1814	2.6	0.65	1074.7	25.6	1086.8	26.7	1111.2	60.7	1111.2	60.7
GRGG-65	71	9165	2.1	12.8735	1.5	1.9495	3.5	0.1820	3.2	0.91	1078.0	31.4	1098.3	23.4	1138.7	29.2	1138.7	29.2
GRGG-42	74	7494	1.5	12.6829	2.2	2.1502	2.9	0.1978	1.9	0.65	1163.4	20.1	1165.1	20.1	1168.3	43.6	1168.3	43.6
GRGG-30	83	11544	3.0	12.6808	2.7	2.1865	3.5	0.2011	2.3	0.64	1181.2	24.3	1176.7	24.6	1168.6	53.8	1168.6	53.8
GRGG-25	90	16599	3.2	12.6671	2.8	2.0963	8.8	0.1926	8.3	0.95	1135.4	86.8	1147.6	60.6	1170.7	56.1	1170.7	56.1
GRGG-53	204	12624	1.3	12.5985	1.8	2.1964	3.5	0.2007	3.0	0.86	1179.0	32.6	1179.9	24.5	1181.5	35.0	1181.5	35.0
GRGG-3	409	40341	3.4	12.4608	2.2	2.1577	3.7	0.1950	3.0	0.81	1148.4	31.7	1167.5	25.9	1203.2	43.4	1203.2	43.4
GRGG-2	134	20139	1.8	12.4157	1.8	2.1480	2.9	0.1934	2.3	0.78	1139.9	24.0	1164.4	20.4	1210.3	36.2	1210.3	36.2
GRGG-49	449	28572	1.6	12.2498	2.3	2.3922	2.9	0.2125	1.7	0.60	1242.3	19.7	1240.3	20.7	1236.7	45.1	1236.7	45.1
GRGG-57	345	4422	3.5	11.9465	6.4	1.8900	6.6	0.1638	1.3	0.19	977.6	11.3	1077.6	43.6	1285.7	125.5	1285.7	125.5
GRGG-27	100	20010	2.0	10.9795	1.9	3.0234	4.9	0.2408	4.5	0.92	1390.6	56.5	1413.5	37.4	1448.2	36.3	1448.2	36.3
GRGG-14	110	19383	2.3	10.9292	2.5	3.1355	7.4	0.2485	6.9	0.94	1430.9	88.9	1441.4	56.8	1457.0	47.9	1457.0	47.9
GRGG-34	88	10584	1.8	10.8607	2.5	3.2492	4.5	0.2559	3.8	0.84	1469.0	49.5	1469.0	35.0	1468.9	46.9	1468.9	46.9
GRGG-7	248	16125	3.6	10.8072	1.6	2.9098	10.1	0.2281	10.0	0.99	1324.4	119.6	1384.5	76.6	1478.3	30.7	1478.3	30.7
GRGG-64	206	27960	2.5	10.5711	1.7	3.3781	2.1	0.2590	1.2	0.59	1484.7	16.3	1499.3	16.4	1520.1	31.9	1520.1	31.9
GRGG-66	71	13491	0.8	10.4123	1.2	3.4976	3.7	0.2641	3.4	0.94	1510.9	46.3	1526.7	28.9	1548.5	23.1	1548.5	23.1
GRGG-38	126	14034	1.4	10.2333	2.3	3.6532	3.1	0.2711	2.1	0.67	1546.6	28.2	1561.2	24.5	1581.1	42.7	1581.1	42.7
GRGG-19	322	47727	1.1	10.0232	1.7	3.7057	3.4	0.2694	2.9	0.86	1537.7	39.5	1572.6	26.9	1619.7	31.8	1619.7	31.8
GRGG-37	57	13467	1.8	9.9135	1.7	4.0181	3.2	0.2889	2.8	0.85	1636.0	39.7	1637.9	26.2	1640.2	31.2	1640.2	31.2
GRGG-21	174	24798	1.3	9.9081	1.8	3.8206	5.0	0.2745	4.7	0.93	1563.8	64.8	1597.1	40.2	1641.2	33.0	1641.2	33.0

TABLE A4
(continued)

Analysis	U (ppm)	$^{206}Pb/^{204}Pb$	U/Th	$^{206}Pb^*/^{207}Pb^*$	± (%)	Isotope Ratios $^{207}Pb^*/^{235}U^*$	± (%)	$^{206}Pb^*/^{238}U$	± (%)	Err. corr	Apparent Ages (Ma) $^{206}Pb^*/^{238}U^*$	± (Ma)	$^{207}Pb^*/^{235}U$	± (Ma)	$^{206}Pb^*/^{207}Pb^*$	± (Ma)	Best age (Ma)	± (Ma)
GRGG-11	518	92985	4.4	9.8621	1.3	3.8370	2.8	0.2744	2.5	0.89	1563.3	35.3	1600.5	23.0	1649.9	23.9	1649.9	23.9
GRGG-20	213	13338	1.6	9.8177	3.0	3.4265	5.1	0.2440	4.1	0.80	1407.4	51.3	1510.5	39.9	1658.2	56.3	1658.2	56.3
GRGG-61	402	18093	1.4	9.8059	2.5	4.0900	4.5	0.2909	3.7	0.83	1645.9	54.0	1652.3	36.5	1660.4	45.8	1660.4	45.8
GRGG-40	151	22101	1.2	9.7841	3.1	4.1154	4.5	0.2920	3.2	0.72	1651.7	46.6	1657.4	36.4	1664.6	57.4	1664.6	57.4
GRGG-52	209	27924	1.2	9.7557	2.3	4.0964	3.1	0.2898	2.1	0.68	1640.7	30.7	1653.6	25.5	1669.9	42.5	1669.9	42.5
GRGG-73	154	21603	2.0	9.6436	1.4	3.8891	2.1	0.2720	1.6	0.77	1551.0	22.5	1611.4	17.1	1691.3	25.1	1691.3	25.1
GRGG-9	105	13998	2.9	9.6324	1.8	4.1468	3.3	0.2897	2.8	0.85	1640.0	40.1	1663.6	26.8	1693.4	32.3	1693.4	32.3
GRGG-72	260	31695	1.0	9.5993	1.1	3.9674	2.6	0.2762	2.4	0.91	1572.3	33.5	1627.6	21.4	1699.8	20.1	1699.8	20.1
GRGG-31	195	15795	1.2	9.5849	3.1	4.3333	3.8	0.3012	2.2	0.58	1697.4	33.1	1699.7	31.7	1702.5	57.9	1702.5	57.9
GRGG-16	217	56580	3.8	9.4129	3.2	4.3936	6.5	0.2999	5.7	0.87	1691.0	84.6	1711.1	53.9	1735.8	58.0	1735.8	58.0
GRGG-13	56	6348	2.2	9.3238	1.8	4.4660	4.5	0.3020	4.1	0.92	1701.2	61.5	1724.7	37.2	1753.2	32.7	1753.2	32.7
GRGG-47	121	19257	3.5	9.0797	1.6	4.7590	3.8	0.3134	3.4	0.90	1757.4	52.3	1777.7	31.5	1801.6	29.1	1801.6	29.1
GRGG-18	929	41310	4.4	9.0600	1.8	4.8189	2.1	0.3166	1.0	0.48	1773.3	15.5	1788.2	17.6	1805.6	33.5	1805.6	33.5
GRGG-32	814	35667	4.0	8.9189	2.4	4.6212	2.9	0.2989	1.7	0.58	1686.0	24.9	1753.1	24.1	1834.1	42.6	1834.1	42.6
GRGG-6	190	24684	3.5	8.8531	1.6	4.9622	4.8	0.3186	4.5	0.94	1783.0	70.7	1812.9	40.8	1847.5	29.7	1847.5	29.7
GRGG-26	76	10413	1.7	8.7327	1.8	5.0927	2.8	0.3225	2.2	0.78	1802.2	34.4	1834.9	23.8	1872.2	31.6	1872.2	31.6
GRGG-70	407	101160	8.7	7.7778	2.0	6.4135	3.5	0.3618	2.9	0.81	1990.6	49.0	2034.1	30.9	2078.5	35.9	2078.5	35.9
GRGG-75	494	8832	2.4	7.0408	6.2	7.2970	9.1	0.3726	6.6	0.73	2041.7	115.5	2148.4	81.3	2252.1	108.0	2252.1	108.0
GRGG-36	44	17595	0.9	5.3900	2.4	12.8389	4.5	0.5019	3.8	0.85	2621.9	81.4	2667.9	42.0	2702.9	39.0	2702.9	39.0
GRGG-43	68	19692	0.6	5.1901	2.4	14.1597	3.0	0.5330	1.8	0.61	2754.1	41.2	2760.5	28.8	2765.1	39.6	2765.1	39.6
GRGG-10	99	39891	1.3	5.0591	2.0	14.2333	3.8	0.5223	3.2	0.85	2708.7	70.8	2765.4	35.9	2807.0	32.9	2807.0	32.9
KMTB-22	236	1905	1.2	19.5860	3.2	0.3402	3.4	0.0483	1.1	0.32	304.2	3.2	297.3	8.6	243.4	73.2	304.2	3.2
KMTB-64	2323	12115	20.6	11.7060	5.2	0.7822	9.4	0.0664	7.8	0.83	414.5	31.4	586.7	41.9	1325.2	100.6	414.5	31.4
KMTB-72	390	3500	1.1	18.2670	2.0	0.5265	2.3	0.0698	1.2	0.53	434.7	5.2	429.5	8.1	401.7	44.0	434.7	5.2
KMTB-53	850	8795	1.8	16.6722	1.7	0.6967	2.9	0.0842	2.3	0.81	521.4	11.6	536.8	11.9	602.8	36.5	521.4	11.6
KMTB-37	500	5920	2.3	16.8819	1.8	0.7905	3.3	0.0968	2.8	0.85	595.6	16.1	591.5	14.9	575.7	38.2	595.6	16.1
KMTB-12	287	4090	4.3	13.6276	1.5	1.5521	1.8	0.1534	1.0	0.55	920.0	8.6	951.3	11.3	1024.5	30.9	1024.5	30.9
KMTB-68	48	2415	1.0	13.3299	2.9	1.9535	3.4	0.1889	1.7	0.49	1115.2	16.9	1099.6	22.5	1069.0	58.6	1069.0	58.6
KMTB-31	106	3295	1.3	13.0260	2.1	2.0009	2.7	0.1890	1.7	0.62	1116.1	16.9	1115.8	18.2	1115.2	42.2	1115.2	42.2
KMTB-47	353	14920	1.8	12.7437	2.2	2.1497	2.6	0.1987	1.4	0.54	1168.3	15.2	1165.0	18.2	1158.8	43.6	1158.8	43.6
KMTB-38	61	1995	2.9	12.1226	3.4	2.4584	3.6	0.2161	1.0	0.28	1261.5	11.5	1259.9	25.8	1257.2	67.0	1257.2	67.0
KMTB-66	158	17230	1.2	11.5350	3.2	2.7399	3.7	0.2292	1.7	0.47	1330.4	20.6	1339.4	27.3	1353.7	62.6	1353.7	62.6
KMTB-42	55	2410	1.3	11.4189	2.2	2.9548	2.5	0.2447	1.0	0.41	1411.1	12.7	1396.1	18.6	1373.1	43.1	1373.1	43.1
KMTB-69	138	5165	1.5	11.3376	2.4	2.8914	3.1	0.2378	2.0	0.63	1375.0	24.5	1379.7	23.6	1386.9	46.6	1386.9	46.6

Table A4
(continued)

Analysis	U (ppm)	$^{206}Pb/^{204}Pb$	U/Th	$^{206}Pb^*/^{207}Pb^*$	± (%)	Isotope Ratios: $^{207}Pb^*/^{235}U^*$	± (%)	$^{206}Pb^*/^{238}U$	± (%)	Err. corr	Apparent Ages (Ma): $^{206}Pb^*/^{238}U^*$	± (Ma)	$^{207}Pb^*/^{235}U$	± (Ma)	$^{206}Pb^*/^{207}Pb^*$	± (Ma)	Best age (Ma)	± (Ma)
KMTB-58	106	21605	1.2	11.2625	1.3	2.8587	1.9	0.2335	1.4	0.74	1352.9	16.8	1371.1	14.0	1399.6	24.0	1399.6	24.0
KMTB-29	105	5910	2.0	11.2007	1.7	3.0498	2.6	0.2478	2.0	0.76	1426.9	25.5	1420.2	20.1	1410.2	32.9	1410.2	32.9
KMTB-70	431	11390	1.6	11.1670	2.4	3.0639	2.6	0.2481	1.0	0.39	1428.9	12.8	1423.7	19.9	1415.9	45.8	1415.9	45.8
KMTB-11	178	3670	2.2	11.1545	3.8	3.1010	3.9	0.2509	1.0	0.25	1443.0	12.9	1432.9	30.2	1418.1	72.7	1418.1	72.7
KMTB-50	119	5100	1.8	11.1473	2.2	2.7207	3.7	0.2200	3.0	0.80	1281.7	34.6	1334.1	27.6	1419.3	42.4	1419.3	42.4
KMTB-30	94	6450	1.8	11.1253	2.4	3.0244	2.6	0.2440	1.0	0.39	1407.6	12.6	1413.8	19.6	1423.1	45.3	1423.1	45.3
KMTB-46	158	9535	1.7	11.1250	1.1	3.0249	2.0	0.2441	1.7	0.84	1407.8	21.4	1413.9	15.3	1423.1	20.7	1423.1	20.7
KMTB-77	204	7520	1.7	11.1135	1.7	3.1081	2.0	0.2505	1.0	0.51	1441.2	12.9	1434.7	15.1	1425.1	32.2	1425.1	32.2
KMTB-44	631	19245	1.7	11.1121	2.0	2.3885	4.7	0.1925	4.2	0.91	1134.9	44.1	1239.2	33.5	1425.3	38.0	1425.3	38.0
KMTB-45	257	8635	1.0	11.1083	2.4	3.0255	3.5	0.2438	2.5	0.72	1406.2	32.0	1414.1	26.8	1426.0	46.6	1426.0	46.6
KMTB-65	109	3400	2.2	11.1009	2.9	3.1870	3.3	0.2566	1.6	0.48	1472.4	21.2	1454.0	25.8	1427.3	55.7	1427.3	55.7
KMTB-27	282	9725	1.9	11.0838	2.7	3.1068	3.5	0.2497	2.3	0.64	1437.2	29.1	1434.4	27.2	1430.2	52.2	1430.2	52.2
KMTB-7	50	3005	1.4	11.0650	4.3	3.0452	4.8	0.2444	2.1	0.45	1409.4	27.0	1419.0	36.5	1433.5	81.6	1433.5	81.6
KMTB-34	594	27325	5.1	11.0227	1.7	2.7011	2.0	0.2159	1.0	0.50	1260.4	11.4	1328.8	14.9	1440.8	33.2	1440.8	33.2
KMTB-80	92	3125	1.6	11.0056	3.0	3.0421	4.0	0.2428	2.7	0.66	1401.3	33.8	1418.2	30.9	1443.7	57.7	1443.7	57.7
KMTB-49	440	16140	0.9	10.9549	1.0	3.2176	2.2	0.2556	2.0	0.89	1467.5	26.2	1461.4	17.4	1452.5	19.4	1452.5	19.4
KMTB-39	163	6155	1.2	10.9292	3.7	3.1244	4.1	0.2477	1.6	0.38	1426.4	20.0	1438.7	31.2	1457.0	71.3	1457.0	71.3
KMTB-10	328	6020	1.4	10.9254	3.3	2.2378	6.5	0.1773	5.7	0.86	1052.3	54.9	1193.0	45.9	1457.6	62.6	1457.6	62.6
KMTB-61	115	4490	1.7	10.9245	2.8	3.1379	3.0	0.2486	1.2	0.38	1431.4	14.8	1442.0	23.1	1457.8	52.8	1457.8	52.8
KMTB-32	434	19415	1.2	10.9213	1.1	3.1326	2.2	0.2481	1.9	0.85	1428.8	23.7	1440.7	16.7	1458.3	21.5	1458.3	21.5
KMTB-2	185	6245	3.6	10.9110	1.7	3.2753	2.1	0.2592	1.4	0.64	1485.7	18.0	1475.2	16.7	1460.1	31.4	1460.1	31.4
KMTB-17	94	11935	1.3	10.9103	1.2	3.1846	2.3	0.2520	2.0	0.86	1448.8	25.4	1453.4	17.6	1460.3	21.9	1460.3	21.9
KMTB-55	150	10705	1.2	10.9049	1.8	3.0474	2.3	0.2410	1.4	0.61	1392.0	17.8	1419.6	17.7	1461.2	34.6	1461.2	34.6
KMTB-74	279	9625	2.0	10.8802	1.9	3.1383	2.2	0.2476	1.1	0.52	1426.3	14.6	1442.1	17.0	1465.5	35.9	1465.5	35.9
KMTB-19	679	56700	7.7	10.1193	2.3	3.7156	2.5	0.2727	1.0	0.40	1554.5	13.8	1574.7	20.1	1602.0	43.1	1602.0	43.1
KMTB-8	57	1665	1.6	10.0431	3.1	3.7193	4.4	0.2709	3.1	0.70	1545.4	42.6	1575.5	35.3	1616.1	58.4	1616.1	58.4
KMTB-82	283	11140	2.2	10.0336	2.0	3.0276	4.8	0.2203	4.4	0.91	1283.6	50.9	1414.6	36.7	1617.8	37.5	1617.8	37.5
KMTB-67	121	5800	1.0	10.0159	3.3	3.7003	3.4	0.2688	1.0	0.29	1534.7	13.7	1571.4	27.3	1621.1	60.6	1621.1	60.6
KMTB-57	57	2130	1.6	9.9678	2.6	3.7833	2.8	0.2735	1.0	0.36	1558.6	13.8	1589.2	22.5	1630.1	48.6	1630.1	48.6
KMTB-6	304	10255	4.3	9.8127	1.8	4.0931	2.0	0.2913	1.0	0.50	1648.0	14.5	1652.9	16.5	1659.2	32.4	1659.2	32.4
KMTB-73	203	22780	4.5	9.7774	1.3	3.9883	2.1	0.2828	1.7	0.79	1605.6	24.0	1631.8	17.3	1665.8	23.9	1665.8	23.9
KMTB-48	93	7415	3.8	9.7260	1.2	4.2332	3.1	0.2986	2.9	0.92	1684.4	42.2	1680.5	25.5	1675.6	22.6	1675.6	22.6
KMTB-79	88	5805	2.1	9.6820	2.1	4.2146	2.4	0.2960	1.0	0.42	1671.2	14.7	1676.9	19.4	1683.9	39.6	1683.9	39.6
KMTB-20	97	5160	2.9	9.6800	2.0	4.0450	2.7	0.2840	1.8	0.67	1611.4	25.4	1643.3	21.7	1684.3	36.7	1684.3	36.7

Table A4
(continued)

Analysis	U (ppm)	$^{206}Pb/^{204}Pb$	U/Th	$^{206}Pb^*/^{207}Pb^*$	± (%)	Isotope Ratios					Apparent Ages (Ma)						Best age (Ma)	± (Ma)
						$^{207}Pb^*/^{235}U^*$	± (%)	$^{206}Pb^*/^{238}U$	± (%)	Err. corr	$^{206}Pb^*/^{238}U^*$	± (Ma)	$^{207}Pb^*/^{235}U$	± (Ma)	$^{206}Pb^*/^{207}Pb^*$	± (Ma)		
KMTB-16	547	25865	2.4	9.6398	2.1	4.0024	2.8	0.2798	1.9	0.67	1590.5	26.6	1634.7	23.1	1692.0	39.1	1692.0	39.1
KMTB-5	230	7070	2.2	9.6355	1.6	4.0273	3.0	0.2814	2.6	0.85	1598.6	36.4	1639.7	24.7	1692.8	29.9	1692.8	29.9
KMTB-28	183	20295	1.5	9.6296	1.0	4.2803	1.4	0.2989	1.0	0.71	1686.1	14.8	1689.6	11.6	1693.9	18.4	1693.9	18.4
KMTB-24	150	8770	3.7	9.5532	2.6	4.2909	2.7	0.2973	1.0	0.36	1677.9	14.8	1691.6	22.6	1708.6	47.1	1708.6	47.1
KMTB-4	287	12405	3.3	9.4986	2.7	4.3445	5.0	0.2993	4.2	0.84	1687.8	62.8	1701.8	41.7	1719.2	50.5	1719.2	50.5
KMTB-81	230	12375	4.5	9.3943	1.3	4.4210	3.0	0.3012	2.7	0.91	1697.3	40.1	1716.3	24.6	1739.4	22.9	1739.4	22.9
KMTB-35	428	32695	4.9	9.3380	2.2	4.5954	5.0	0.3112	4.5	0.90	1746.8	68.2	1748.4	41.5	1750.4	40.5	1750.4	40.5
KMTB-76	296	14650	2.9	9.3103	2.3	4.6714	5.0	0.3154	4.5	0.89	1767.4	69.7	1762.1	42.2	1755.9	41.4	1755.9	41.4
KMTB-23	170	8975	2.7	9.1215	1.8	4.8742	2.8	0.3225	2.1	0.76	1801.7	33.6	1797.8	23.7	1793.3	33.3	1793.3	33.3
KMTB-26	244	17090	1.3	9.1150	1.6	4.7861	3.1	0.3164	2.7	0.86	1772.1	41.4	1782.5	26.1	1794.6	29.0	1794.6	29.0
KMTB-62	94	9690	1.2	8.9714	1.9	5.0274	2.1	0.3271	1.0	0.48	1824.4	15.9	1823.9	17.8	1823.4	33.6	1823.4	33.6
KMTB-51	242	13340	1.9	8.9275	1.9	5.0832	2.3	0.3291	1.2	0.51	1834.2	18.5	1833.3	19.1	1832.3	35.0	1832.3	35.0
KMTB-63	857	28910	6.3	8.8503	5.3	4.4032	6.5	0.2826	3.7	0.57	1604.6	52.3	1712.9	53.6	1848.0	96.3	1848.0	96.3
KMTB-71	44	2435	1.8	8.5154	1.6	5.5971	2.9	0.3457	2.5	0.84	1913.9	40.6	1915.6	25.2	1917.5	28.6	1917.5	28.6
KMTB-59	29	1825	0.9	7.4807	2.2	6.6654	3.0	0.3616	2.0	0.67	1989.9	34.4	2068.1	26.5	2146.8	38.9	2146.8	38.9
WADC401-58	110	5355	0.9	18.7683	30.6	0.0752	30.8	0.0102	3.5	0.11	65.7	2.3	73.6	21.9	340.8	707.9	65.7	2.3
WADC401-4	3215	12585	5.2	18.9574	4.4	0.0759	4.9	0.0104	2.3	0.46	66.9	1.5	74.3	3.5	318.0	99.2	66.9	1.5
WADC401-63	656	3330	0.7	22.1824	6.6	0.0750	6.7	0.0121	1.0	0.15	77.3	0.8	73.4	4.7	-51.3	161.1	77.3	0.8
WADC401-71	1128	8200	2.2	21.0577	3.5	0.0790	3.6	0.0121	1.0	0.28	77.3	0.8	77.2	2.7	73.8	82.9	77.3	0.8
WADC401-53	260	2320	0.8	22.4805	12.4	0.0748	12.5	0.0122	1.0	0.08	78.2	0.8	73.3	8.8	-83.9	305.4	78.2	0.8
WADC401-6	1197	3410	1.8	16.1744	7.4	0.1127	7.8	0.0132	2.4	0.31	84.7	2.0	108.4	8.0	668.1	159.2	84.7	2.0
WADC401-1	597	2225	0.8	20.5415	12.9	0.0929	13.9	0.0138	5.2	0.38	88.6	4.6	90.2	12.0	132.5	304.5	88.6	4.6
WADC401-31	1541	12530	0.9	20.6158	2.9	0.0987	4.8	0.0148	3.9	0.80	94.5	3.6	95.6	4.4	124.0	68.6	94.5	3.6
WADC401-28	388	2635	2.4	21.6472	5.1	0.0979	5.4	0.0154	1.8	0.33	98.3	1.7	94.8	4.9	7.8	122.4	98.3	1.7
WADC401-11	185	1175	2.6	24.4567	17.1	0.0937	17.2	0.0166	1.2	0.07	106.2	1.3	90.9	15.0	-294.5	440.4	106.2	1.3
WADC401-21	700	6285	1.6	20.4228	5.3	0.1638	5.5	0.0243	1.5	0.27	154.6	2.2	154.1	7.8	146.1	123.3	154.6	2.2
WADC401-42	121	1045	0.7	23.3292	17.2	0.1446	18.3	0.0245	6.2	0.34	155.8	9.5	137.1	23.5	-175.4	432.1	155.8	9.5
WADC401-41	316	5920	2.0	20.3485	6.5	0.1872	7.0	0.0276	2.8	0.39	175.7	4.8	174.3	11.2	154.7	151.2	175.7	4.8
WADC401-15	317	8690	5.7	18.4416	3.6	0.4006	3.9	0.0536	1.6	0.41	336.5	5.3	342.1	11.4	380.4	80.8	336.5	5.3
WADC401-18	195	25720	1.2	11.1910	2.0	3.0368	3.4	0.2465	2.8	0.82	1420.3	35.6	1416.9	26.1	1411.8	37.9	1411.8	37.9
WADC401-14	499	60955	1.3	11.1859	1.7	3.0606	2.0	0.2483	1.0	0.51	1429.7	13.0	1422.9	15.1	1412.7	32.5	1412.7	32.5
WADC401-43	492	38705	2.0	11.1162	1.9	2.9687	2.1	0.2393	1.0	0.47	1383.3	12.4	1399.7	16.2	1424.6	35.9	1424.6	35.9
WADC401-29	106	12945	1.5	10.9291	1.9	3.2742	2.2	0.2595	1.2	0.53	1487.4	15.4	1474.9	17.1	1457.0	35.4	1457.0	35.4
WADC401-38	145	18530	1.5	10.8200	2.3	3.3800	3.7	0.2652	2.9	0.78	1516.6	38.8	1499.8	28.8	1476.0	43.5	1476.0	43.5

TABLE A4
(continued)

Analysis	U (ppm)	$^{206}Pb/^{204}Pb$	U/Th	$^{206}Pb^*/^{207}Pb^*$	± (%)	Isotope Ratios $^{207}Pb^*/^{235}U^*$	± (%)	$^{206}Pb^*/^{238}U$	± (%)	Err. corr	Apparent Ages (Ma) $^{206}Pb^*/^{238}U^*$	± (Ma)	$^{207}Pb^*/^{235}U$	± (Ma)	$^{206}Pb^*/^{207}Pb^*$	± (Ma)	Best age (Ma)	± (Ma)
WADC401-20	702	62800	2.1	10.7611	1.4	3.3446	2.9	0.2610	2.5	0.87	1495.1	33.9	1491.5	22.8	1486.4	27.1	1486.4	27.1
WADC401-45	471	42290	3.1	10.7431	1.7	2.6342	2.3	0.2053	1.5	0.67	1203.5	16.9	1310.3	16.9	1489.6	32.2	1489.6	32.2
WADC401-32	1944	82395	2.6	9.9876	2.5	2.9847	3.4	0.2162	2.3	0.68	1261.8	26.6	1403.7	26.1	1626.4	46.9	1626.4	46.9
WADC401-50	207	36475	2.9	9.8191	1.7	3.9717	3.1	0.2828	2.7	0.85	1605.7	37.7	1628.4	25.4	1657.9	30.7	1657.9	30.7
WADC401-3	269	15885	1.9	9.7518	1.8	3.1050	5.1	0.2196	4.7	0.94	1279.8	54.9	1433.9	38.9	1670.7	33.1	1670.7	33.1
WADC401-65	1811	6085	4.6	9.7516	2.0	0.6821	6.3	0.0482	6.0	0.95	303.7	17.7	528.0	26.0	1670.7	37.7	1670.7	37.7
WADC401-7	119	10855	1.0	9.6938	2.3	4.1035	2.5	0.2885	1.0	0.40	1634.0	14.4	1655.0	20.6	1681.7	42.7	1681.7	42.7
WADC401-13	361	51070	2.7	9.6909	1.0	4.2587	1.4	0.2993	1.0	0.69	1688.0	14.9	1685.4	11.9	1682.2	19.2	1682.2	19.2
WADC401-2	227	26655	1.5	9.6658	3.7	4.3897	3.8	0.3077	1.0	0.26	1729.5	15.2	1710.4	31.5	1687.0	67.7	1687.0	67.7
WADC401-52	178	42265	1.4	9.6191	3.0	4.3414	3.2	0.3029	1.0	0.32	1705.6	15.0	1701.3	26.0	1696.0	55.1	1696.0	55.1
WADC401-5	610	46405	4.1	9.6052	2.4	3.7558	3.6	0.2616	2.7	0.76	1498.2	36.6	1583.4	29.0	1698.6	43.3	1698.6	43.3
WADC401-60	140	28855	1.7	9.5818	1.6	4.1599	2.3	0.2891	1.7	0.74	1637.0	25.2	1666.2	19.2	1703.1	28.9	1703.1	28.9
WADC401-75	849	100735	15.0	9.5654	1.1	4.1466	1.5	0.2877	1.0	0.69	1629.9	14.4	1663.5	11.9	1706.3	19.5	1706.3	19.5
WADC401-73	247	44220	1.3	9.5146	4.9	3.9986	6.7	0.2759	4.6	0.69	1570.8	64.0	1633.9	54.4	1716.1	89.4	1716.1	89.4
WADC401-62	479	45490	4.1	9.4885	1.2	3.9025	3.5	0.2686	3.3	0.94	1533.5	44.5	1614.2	28.2	1721.1	22.6	1721.1	22.6
WADC401-47	305	61230	2.3	9.4810	2.1	4.5091	2.7	0.3101	1.7	0.63	1741.0	25.6	1732.7	22.3	1722.6	38.4	1722.6	38.4
WADC401-54	628	144510	6.8	9.4604	1.9	3.9662	3.2	0.2721	2.5	0.80	1551.6	34.9	1627.3	25.6	1726.6	34.5	1726.6	34.5
WADC401-69	199	40100	1.9	9.4528	2.0	4.5072	2.3	0.3090	1.3	0.55	1735.8	19.5	1732.3	19.4	1728.1	35.8	1728.1	35.8
WADC401-8	1492	63250	22.3	6.4602	2.3	9.7051	2.5	0.4547	1.0	0.39	2416.2	20.2	2407.2	23.3	2399.6	39.6	2399.6	39.6

TABLE A5

References for paleoflow directions depicted in figure

Label in Figure 7	Reference(s)
1 – Northwest GGRB	(Steidtmann, 1969; West and Dawson, 1973; Anderson and Picard, 1974; Dorr and others, 1977)
2 – Northwest WRB	(Bauer, 1934; Love, 1939; Van Houten, 1955; Keefer, 1957; Van Houten, 1964; Keefer, 1965; Soister, 1968; Love, 1970; MacGinitie, 1974; Emry, 1975; Boles and Surdam, 1979; Korth, 1982; Stucky, ms, 1982; Stucky, 1984)
3 – Northeast GGRB	(Sklenar and Anderson, 1985)
4 – Southwest GGRB	(Oriel, 1961; Lawrence, 1963; Rubey and others, 1975; Zonneveld and others, 2003)
5 – Southeast GGRB / Northern PCB	(Trudell and others, 1970; Roehler, 1973b; Roehler, 1974; Trudell and others, 1974; Duncan and others, 1974; O'Sullivan, 1974; O'Sullivan, 1975; Hail, 1977; Surdam and Stanley, 1980; Johnson, 1981; Donnell, 1982; Johnson 1984; Hail, 1987; O'Sullivan, 1987; Hail, 1990; Franczyk and others, 1992; Hail, 1992; Hail and Smith, 1994)
6 – Western UB	(Stagner, 1941; Stanley and Collinson, 1979; Weiss, 1982; Fouch and others, 1983; Bruhn and others, 1986; Lawton, 1986; Lawton and others, 1993; Talling and others, 1995)
7 – Eastern UB / Western PCB	(Dane, 1954; Cashion and Donnell, 1972; Moncure, ms, 1979; Moncure and Surdam, 1980; Cole, 1985)
8 – Southern UB	(Spieker, 1946; Cashion, 1967; Marcantel, 1968; Fouch and others, 1976; Peterson, 1976; Volkert, ms, 1980; Pitman and others, 1982; Zawiskie and others, 1982; Smith, 1986; Bruhn and others, 1986; Dickinson and others, 1986; Willis, 1986; Fouch and others, 1987; Franczyk and others, 1991; Franczyk and Pitman, 1991; Morris and others, 1991)
9 – Southeast PCB	(Donnell, 1961; Donnell, 1969; Kihm, 1984)
10 – SCB	(Janecke, 1994; Janecke and others, 2000)
11 – Northwest GGRB	(Culbertson, 1962; Ebens, ms, 1963; McGrew and Sullivan, 1970; Kistner, ms, 1973; Gustav, ms, 1974; Wolfbauer and Surdam, 1974; Surdam and Stanley, 1980)
12 – Northwest WRB / Northeast GGRB	(Oriel, 1961; Oriel, 1962; Roehler, 1969; Roehler, 1970; Roehler, 1973a; Roehler, 1973b; Braunagel, 1977; Mauger, 1977; Stanley and Surdam, 1978; Surdam and Stanley, 1979; Surdam and Stanley, 1980; Roehler, 1988; Roehler, 1990; Stucky and others, 1996)
13 – Southeast GGRB / Northwest PCB/ Eastern UB	(Cashion and Donnell, 1972; Cashion and Donnell, 1974; Roehler, 1992; Prothero, 1996; Bartov and others, 2007; Bartov and others, 2008; Sarg and others, 2009)
14 – Northern UB	(Kay, 1934; Anderson and Picard, 1972; Anderson and Picard, 1974)

TABLE A6

References for strontium isotope ratios of exposure depicted in figure 1

Location and Rock Type	Reference(s)
Precambrian Cores of Laramide Uplifts	
Uinta Uplift (UU)	(Crittenden and Peterman, 1975; Bouchard and others, 1998; Gerner and others, 2007)
Wind River Uplift (WRU)	(Frost and others, 1998)
Sierra Madre Uplift (SMU)	(Divis, 1977)
Front Range Uplift (FRU)	(Hedge and others, 1967)
Owl Creek Uplift (OCU)	(Mueller and others, 1985)
Granite Uplift (GU)	(Peterman and Hildreth, 1978)
Laramie Uplift (LU)	(Zielinski and others, 1981; Patel and others, 1999)
Sawatch-San Luis Uplift (SSU)	(Pearson and others, 1966; Moorbath and others, 1967)
Sangre de Cristo Uplift (SCU)	(Nelson and DePaolo, 1988)
Precambrain, Paleozoic and Mesozoic Carbonates	(Paces and others, 2007; Bright, 2009)
Tertiary Volcanic Provinces	(Peterman and others, 1970; Meen and Eggler, 1987; Norman and Leeman, 1989; Cunningham and others, 1998; Vogel and others, 2001)
Absaroka	(Peterman and others, 1970; Meen and Eggler, 1987)
Challis	(Norman and Leeman, 1989)
Keetley	(Vogel and others, 2001)
Marysvale	(Cunningham and others, 1998)

REFERENCES

Anderson, D. W., and Picard, M. D., 1972, Stratigraphy of the Duchesne River Formation (Eocene-Oligocene?), Northern Uinta Basin, Northeastern Utah: Utah Geological and Mineralogical Survey Bulletin, v. 97, p. 1–23.

——— 1974, Evolution of synorogenic clastic deposits in the intermontane Uinta Basin of Utah *in* Dickinson, W. R., editor, Tectonics and Sedimentation: SEPM Special Publication, v. 22, p. 167–189.

Axen, G. J., Taylor, W. J., and Bartley, J. M., 1993, Space-time patterns and tectonic controls of Tertiary magmatism in the Great Basin of the western United States: Geological Society of America Bulletin, v. 105, p. 56–76, doi:10.1130/0016-7606(1993)105⟨0056:STPATC⟩2.3.CO;2.

Bartov, Y., Picha, M., and Daub, J., 2007, Oil shale of the Piceance Creek and eastern Uinta Basins, 27th Oil Shale Symposium: Golden, Colorado, Colorado School of Mines.

Bartov, Y., Nummendal, D., and Sarg, R., 2008, The depositional system of the Green River oil shale in western Colorado: San Antonio, Texas, AAPG Annual Convention, Search and Discovery Article #90078.

Bauer, C. M., 1934, Wind River Basin [Wyoming]: Geological Society of America Bulletin, v. 45, p. 665–696.

Bohacs, K. M., Carroll, A. R., Neal, J. E., and Mankiewicz, P. J., 2000, Lake-basin type, source potential, and hydrocarbon character: an integrated sequence-stratigraphic-geochemical framework, *in* Gierlowski-Kordesch, E. H., and Kelts, K. R., editors, Lake basins through space and time: AAPG Studies in Geology No. 46, p. 3–34.

Boles, J. R., and Surdam, R. C., 1979, Diagenesis of volcanogenic sediments in a Tertiary saline lake; Wagon Bed Formation, Wyoming: American Journal of Science, v. 279, p. 832–853.

Bouchard, D. P., Kaufman, D. S., Hochberg, A., and Quade, J., 1998, Quaternary history of the Thatcher Basin, Idaho, reconstructed from the $^{87}Sr/^{86}Sr$ and amino acid composition of lacustrine fossils: implications for the diversion of the Bear River into the Bonneville Basin: Palaeogeography, Palaeoclimatology, Palaeoecology, v. 141, p. 95–114, doi:10.1016/S0031-0182(98)00005-4.

Bowen, G. J., and Bowen, B. B., 2008, Mechanisms of PETM global change constrained by a new record from central Utah: Geology, v. 36, p. 379–382, doi: 10.1130/G24597A.1.

Bowen, G. J., Daniels, A. L., and Bowen, B. B., 2008, Paleoenvironmental isotope geochemistry and paragenesis of lacustrine and palustrine carbonates, Flagstaff Formation, central Utah, USA: Journal of Sedimentary Research, v. 78, p. 162–174.

Bradley, W. H., 1931, Origin and microfossils of the oil shale of the Green River Formation of Colorado and Utah: United States Geological Survey Professional Paper, v. 168, 58 p.
Brass, G. W., 1975, The effect of weathering on the distribution of strontium isotopes in weathering profiles: Geochimica et Cosmochimica Acta, v. 39, p. 1,647–1,653, doi:10.1016/0016-7037(75)90086-1.
Braunagel, L. H., and Stanley, K. O., 1977, Origin of variegated redbeds in the Cathedral Bluffs Tongue of the Wasatch Formation (Eocene), Wyoming: Journal of Sedimentary Petrology, v. 47, p. 1,201–1,219.
Bright, J., 2009, Isotope and major-ion chemistry of groundwater in Bear Lake Valley, Utah and Idaho, with emphasis on the Bear River Range, *in* Rosenbaum, J. G., and Kaufman, D. S., editors, Paleoenvironments of Bear Lake, Utah and Idaho, and its catchment: Geological Society of America Special Paper 150, p. 105–132.
Brobst, D. A., and Tucker, J. D., 1973, X-ray mineralogy of the Parachute Creek Member, Green River Formation, in the Northern Piceance Creek Basin, Colorado: United States Geological Survey Professional Paper 803, p. 1–53.
Bruhn, R. L., Picard, M. D., and Isby, J. S., 1986, Tectonics and sedimentology of Uinta Arch, western Uinta Mountains, and Uinta Basin, *in* Peterson, J. A., editor, Paleotectonics and sedimentation in the Rocky Mountain region, United States: American Association of Petroleum Geologists Memoir, v. 41, p. 333–352.
Carroll, A. R., and Bohacs, K. M., 1999, Stratigraphic classification of ancient lakes: Balancing tectonic and climatic controls: Geology, v. 27, p. 99–102, doi:10.1130/0091-7613(1999)027⟨0099:SCOALB⟩2.3.CO;2.
Carroll, A. R., Chetel, L. M., and Smith, M. E., 2006, Feast to famine: Sediment supply control on Laramide basin fill: Geology, v. 34, p. 197–200, doi:10.1130/G22148.1.
Carroll, A. R., Doebbert, A. C., Booth, A. L., Chamberlain, C. P., Rhodes-Carson, M. K., Smith, M. E., Johnson, C. M., and Beard, B. L., 2008, Capture of high altitude precipitation by a low altitude Eocene lake, western U.S.: Geology, v. 36, p. 791–794, doi: 10.1130/G24783A.1.
Cashion, W. B., 1967, Geology and fuel resources of the Green River Formation Southeastern Uinta Basin Utah and Colorado: U.S. Geological Survey Professional Paper n. 548, p. 48.
Cashion, W. B., and Donnell, J. R., 1972, Chart showing correlation of selected key units in the organic-rich sequence of Green River Formation, Piceance Creek basin, Colorado, and Uinta basin, Utah: U.S. Geological Survey Oil and Gas Investigations Chart OC 65.
——— 1974, Revision of Nomenclature of the Upper Part of the Green River Formation, Piceance Creek Basin, Colorado, and Eastern Uinta Basin, Utah: U.S. Geological Survey Bulletin, v. 1394-G, p. 1–9.
Chamberlain, C. P., and Poage, M. A., 2000, Reconstructing the paleotopography of mountain belts from the isotopic composition of authigenic minerals: Geology, v. 28, p. 115–118, doi:10.1130/0091-7613(2000)28⟨115:RTPOMB⟩2.0.CO;2.
Christensen, R. L., and Yeats, R. L., 1992, Post-Laramide geology of the U.S. Cordilleran region, *in* Burchfiel, B. C., Lipman, P. W., and Zoback, M. L. C., editors, The Cordilleran Orogen: Conterminous U.S.: Geology of North America: Boulder, Colorado, Geological Society of America, v. g-3, p. 261–406.
Cole, R. D., 1985, Depositional environments of oil-shale in the Green River Formation, Douglas Creek Arch, Colorado and Utah, *in* Picard, M. D., editor, Geology and Energy Resources, Uinta Basin of Utah: Salt Lake City, Utah Geological Association, p. 211–224.
Crittenden, M. D., Jr., and Peterman, Z. E., 1975, Provisional Rb/Sr age of the Precambrian Uinta Mountain Group, northeastern Utah: Utah Geology, v. 2, p. 75–77.
Culbertson, W. C., 1962, Laney Shale Member and Tower Sandstone Lentil of the Green River Formation, Green River Area, Wyoming: U.S. Geological Survey Professional Paper, v. 450-C, p. 54–57.
Cunningham, C. G., Unruh, D. M., Steven, T. A., Rowley, P. D., Naeser, C. W., Mehnert, H. H., Hedge, C. E., and Ludwig, K. R., 1998, Geochemistry of Volcanic Rocks in the Marysvale Volcanic Field, West-Central Utah: U.S. Geological Survey Bulletin, v. 2158, p. 223–231.
Dane, C. H., 1954, Stratigraphic and facies relationships of upper part of Green River Formation and lower part of the Uinta Formation in Duchesne, Uintah, and Wasatch counties: Bulletin of the American Association of Petroleum Geologists, v. 38, p. 405–425.
Davis, S. J., Wiegand, B. A., Carroll, A. R., and Chamberlain, C. P., 2008, The Effect of Drainage Reorganization on Paleoaltimetry Studies: An Example from the Paleogene Laramide Foreland: Earth and Planetary Science Letters, v. 275, p. 258–268, doi:10.1016/j.epsl.2008.08.009.
Davis, S. J., Mulch, A., Carroll, A. R., Horton, T. W., and Chamberlain, C. P., 2009, Paleogene landscape evolution of the central North American Cordillera: Developing topography and hydrology in the Laramide foreland: Geological Society of America Bulletin, v. 121, p. 100–116, doi: 10.1130/B26308.1.
de Villiers, S., Greaves, M., and Elderfield, H., 2002, An intensity ratio calibration method for the accurate determination of Mg/Ca and Sr/Ca of marine carbonates by ICP-AES: Geochemistry Geophysics Geosystems, v. 3, paper number 2001GC000169, 10.1029/2001GC000169.
DeCelles, P. G., 1988, Lithologic provenance modeling applied to the Late Cretaceous synorogenic Echo Canyon Conglomerate, Utah: A case of multiple source areas: Geology, v. 16, p. 1,039–1,043, doi:10.1130/0091-7613(1988)016⟨1039:LPMATT⟩2.3.CO;2.
——— 2004, Late Jurassic to Eocene Evolution of the Cordilleran Thrust Belt and Foreland Basin System, Western U.S.A.: American Journal of Science, v. 304, p. 105–168, doi:10.2475/ajs.304.2.105.
DeCelles, P. G., Lawton, T. F., and Mitra, G., 1995, Thrust timing, growth of structural culminations, and synorogenic sedimentation in the type Sevier orogenic belt, western United States: Geology, v. 23, p. 699–702, doi:10.1130/0091-7613(1995)023⟨0699:TTGOSC⟩2.3.CO;2.
Dettman, D. L., and Lohmann, K. C., 2000, Oxygen isotope evidence for high-altitude snow in the Laramide Rocky Mountains of North America during the Late Cretaceous and Paleogene: Geology, v. 28, p. 243–246, doi:10.1130/0091-7613(2000)28⟨243:OIEFHS⟩2.0.CO;2.
Dickinson, W. R., 2004, Evolution of the North American Cordillera: Annual Review of Earth and Planetary Sciences, v. 32, p. 13–45, doi:10.1146/annurev.earth.32.101802.120257.

Dickinson, W. R., and Gehrels, G. E., 2003, U-Pb ages of detrital zircons from Permian and Jurassic eolian sandstones of the Colorado Plateau, USA: paleogeographic implications: Sedimentary Geology, v. 163, p. 29–66, doi:10.1016/S0037-0738(03)00158-1.

Dickinson, W. R., Lawton, T. F., and Inman, K. F., 1986, Sandstone detrital modes, central Utah foreland region: stratigraphic record of Cretaceous-Paleogene tectonic evolution: Journal of Sedimentary Petrology, v. 56, p. 276–293.

Dickinson, W. R., Klute, M. A., Hayes, M. J., Janecke, S. U., Lundin, E. R., McKittrick, M. A., and Olivares, M. D., 1988, Paleogeographic and paleotectonic setting of Laramide sedimentary basins in the central Rocky Mountain region: Geological Society of America Bulletin, v. 100, p. 1,023–1,039, doi:10.1130/0016-7606(1988)100⟨1023:PAPSOL⟩2.3.CO;2.

Divis, A. F., 1977, Isotopic studies on a Precambrain geochronologic boundary, Sierra Madre Mountains, Wyoming: Geological Society of America Bulletin, v. 88, p. 96–100.

Donnell, J. R., 1961, Tripartition of the Wasatch Formation near De Beque in northwestern Colorado: U.S. Geological Survey Professional Paper, v. 424-B, p. 147–148.

——— 1969, Paleocene and Lower Eocene Units in the Southern Part of the Piceance Creek Basin Colorado *in* Contributions to Stratigraphy: U.S. Geological Survey Bulletin, v. 1274-M, p. M1–M18.

——— 1982, Tongues of the Green River and Uinta Formations in the Piceance Creek Basin, *in* Gary, J. H., editor, Fifteenth Oil Shale Symposium Proceedings: Golden, Colorado, Colorado School of Mines Press, p. 29–37.

Dorr, J. A., Jr., Spearing, D. R., and Steidtmann, J. R., 1977, Deformation and deposition between a foreland uplift and an impinging thrust belt: Hoback Basin, Wyoming: Geological Society of America Special Paper, v. 177, 82 p.

Drummond, C. N., Wilinson, B. H., Lohmann, K. C., and Smith, G. R., 1993, Effect of regional topography and hydrology on the lacustrine isotopic record of Miocene paleoclimate in the Rocky Mountains: Palaeogeography, Palaeoclimatology, Palaeoecology, v. 101, p. 67–79, doi:10.1016/0031-0182(93)90152-9.

Dubiel, R. F., Potter, C. J., Good, S. C., and Snee, L. W., 1996, Reconstructing an Eocene extensional basin: the White Sage Formation, eastern Great Basin, *in* Beratan, K. K., editor, Reconstructing the history of Basin and Range extension using sedimentology and stratrigraphy: Geological Society of America Special Paper, v. 303, p. 1–14.

Duncan, D. C., Hail, W. J., Jr., O'Sullivan, R. B., and Pipiringos, G. N., 1974, Four Newly Named Tongues of Eocene Green River Formation, Northern Piceance Creek Basin, Colorado *in* Contributions to Stratigraphy: U.S. Geological Survey Bulletin, v. 1394-F, p. FF–F13.

Ebens, R. J., ms, 1963, Petrography of the Eocene Tower Sandstone lenses at Green River, Sweetwater County, Wyoming: Laramie, University of Wyoming, Masters Thesis, p. 46.

Elston, D. P., and Young, R. A., 1991, Cretaceous-Eocene (Laramide) landscape development and Oligocene-Pliocene drainage reorganization of Transition Zone and Colorado Plateau, Arizona: Journal of Geophysical Research, v. 96(B7), p. 12,389–12,406, doi:10.1029/90JB01978.

Emry, R. J., 1975, Revised Tertiary stratigraphy and paleontology of the western Beaver Divide, Fremont County, Wyoming: Smithsonian Contributions to Paleobiology, v. 25, p. 20.

Epis, R. C., and Chapin, C. E., 1975, Geomorphic and tectonic implications of the post-Laramide, late Eocene erosion surface in the Southern Rocky Mountains, *in* Curtis, B. F., editor, Cenozoic history of the Southern Rocky Mountains: Geological Society of America Memoir, v. 144, p. 45–74.

Eugster, H. P., and Kelts, K., 1983, Lacustrine chemical sediments, *in* Goudie, A. S., and Pye, K., editors, Chemical sediments and geomorphology: precipitates and residua in the near-surface environment: San Francisco, Academic Press, p. 321–368.

Flowers, R. M., Wernicke, B. P., and Farley, K. A., 2008, Unroofing, incision, and uplift history of the southwestern Colorado Plateau from apatite (U-Th)/He thermochronometry: Geological Society of America Bulletin, v. 120, p. 571–587, doi:10.1130/B26231.1.

Foster, D. A., Mueller, P. A., Mogk, D. W., Wooden, J. L., and Vogl, J. J., 2006, Proterozoic evolution of the western margin of the Wyoming craton: implications for the tectonic and magmatic evolution of the northern Rocky Mountains: Canadian Journal of Earth Sciences, v. 43, p. 1,601–1,619, doi:10.1139/E06-052.

Fouch, T. D., 1979, Character and paleogeographic distribution of Upper Cretaceous (?) and Paleogene nonmarine sedimentary rocks in east-central Nevada, *in* Armentrout, J. M., Cole, M. R., and TerBest, H., editors, Cenozoic paleogeography of the western United States, Pacific Coast Paleogeography Symposium 3: Pacific Section, Society of Economic Paleontologists and Mineralogists, p. 97–111.

Fouch, T. D., Cashion, W. B., Ryder, R. T., and Campbell, J. A., 1976, Field guide to lacustrine and related nonmarine depositional environments in Tertiary rocks, Uinta basin, Utah, *in* Epis, R. C., and Weimer, R. J., editors, Studies in Colorado field geology: Colorado School of Mines, Professional Contributions No. 8, p. 358–385.

Fouch, T. D., Lawton, T. F., Nichols, D. J., Cashion, W. B., and Cobban, W. A., 1983, Patterns and timing of synorogenic sedimentation in Upper Cretaceous rocks of central and northeast Utah, *in* Reynolds, M. W., and Dolly, E. D., editors, Mesozoic paleogeography of the west-central United States: Rocky Mountain Paleogeography Symposium 2, SEPM, p. 305–328.

Fouch, T. D., Hanley, J. H., Forester, R. M., Keighin, C. W., Pitman, J. K., and Nichols, D. J., 1987, Chart showing lithology, mineralogy, and paleontology of the nonmarine North Horn Formation and Flagstaff Member of the Green River Formation, Price Canyon, central Utah: A principal reference section: U.S. Geological Survey Miscellaneous Investigations Series Map, I-1797-A, 8 p., 1 sheet.

Franczyk, K. J., and Pitman, J. K., 1991, Latest Cretaceous Nonmarine depositional systems in the Wasatch Plateau area: Reflections of foreland to intermontane basin transition, *in* Chidsey, T. C., editor, Geology of east-central Utah: Salt Lake City, Utah, Utah Geological Association Publication 19, p. 77–93.

Franczyk, K. J., Hanley, J. H., Pitman, J. K., and Nichols, D. J., 1991, Paleocene depositional systems in the western Roan Cliffs, Utah, *in* Chidsey, T. C., editor, Geology of east-central Utah: Utah Geological Association Publication 19, p. 111–127.

Franczyk, K. J., Fouch, T. D., Johnson, R. C., Molenaar, C. M., and Cobban, W. A., 1992, Cretaceous and Tertiary paleogeographic reconstructions for the Uinta-Piceance Basin study area, Colorado and Utah: U.S. Geological Survey Bulletin, v. 1787-Q, p. 1–37.

Fricke, H. C., 2003, Investigation of early Eocene water-vapor transport and paleoelevation using oxygen isotope data from geographically widespread mammal remains: Geological Society of America Bulletin, v. 115, p. 1088–1096, doi:10.1130/B25249.1.

Fricke, H. C., Clyde, W. C., O'Neil, J. R., and Gingerich, P. D., 1998, Evidence for rapid climate change in North America during the latest Paleocene thermal maximum: oxygen isotope compositions of biogenic phosphate from the Bighorn Basin (Wyoming): Earth and Planetary Science Letters, v. 160, p. 193–208, doi:10.1016/S0012-821X(98)00088-0.

Frost, C. D., Frost, B. R., Chamberlain, K. R., and Hulsebosch, T. P., 1998, The Late Archean history of the Wyoming province as recorded by granitic magmatism in the Wind River Range, Wyoming: Precambrian Research, v. 89, p. 145–173, doi:10.1016/S0301-9268(97)00082-X.

Garzione, C. N., Dettman, D. L., Quade, J., DeCelles, P. G., and Butler, R. F., 2000, High times on the Tibetan Plateau: Paleoelevation of the Thakkola graben, Nepal: Geology, v. 28, p. 339–342, doi:10.1130/0091-7613(2000)28⟨339:HTOTTP⟩2.0.CO;2.

Gehrels, G. E., Valencia, V., and Ruiz, J., 2008, Enhanced precision, accuracy, efficiency, and spatial resolution of U-Pb ages by laser ablation-multicollector- inductively coupled plasma-mass spectrometry: Geochemistry Geophysics Geosystems, v. 9, p. Q03017, doi:10.1029/2007GC001805.

Gerner, S. J., Spangler, L. E., Kimball, B. A., and Naftz, D. L., 2007, Characterization of dissolved solids in water resources of agricultural lands near Manila, Utah, 2004–05: U.S. Geological Survey, Scientific Investigations Report 2006-5211, p. 45.

Gierlowski-Kordesch, E. H., Jacobson, A. D., Blum, J. D., and Valero-Garcés, B. L., 2008, Watershed reconstruction of a Paleocene-Eocene lake basin using Sr isotopes in carbonate rocks: Geological Society of America Bulletin, v. 120, p. 85–95, doi:10.1130/B26070.1.

Goldstrand, P. M., 1994, Tectonic development of Upper Cretaceous to Eocene strata of southwestern Utah: Geological Society of America Bulletin, v. 106, p. 145–154, doi:10.1130/0016-7606(1994)106⟨0145:TDOUCT⟩2.3.CO;2.

Good, S. C., 1987, Mollusc-based interpretations of lacustrine paleoenvironments of the Sheep Pass Formation (Latest Cretaceous to Eocene) of east central Nevada: PALOIS, v. 2, p. 467–478.

Graham, S. A., Chamberlain, C. P., Yue, Y., Ritts, B. D., Hanson, A. D., Horton, T. W., Waldbauer, J. R., Poage, M. A., and Feng, X., 2005, Stable isotope records of Cenozoic climate and topography, Tibetan Plateau and Tarim Basin: American Journal of Science, v. 305, p. 101–118, doi:10.2475/ajs.305.2.101.

Gustav, S. H., ms, 1974, The sedimentology and paleogeography of the Bridger Formation, (Eocene) of southwestern Wyoming: Boston, University of Massachusetts, p. 82.

Hail, W. J., Jr., 1977, Stewart Gulch Tongue—A New Tongue of the Eocene Green River Formation, Piceance Creek Basin, Colorado, *in* Contributions to Stratigraphy: U.S. Geological Survey Bulletin, v. 1422-E, p. 1–8.

——— 1987, Chart showing intertongued units of the Eocene Green River and Uinta Formations, Northwestern Piceance Creek Basin, Northwestern Colorado: U.S. Geological Survey, Miscellaneous Investigations Series, Map I-1797-B.

——— 1990, Geology of the Lower Yellow Creek Area, Northwestern Colorado: U.S. Geological Survey Bulletin, v. 1787-O, p. 1–45.

——— 1992, Geology of the Central Roan Plateau Area, Northwestern Colorado: U.S. Geological Survey Bulletin, v. 1787-R, p. 1–26.

Hail, W. J., Jr., and Smith, M. C., 1994, Geologic map of the northern part of the Piceance Creek basin, northwestern Colorado: U.S. Geological Survey, Miscellaneous Investigations Series, map-I-2400.

Hansen, W. R., 1965, Geology of the Flaming Gorge area, Utah-Colorado-Wyoming: U.S. Geological Survey Professional Paper, v. 400-B, p. 260–261.

——— 1985, Drainage development of the Green River Basin in southwestern Wyoming and its bearing on fish biogeography, neotectonics, and paleoclimates: Mountain Geologist, v. 22, p. 192–204.

Hart, W. S., Quade, J., Madsen, D. B., Kaufman, D. S., and Oviatt, C. G., 2004, The $^{87}Sr/^{86}Sr$ ratios of lacustrine carbonates and lake-level history of the Bonneville paleolake system: Geological Society of America Bulletin, v. 116, p. 1,107–1,119, doi: 10.1130/B25330.1.

Hayden, F. V., 1869, Preliminary field report of the United States Geological Survey of Colorado and New Mexico: U.S. Geological Survey of the Territories, v. Third Annual Report, 155 p.

Hedge, C. E., Peterman, Z. E., and Braddock, W. A., 1967, Age of the major Precambrian regional metamorphism in the northern Front Range, Colorado: Geological Society of America Bulletin, v. 78, p. 551–558, doi: 10.1130/0016-7606(1967)78[551:AOTMPR]2.0.CO;2.

Henry, C. D., 2008, Ash-flow tuffs and paleovalleys in northeastern Nevada: Implications for Eocene paleogeography and extension in the Sevier hinterland, northern Great Basin: Geosphere, v. 4, p. 1–35, doi:10.1130/GES00122.1/.

Horton, T. W., Sjostrom, D. J., Abruzzese, M. J., Poage, M. A., Waldbauer, J. R., Hren, M., Wooden, J., and Chamberlain, C. P., 2004, Spatial and temporal variation of Cenozoic surface elevation in the Great Basin and Sierra Nevada: American Journal of Science, v. 304, p. 862–888, doi:10.2475/ajs.304.10.862.

Ingersoll, R. V., Cavazza, W., Baldridge, W. S., and Shafiqullah, M., 1990, Cenozoic sedimentation and paleotectonics of north-central New Mexico: Implications for initiation and evolution of the Rio Grande rift: Geological Society of America Bulletin, v. 102, p. 1,280–1,296, doi:10.1130/0016-7606(1990)102⟨1280:CSAPON⟩2.3.CO;2.

Jacobsen, A. D., and Blum, J. D., 2000, Ca/Sr and $^{87}Sr/^{86}Sr$ geochemistry of disseminated calcite in Himalayan silicate rocks from Nanga Parbat: Influence on river-water chemistry: Geology, v. 28, p. 463–466, doi:10.1130/0091-7613(2000)28⟨463:SASGOD⟩2.0.CO;2.

Janecke, S. U., 1994, Sedimentation and paleogeography of an Eocene to Oligocene rift zone, Idaho and Montana: Geological Society of America Bulletin, v. 106, p. 1,083–1,095, doi: 10.1130/0016-7606(1994)106⟨1083:SAPOAE⟩2.3.CO;2.

Janecke, S. U., VanDenburg, C. J., Blankenau, J. J., and M'Gonigle, J. W., 2000, Long-distance longitudinal transport of gravel across the Cordilleran thrust belt of Montana and Idaho: Geology, v. 28, p. 439–442, doi:10.1130/0091-7613(2000)28⟨439:LLTOGA⟩2.0.CO;2.

Johnson, R. C., 1981, Stratigraphic evidence for a deep Eocene Lake Uinta, Piceance Creek Basin, Colorado: Geology, v. 9, p. 55–62, doi: 10.1130/0091-7613(1981)9⟨55:SEFADE⟩2.0.CO;2.

——— 1984, New Names for Units in the Lower Part of the Green River Formation, Piceance Creek Basin, Colorado: U.S. Geological Survey Bulletin, v. 1529-I, p. 1–20.

Jones, L. M., and Faure, G., 1972, Strontium isotope geochemistry of Great Salt Lake, Utah: Geological Society of America Bulletin, v. 83, p. 1,875–1,880, doi:10.1130/0016-7606(1972)83[1875:SIGOGS]2.0.CO;2.

Kay, J. L., 1934, The Tertiary formations of the Uinta Basin, Utah: Annals of the Carnegie Museum, v. 23, p. 357–371.

Keefer, W. R., 1957, Geology of the Du Noir area Fremont County Wyoming: U.S. Geological Survey Professional Paper, v. 294-E, p. 155–221.

——— 1965, Stratigraphy and geologic history of the uppermost Cretaceous, Paleocene, and Lower Eocene rocks in the Wind River Basin, Wyoming: U.S. Geological Survey Professional Paper, v. 495-A, p. 77.

Kelts, K., 1988, Environments of deposition of lacustrine petroleum source rocks: an introduction, *in* Fleet, A. J., Kelts, K., and Talbot, M. R., editors, Lacustrine Petroleum Source Rocks: London, Geological Society Special Publication, v. 40, p. 3–26.

Kent-Corson, M. L., Sherman, L. S., Mulch, A., and Chamberlain, C. P., 2006, Cenozoic topographic and climatic response to changing tectonic boundary conditions in Western North America: Earth and Planetary Science Letters, v. 252, p. 453–466, doi:10.1016/j.epsl.2006.09.049.

Kihm, A. J., ms, 1984, Early Eocene Mammalian Faunas of the Piceance Creek Basin Northwestern Colorado: Boulder, Colorado, University of Colorado at Boulder, Ph. D. thesis, p. 390.

Kistner, F. B., ms, 1973, Stratigraphy of the Bridger Formation in the Big Island-Blue Rim area, Sweetwater County, Wyoming: Laramie, University of Wyoming, Master's thesis, p. 174.

Koch, P. L., Zachos, J. C., and Dettman, D. L., 1995, Stable isotope stratigraphy and paleoclimatology of the Paleogene Bighorn Basin (Wyoming, USA): Palaeogeography, Palaeoclimatology, Palaeoecology, v. 115, p. 61–89, doi:10.1016/0031-0182(94)00107-J.

Korth, W. W., 1982, Revision of the Wind River faunas, early Eocene of central Wyoming. Part 2. Geologic setting: Annals of the Carnegie Museum, v. 51, p. 57–78.

Lawrence, J. C., 1963, Origin of the Wasatch Formation, Cumberland Gap area, Wyoming: University of Wyoming Contributions to Geology (Rocky Mountain Geology), v. 2, p. 151–158.

Lawton, T. F., 1986, Fluvial systems of the Upper Cretaceous Mesaverde Group and Paleocene North Horn Formation, central Utah: A record of transition from thin-skinned to thick-skinned deformation in the foreland region, *in* Peterson, J. A., editor, Paleotectonics and Sedimentation in the Rocky Mountain Region, United States: American Association of Petroleum Geologists Memoir, v. 41, p. 423–442.

Lawton, T. F., Talling, P. J., Hobbs, R. S., Trexler, J. H., Jr., Weiss, M. P., and Burbank, D. W., 1993, Structure and Stratigraphy of Upper Cretaceous and Paleocene Strata (North Horn Formation), Eastern San Pitch Mountains, Utah—Sedimentation at the Front of the Sevier Orogenic Belt, *in* Evolution of Sedimentary Basins; Uinta and Piceance basins: U.S. Geological Survey Bulletin B 1787-II, p. 1–36.

Lipman, P. W., Prostka, H. J., and Christensen, R. L., 1972, Cenozoic volcansim and plate tectonic evolution of the western United States. I. Early and Middle Cenozoic: Philosophical Transactions of the Royal Society of London, Series A, Mathematical and Physical Sciences, v. 271, p. 217–248.

Love, J. D., 1939, Geology along the southern margin of the Absaroka Range, Wyoming: Geological Society of America Special Paper, v. 20, 134 p.

——— 1970, Cenozoic geology of the Granite Mountains area, central Wyoming: U.S. Geological Survey Professional Paper, v. 495-C, p. 154.

Ludwig, K. R., 2001, SQUID 1.02; a users manual: Berkeley, California, Berkeley Geochronology Center Special Publication n. 2.

MacGinitie, H. D., 1974, An early middle Eocene flora from the Yellowstone-Absaroka Volcanic Province, northwestern Wind River Basin, Wyoming: Berkeley, California, University of California Publications in Geological Sciences, v. 108, 103 p.

Marcantel, E. L., and Weiss, M. P., 1968, Colton Formation (Eocene: Fluviatile) and associated lacustrine beds, Gunnison Plateau, central Utah: The Ohio Journal of Science, v. 68, p. 40–49.

Mauger, R. L., 1977, K-Ar ages of biotites from tuffs in Eocene rocks of the Green River, Washakie, and Uinta basins, Utah, Wyoming, and Colorado: University of Wyoming Contributions to Geology (Rocky Mountain Geology), v. 15, p. 17–41.

McCrea, J. M., 1950, On the isotopic chemistry of carbonates and a paleotemperature scale: The Journal of Chemical Physics, v. 18, p. 849–857, doi:10.1063/1.1747785.

McGrew, P. O., and Sullivan, R., 1970, The stratigraphy and paleontology of Bridger A: University of Wyoming, Contributions to Geology, v. 9, p. 66–85.

McMillan, M. E., Heller, P. L., and Wing, S. L., 2006, History and causes of post-Laramide relief in the Rocky Mountain orogenic plateau: Geological Society of America Bulletin, v. 118, p. 393–405, doi:10.1130/B25712.1.

Meen, J. K., and Eggler, D. H., 1987, Petrology and geochemistry of the Cretaceous Independence volcanic suite, Absaroka Mountains, Montana: Clues to the composition of the Archean sub-Montana mantle: Geological Society of America Bulletin, v. 98, p. 238–247, doi: 10.1130/0016-7606(1987)98⟨238:PAGOTC⟩2.0.CO;2.

Moncure, G. K., ms, 1979, Depositional environment of the Green River Formation in the vicinity of the Douglas Creek Arch, Colorado and Utah: Laramie, University of Wyoming, Master's thesis, p. 55.

Moncure, G., and Surdam, R. C., 1980, Depositional environment of the Green River Formation in the vicinity of the Douglas Creek Arch, Colorado and Utah: University of Wyoming Contributions to Geology, v. 19, p. 9–24.

Moorbath, S., Hurley, P. M., and Fairbairn, H. W., 1967, Evidence for the origin and age of some mineralized Laramide intrusives in the southwestern United States from strontium isotope and rubidium-strontium measurements: Economic Geology, v. 62, p. 228–236, doi: 10.2113/gsecongeo.62.2.228.

Morrill, C., and Koch, P. L., 2002, Elevation or alteration? Evaluation of isotopic constraints on paleoaltitudes surrounding the Eocene Green River Basin: Geology, v. 30, p. 151–154, doi:10.1130/0091-7613(2002)030⟨0151:EOAEOI⟩2.0.CO;2.

Morris, T. H., Richmond, D. R., and Marino, J. E., 1991, The Paleocene/Eocene Colton Formation: A Fluvial-dominated lacustrine deltaic system, Roan Cliffs, Utah, *in* Chidsey, T. C., Jr., editor, Geology of east-central Utah: Utah Geological Association Publication, v. 19, p. 129–139.

Mueller, P. A., Peterman, Z. E., and Granath, J. W., 1985, A bimodal Archean volcanic series, Owl Creek Mountains, Wyoming: Journal of Geology, v. 93, p. 701–712.

Müller, G., Irion, G., and Forstner, U., 1972, Formation and diagenesis of inorganic Ca-Mg carbonates in the lacustrine environment: Naturwissenchaften, v. 59, p. 158–164, doi:10.1007/BF00637354.

Nelson, B. K., and DePaolo, D. J., 1988, Comparison of isotopic and petrographic provenance indicators in sediments from Tertiary continental basins of New Mexico: Journal of Sedimentary Petrology (Journal of Sedimentary Research), v. 58, p. 348–357.

Nelson, S. T., Wood, M. J., Mayo, A. L., Tingey, D. G., and Eggett, D., 2005, Shoreline tufa and tufaglomerate from Pleistocene Lake Bonneville, Utah, USA: stable isotopic and mineralogical records of lake conditions, processes, and climate: Journal of Quaternary Science, v. 20, p. 3–19, doi:10.1002/jqs.889.

Norris, R. D., Jones, L. S., Corfield, R. M., and Cartlidge, J. E., 1996, Skiing in the Eocene Uinta Mountains? Isotopic evidence in the Green River Formation for snow melt and large mountains: Geology, v. 24, p. 403–406, doi:10.1130/0091-7613(1996)024⟨0403:SITEUM⟩2.3.CO;2.

Norman, M. D., and Leeman, W. P., 1989, Geochemical evolution of Cenozoic-Cretaceous magmatism and its relation to tectonic setting, southwestern Idaho, U.S.A.: Earth and Planetary Science Letters, v. 94, p. 78–96, doi:10.1016/0012-821X(89)90085-X.

O'Sullivan, R. B., 1974, Chart showing correlation of selected restored stratigraphic diagram units of the Eocene Uinta and Green River Formations, east-central Piceance Creek Basin, northwestern Colorado: U.S. Geological Survey Oil and Gas Investigations Chart, Report # 67, p. 1.

——— 1975, Coughs Creek Tongue—A New Tongue of the Eocene green River Formation, Piceance Creek Basin, Colorado: U.S. Geological Survey Bulletin, v. 1395-G, p. G1–G7.

——— 1987, Chart showing the correlation of selected parts of the Eocene Uinta and Green River Formations, southeastern Piceance Creek Basin, Colorado: U.S. Geological Survey Miscellaneous Field Studies Map, MF-1986.

Oriel, S. S., 1961, Tongues of the Wasatch and Green River Formations, Fort Hill area, Wyoming: U.S. Geological Survey Professional Paper, v. 424-B, p. B151–B152.

——— 1962, Main body of the Wasatch Formation near La Barge, Wyoming: American Association of Petroleum Geologists Bulletin, v. 46, p. 2,161–2,173.

Oviatt, C. G., 1988, Late Pleistocene and Holocene lake fluctuations in the Sevier Lake Basin, Utah, USA: Journal of Paleolimnology, v. 1, p. 9–21, doi:10.1007/BF00202190.

Oviatt, C. G., Habiger, G. D., and Hay, J. E., 1994, Variation in the composition of Lake Bonneville marl: a potential key to lake-level fluctuations and paleoclimate: Journal of Paleolimnology, v. 11, p. 19–30, doi:10.1007/BF00683268.

Paces, J. B., Peterman, Z. E., Futa, K., Oliver, T. A., and Marshall, B. D., 2007, Strontium isotopic composition of Paleozoic carbonate rocks in the Nevada Test Site vicinity, Clark, Lincoln, and Nye Counties, Nevada, and Inyo County, California: U.S. Department of Interior, U.S. Geological Survey, Data Series 280.

Palmer, M. R., and Edmond, J. M., 1992, Controls over the strontium isotope composition of river water: Geochimica et Cosmochimica Acta, v. 56, p. 2,099–2,111, doi:10.1016/0016-7037(92)90332-D.

Patel, S. C., Frost, C. D., and Frost, B. R., 1999, Contrasting responses of Rb-Sr systematics to regional and contact metamorphism, Laramie Mountains, Wyoming, USA: Journal of Metamorphic Geology, v. 17, p. 259–269, doi: 10.1046/j.1525-1314.1999.00411.x.

Pearson, R. C., Hedge, C. E., Thomas, H. H., and Stern, T. W., 1966, Geochronology of the St. Kevin Granite and neighboring Precambrian rocks, northern Sawatch Range, Colorado: Geological Society of America Bulletin, v. 77, p. 1,109–1,120.

Peterman, Z. E., and Hildreth, R. A., 1978, Reconnaissance geology and geochronology of the Precambrian of the Granite Mountains, Wyoming: U.S. Geological Survey Professional Paper 1055, p. 22.

Peterman, Z. E., Doe, B. R., and Prostka, H. J., 1970, Lead and Strontium Isotopes in Rocks of the Absaroka Volcanic Field, Wyoming: Contributions to Mineralogy and Petrology, v. 27, p. 121–130, doi:10.1007/BF00371979.

Peterson, A. R., 1976, Paleoenvironments of the Colton Formation, Colton, Utah: Brigham Young University Geology Studies, v. 23, p. 7–35.

Pipiringos, G. N., and Johnson, R. C., 1975, Preliminary geologic map of the Buckskin Point Quadrangle, Rio Blanco County, Colorado: U.S. Geological Survey Miscellaneous Field Studies Map 651.

Pitman, J. K., Fouch, T. D., and Goldhaber, M. B., 1982, Depositional setting and diagenetic evolution of some Tertiary unconventional reservoir rocks, Uinta Basin, Utah: American Association of Petroleum Geologists Bulletin, v. 66, p. 1,581–1,596.

Potter, C. J., Dubiel, R. F., Snee, L. W., and Good, S. C., 1995, Eocene extension of early Eocene lacustrine strata in a complexly deformed Sevier-Laramide hinterland, northwest Utah and northeast Nevada: Geology, v. 23, p. 181–184, doi:10.1130/0091-7613(1995)023⟨0181:EEOEEL⟩2.3.CO;2.

Prothero, D. R., 1990, Magnetostratigraphy and $^{40}Ar/^{39}Ar$ dating of the Middle Eocene Uinta Formation, Uinta Basin, Utah: GSA Abstracts with Programs.

——— 1996, Magnetic stratigraphy and biostratigraphy of the Middle Eocene Uinta Formation, Uinta Basin, Utah, *in* Prothero, D. R., and Emry, R. J., editors, The Terrestrial Eocene-Oligocene Transition in North America: Cambridge, Cambridge University Press, p. 3–24.

Quade, J., Roe, L., DeCelles, P. G., and Ojha, T. P., 1997, The Late Neogene $^{87}Sr/^{86}Sr$ record of lowland Himalayan rivers: Science, v. 276, p. 1,828–1,831.

Rhodes, M. K., Carroll, A. R., Pietras, J. T., Beard, B. L., and Johnson, C. M., 2002, Strontium isotope record of paleohydrology and continental weathering, Eocene Green River Formation, Wyoming: Geology, v. 30, p. 167–170, doi:10.1130/0091-7613(2002)030⟨0167:SIROPA⟩2.0.CO;2.

Roehler, H. W., 1969, Stratigraphy and oil-shale deposits of Eocene rocks in the Washakie Basin, Wyoming, *in* Barlow, J. A., editor, Symposium on Tertiary Rocks of Wyoming: Casper, Wyoming, Wyoming Geological Association Field Conference Guidebook, n. 21, p. 197–206.

——— 1970, Non-opaque heavy minerals from sandstone of Eocene age in the Washakie Basin, Wyoming: U.S. Geological Survey Professional Paper, v. 700-D, p. D181–D187.

——— 1973a, Stratigraphic divisions and geologic history of the Laney member of the Green River Formation in the Washakie Basin in southwestern Wyoming: U.S. Geological Survey Bulletin, v. 1372-E, p. 28.

——— 1973b, Stratigraphy of the Washakie Formation in the Washakie Basin, Wyoming: U.S. Geological Survey Bulletin, v. 1369, p. 40.

——— 1974, Depositional environments of rocks in the Piceance Creek basin, Colorado, *in* Murray, D. K., editor, Energy Resources of the Piceance Creek Basin, Colorado: Denver, Colorado, Rocky Mountain Association of Geologists, p. 57–64.

——— 1988, Geology of the Cottonwood Creek Delta in the Eocene Tipton Tongue of the Green River Formation, southeast Washakie Basin, Wyoming, *in* Roehler, H. W., Hanley, J. H., and Honey, J. G., editors, Geology and paleoecology of the Cottonwood Creek delta in the Eocene Tipton Tongue of the Green River Formation and a mammalian fauna from the Eocene Cathedral Bluffs Tongue of the Wasatch Formation, Southeast Washakie Basin, Wyoming: U.S. Geological Survey Bulletin, v. 1669-A–C, p. 14.

——— 1990, Sedimentology of freshwater lacustrine shorelines in the Eocene Scheggs Bed of the Tipton Tongue of the Green River Formation, Sand Wash Basin, northwest Colorado: U.S. Geological Survey Bulletin, v. 1911, 12 p.

——— 1992, Correlation, composition, areal distribution and thickness of Eocene stratigraphic units, Greater Green River Basin, Wyoming, Utah and Colorado: U.S. Geological Survey Professional Paper, v. 1506-E, p. 1–49.

——— 1993, Eocene climates, depositional environments, and geography, greater Green River basin, Wyoming, Utah, and Colorado: U.S. Geological Survey Professional Paper, v. 1506-F, p. 74 p.

Rubey, W. W., Oriel, S. S., and Tracey, J. I., Jr., 1975, Geology of the Sage and Kemmerer 15-minute quadrangles, Lincoln County, Wyoming: U.S. Geological Survey Professional Paper, v. 855, 18 p.

Sarg, R., Bartov, Y., Carroll, A. R., and Lowenstein, T. K., 2009, The stratigraphy and depositional systems of the Green River oil shale in the Piceance Creek and Greater Green River basins, Colorado and Wyoming, AAPG Annual Convention and Exhibition, Denver, Colorado, June 7–10, 2009: Search and Discovery: Denver, Colorado, American Association of Petroleum Geologists Search and Discovery Article #90090.

Sheldon, N. D., and Retallack, G. J., 2004, Regional paleoprecipitation records from the Late Eocene and Oligocene of North America: The Journal of Geology, v. 112, p. 487–494, doi:10.1086/421076.

Sklenar, S. E., and Anderson, D. W., 1985, Origin and early evolution of an Eocene lake system within the Washakie Basin of southwestern Wyoming, *in* Flores, R. M., and Kaplan, S. S., editors, Cenozoic paleogeography of the west central United States: Denver, Colorado, Society of Economic Paleontologists and Mineralogists, p. 231–245.

Smith, J. D., 1986, Depositional environments of the Tertiary Colton and basal Green River Formations in Emma Park, Utah: Brigham Young University Geology Studies, v. 33, p. 135–174.

Smith, M. E., Carroll, A. R., and Singer, B. S., 2008a, Synoptic reconstruction of a major ancient lake system: Eocene Green River Formation, western United States: Geological Society of America Bulletin, v. 120, p. 54–84, doi:10.1130/B26073.1.

Smith, M. E., Carroll, A. R., and Mueller, E. R., 2008b, Elevated weathering rates in the Rocky Mountains during the Early Eocene Climatic Optimum: Nature Geoscience, v. 1, p. 370–374, doi:10.1038/ngeo205.

Soister, P. E., 1968, Stratigraphy of the Wind River Formation in south-central Wind River Basin, Wyoming: U.S. Geological Survey Professional Paper, v. 594-A, 50 p.

Spencer, R. J., Baedecker, M. J., Eugster, H. P., Forester, R. M., Goldhaber, M. B., Jones, B. F., Kelts, K., Mckenzie, J., Madsen, D. B., Rettig, S. L., Rubin, M., and Bowser, C. J., 1984, Great Salt Lake, and precursors, Utah: the last 30,000 years: Contributions to Mineralogy and Petrology, v. 86, p. 321–334, doi:10.1007/BF01187137.

Spieker, E. M., 1946, Late Mesozoic and early Cenozoic history of central Utah: U.S. Geological Survey Professional Paper, v. 205-D, p. 117–161.

Stagner, W. L., 1941, The paleogeography of the eastern part of the Uinta Basin during Uinta B (Eocene) time: Annals of Carnegie Museum, v. 28, p. 273–308.
Stanley, K. O., and Collinson, J. W., 1979, Depositional history of Paleocene-lower Eocene Flagstaff Limestone and Coeval Rocks, Central Utah: American Association of Petroleum Geologists Bulletin, v. 63, p. 311–323.
Stanley, K. O., and Surdam, R. C., 1978, Sedimentation on the front of Eocene Gilbert-type deltas, Washakie Basin, Wyoming: Journal of Sedimentary Petrology, v. 48, p. 557–573.
Steidtmann, J. R., 1969, Stratigraphy of the Eocene Pass Peak Formation, central-western Wyoming, *in* Barlow, J. A., editor, Symposium on Tertiary rocks of Wyoming: Casper, Wyoming Geological Association, 21st Annual Field Conference Guidebook, p. 55–63.
Stucky, R. K., ms, 1982, Mammalian fauna and biostratigraphy of the upper part of the Wind River Formation (early to middle Eocene), Natrona County, Wyoming, and the Wasatchian-Bridgerian Boundary: Boulder, University of Colorado, Ph. D. thesis, p. 285.
——— 1984, Revision of the Wind River faunas, early Eocene of central Wyoming. Part 5. Geology and biostratigraphy of the upper part of the Wind River Formation, northeastern Wind River Basin: Annals of Carnegie Museum, v. 53, p. 231–294.
Stucky, R. K., Prothero, D. R., Lohr, W. G., and Snyder, J. R., 1996, Magnetic stratigraphy, sedimentology, and mammalian faunas of the early Uintan Washakie Formation, Sand Wash Basin, Northwestern Colorado, *in* Prothero, D. R., and Emry, R. J., editors, The Terrestrial Eocene-Oligocene Transition in North America: Cambridge, Cambridge University Press, p. 40–51.
Surdam, R. C., and Stanley, K. O., 1979, Lacustrine sedimentation during the culminating phase of Eocene Lake Gosiute, Wyoming (Green River Formation): Geological Socieity of American Bulletin, v. 90, p. 93–110.
——— 1980, Effects of changes in drainage-basin boundaries on sedimentation in Eocene Lakes Gosiute and Uinta of Wyoming, Utah, and Colorado: Geology, v. 8, p. 135–139, doi:10.1130/0091-7613(1980)8⟨135:EOCIDB⟩2.0.CO;2.
Talbot, M. R., 1990, A review of the paleohydrological interpretation of carbon and oxygen isotopic ratios in primary lacustrine carbonates: Chemical Geology: Isotope Geoscience Section, v. 80, p. 261–279.
Talbot, M. R., and Kelts, K., 1990, Paleolimnological signatures from carbon and oxygen isotopic ratios in carbonates from organic carbon-rich lacustrine sediments, *in* Katz, B., editor, Lacustrine Basin Exploration: Case Studies and Modern Analogs: American Association of Petroleum Geologists Memoir, v. 50, p. 99–112.
Talling, P. J., Lawton, T. F., Burbank, D. W., and Hobbs, R. S., 1995, Evolution of latest Cretaceous-Eocene nonmarine deposystems in the Axhandle piggyback basin of central Utah: Geological Society of America Bulletin, v. 107, p. 297–315.
Trudell, L. G., Beard, T. N., and Smith, J. W., 1970, Green River Formation lithology and oil-shale correlations in the Piceance Creek Basin, Colorado: U.S. Bureau of Mines Report of Investigations, v. 7357, 226 p.
——— 1974, Stratigraphic framework of Green River Formation oil shales in the Piceance Creek Basin, Colorado, *in* Murray, D. K., editor, Guidebook to the Energy Resources of the Piceance Creek Basin, Colorado: Denver, Colorado, Rocky Mountain Association of Geologists, 25th Annual Field Conference, p. 65–69.
Van Houten, F. B., 1955, Volcanic-rich middle and upper Eocene sedimentary rocks northwest of Rattlesnake Hills, central Wyoming: U.S. Geological Survey Professional Paper, v. 274-A., 14 p.
——— 1964, Tertiary geology of the Beaver Rim area, Fremont and Natrona counties, Wyoming: U.S. Geological Survey Bulletin, v. 1164, 99 p.
Vogel, T. A., Cambray, F. W., and Constenius, K. N., 2001, Origin and emplacement of igneous rocks in the central Wasatch Mountains, Utah: Rocky Mountain Geology, v. 36, p. 119, doi: 10.2113/gsrocky.36.2.119.
Volkert, D. G., ms, 1980, Stratigraphy and petrology of the Colton Formation (Eocene), Gunnison Plateau, central Utah: DeKalb, Illinois, Northern Illinois University, Master's thesis, p. 132.
Weber, J. N., 1964, Carbon-oxygen isotopic composition of Flagstaff carbonate rocks and its bearing on the history of Paleocene-Eocene Lake Flagstaff of central Utah: Geochimica et Cosmochimica Acta, v. 28, p. 1,219–1,242, doi:10.1016/0016-7037(64)90125-5.
Weiss, M. P., 1982, Relation of the Crazy Hollow Formation to the Green River Formation, Central Utah, Overthrust Belt of Utah: Utah Geological Association Publication 10, p. 285–289.
West, R. M., and Dawson, M. R., 1973, Fossil mammals from the upper part of the Cathedral Bluffs Tongue of the Wasatch Formation (Early Bridgerian), northern Green River Basin, Wyoming: University of Wyoming Contributions to Geology, v. 12, p. 33–41.
Willis, G. C., 1986, Geologic Map of the Salina Quadrangle, Sevier County, Utah: Utah Geological and Mineral Survey Map, M-83, 20 p. 1 sheet, scale 1:24,000.
Winfrey, W. M., 1960, Stratigraphy, correlation, and oil potential of the Sheep Pass Formation, east-central Nevada, *in* Boettcher, J. W., and Sloan, W. W., editors, Guidebook to the Geology of east central Nevada: Intermountain Association of Petroleum Geologists, 11th annual Field Conference, Guidebook, p. 126–133.
Wingate, F. H., 1983, Palynology and age of the Elko Formation (Eocene) near Elko, Nevada: Palynology, v. 7, p. 93–132.
Wolfbauer, C. A., and Surdam, R. C., 1974, Origin of nonmarine dolomite in Eocene Lake Gosiute, Green River Basin, Wyoming: GSA Bulletin, v. 85, p. 1,733–1,740, doi: 10.1130/0016-7606(1974)85⟨1733:OONDIE⟩2.0.CO;2.
Wolfe, J. A., 1994, Tertiary climatic changes at middle latitudes of western North America: Palaeogeography, Palaeoclimatology, Palaeoecology, v. 108, p. 195–205, doi:10.1016/0031-0182(94)90233-X.

Zachos, J., Pagani, M., Sloan, L., Thomas, E., and Billups, K., 2001, Trends, rhythms, and aberrations in global climate 65 Ma to Present: Science, v. 292, p. 686–693, doi:10.1126/science.1059412.

Zawiskie, J., Chapman, D., and Alley, R., 1982, Depositional history of the Paleocene-Eocene Colton Formation, north-central Utah, *in* Nielson, D. L., editor, Overthrust Belt of Utah: Utah Geological Association Publication 10, p. 273–284.

Zielinski, R. A., Peterman, Z. E., Stuckless, J. S., Rosholt, J. N., and Nkomo, I. T., 1981, The chemical and isotopic record of rock-water interaction in the Sherman Granite, Wyoming and Colorado: Contributions to Mineralogy and Petrology, v. 78, p. 209–219, doi:10.1007/BF00398915.

Zonneveld, J.-P., Bartels, W. S., and Clyde, W. C., 2003, Stratal architecture of an Early Eocene fluvial-lacustrine depositional system, Little Muddy Creek area, southwestern Green River Basin, Wyoming, *in* Raynolds, R. G., and Flores, R. M., editors, Cenozoic Systems of the Rocky Mountain Region: Denver, Rocky Mountain Section, RMS-SEPM (Society for Sedimentary Geology) Special Publication, p. 253–288.